SYSTEM ARCHITECTURE OF SMALL UNMANNED AERIAL SYSTEM FOR FLIGHT BEYOND VISUAL LINE-OF-SIGHT

THESIS

Kwee Siam Seah, Military Expert 5 (Major), Republic of Singapore Air Force

AFIT-ENV-MS-15-S-047

DEPARTMENT OF THE AIR FORCE
AIR UNIVERSITY

AIR FORCE INSTITUTE OF TECHNOLOGY

Wright-Patterson Air Force Base, Ohio

AFIT-ENV-MS-15-S-047

SYSTEM ARCHITECTURE OF SMALL UNMANNED AERIAL SYSTEM FOR FLIGHT BEYOND VISUAL LINE-OF-SIGHT

THESIS

Presented to the Faculty

Department of Systems Engineering and Management

Graduate School of Engineering and Management

Air Force Institute of Technology

Air University

Air Education and Training Command

In Partial Fulfillment of the Requirements for the

Degree of Master of Science in Systems Engineering

Kwee Siam Seah, BS (Hons)

Military Expert 5 (Major), Republic of Singapore Air Force

September 2015

AFIT-ENV-MS-15-S-047

SYSTEM ARCHITECTURE OF SMALL UNMANNED AERIAL SYSTEM FOR FLIGHT BEYOND VISUAL LINE-OF-SIGHT

Kwee Siam Seah, BS (Hons)

Military Expert 5 (Major), Republic of Singapore Air Force

Committee Membership:

Dr. David R. Jacques
Chair

Dr. John M. Colombi
Member

Maj Scott Pierce, PhD
Member

Abstract

Small Unmanned Aerial Systems (UAS) have increasingly been used in military application. The application in expanding scope of operations has pushed existing small UAS beyond its designed capabilities. This resulted in frequent modifications or new designs. A common requirement in modification or new design of small UAS is to operate beyond visual Line-Of-Sight (LOS) of the ground pilot. Conventional military development for small UAS adopts a design and built approach. Modification of small Remote Control (RC) aircraft, using Commercial-Off-The Shelf (COTS) equipment, offers a more economical alternative with the prospect of shorter development time compared to conventional approach. This research seeks to establish and demonstrate an architecture framework and design a prototype small UAS for operation beyond visual LOS. The aim is to achieve an effective and reliable development approach that is relevant to the military's evolving requirements for small UASs. Key elements of the architecture include Failure Mode Effect and Criticality Analysis (FMECA), fail safe design for loss of control or communication, power management, interface definition, and configuration control to support varying onboard payloads. Flight test was conducted which successfully demonstrated a control handoff between local and remote Ground Station (GS) for beyond visual LOS operations.

AFIT-ENV-MS-15-S-047

Dedicated to my dear wife for your love and patience. To my 2 sons for being my motivation in the period of research. To my parents and the rest of my family, for your continual support.

Acknowledgments

I would like to thank my thesis committee, Dr David Jacques, Dr John Colombi and Maj Scott Pierce. This thesis would not be possible without your guidance, invaluable academic instruction and encouragement.

Kwee Siam

Table of Contents

Page

Page

Page

List of Figures

Page

Page

List of Tables

Page

Page

List of Abbreviations

AFIT	Air Force Institute of Technology
AP	Auto-Pilot
BEC	Battery Elimination Circuit
BOM	Bill of Material
C2	Command and Control
CA	Critical Analysis
CFR	Code of Federal Regulation
COA	Certification Of Approval
COTS	Commercial-Of-The Shelf
DoD	Department of Defense
ESC	Electronic Speed Controller
EIRP	Effective Isotropic radiate Power
FAA	Federal Aviation Authority
FMEA	Failure Mode and Effect Analysis
FMECA	Failure Mode Effect and Criticality Analysis
FPV	First Person View
GS	Ground Station
ISR	Intelligence, Surveillance, and Reconnaissance
LiPo	Lithium Polymer
LOS	Line of Sight
MFR	Military Flight Release

NTIA	National Telecommunications and Information Administration
PID	Proportion-Integral-Derivative
PWM	Pulse Width Modulation
RC	Remote Control
RF	Radio Frequency
SEP	System Engineering Process
SOF	Safety of Flight
SRB	Safety Review Board
RAF	Royal Air Force
UAS	Unmanned Aerial System
UAV	Unmanned Aerial Vehicle
USAF	United States Air Force
TRB/SRB	Technical and Safety Review Board
TX	Transmission

SYSTEM ARCHITECTURE OF SMALL UNMANNED AERIAL VEHICLE FOR FLIGHT BEYOND VISUAL LINE-OF-SIGHT

I. Introduction

The Unmanned Aerial System (UAS) is increasingly used in modern military operations and this trend will continue to proliferate into the 21st century (Miller, 2013) (Gertler, 2012:1). Sophisticated UASs such as Global Hawk (RQ-4) and Reaper (MQ-9) are costly which discourages their use in operation where the risk of losing the platform is high. Stepping up to fulfill these 'dangerous and dirty' operations is the small and expendable UAS (Abatti, 2005). The small UASs are classified under Group 1 or 2 (Small Tactical) UASs and can weigh up to 55 lbs (Department of Defense, 2013:6).

Military systems are conventionally designed and built with strict performance and reliability requirements. Consequently, it is generally more expensive than Commercial-Off-The Shelf (COTS) system. The dollar per pound of the empty weight cost of an UAS is estimated at $1,500/lbs (Department of Defense, 2002:33). This is the cost to acquire a basic UAS that is operated by a ground pilot but has no other operational capability. However, this relationship between cost (empty weight) and weight is not linear for small UAS. Citing an example, the "*Dragon Eye*" weighs 3.5 lbs but the empty weight cost is estimated at $35,000 (Department of Defense, 2002:33) (Sam Perlo-Freeman et al., 2014) . A similar size "*Raven*" that weighs 4.2 lbs has an empty weight cost of $56,000 (Economist, 2011). Taking the official published cost of "*Dragon Eye*"

the dollar per pound of the empty weight is $10,000/lbs. With decreasing military budget in the projected future (Office of Management and Budget, 2015:59), there is an impetus to seek a more austere approach to lower the acquisition cost of small UASs so as to decrease the associated monetary value of losing the UAS during operation.

Conversion of a Remote Control (RC) aircraft models to small UAS, using COTS equipments, offers an economical alternative to lower acquisition cost. This approach is viable as small UAS with basic autonomous flying capability that cost less than $500 have been developed (Long Di and Chen, 2011:49, 73). The desired capability of the UAS dictates the necessary payload which in turn determines the eventual size and cost. Some examples of the capabilities (non-prescriptive) to facilitate ISR operation include autonomous navigation, image recognition and night vision. A commonly required capability is to operate the small UAS beyond visual Line-Of-Sight (LOS). This extends the operating range of the UAS and reduces the danger of enemy attack on the GS.

The definition of LOS is having a clear path between the Unmanned Aerial Vehicle (UAV) and Ground Station (GS). This will enable wireless data to be transmitted between two sub-systems (Gundlach, 1975: 472). The range of wireless transmission is dependent on numerous factors. These include power level, signal frequency and environmental signal noise (Gundlach, 1975: 475). The detail on the factors affecting transmission range will be covered in Section 2.4.

LOS is lost when there is a blockage by terrain or when the operating distance is so far that the curvature of earth prevents a straight line between the UAS and GS (Gundlach, 1975:507). Due to the physical size, small UAS tend to be non observable

beyond relatively small distances without visual aiding equipment. In such instances the UAS is operating beyond visual LOS even though there is still a clear wireless signal LOS. In addition, operating a UAS designed for visual LOS beyond its intended range, may also possibly exceed the transmission range of the system

This research incorporates COTS equipment on a RC aircraft. The aim is to establish a framework to effectively and reliably develop a small UAS architecture that has the capability to safely conduct operations beyond visual LOS. To ensure airworthiness, the operating risks of the designed architecture are identified through Failure Mode Effect and Criticality Analysis (FMECA) to analyze its effect on Safety of Flight (SOF). Corresponding mitigation such as fail safe designs and contingency processes are subsequently implemented to address the risk. Thereafter, the residual risks are re-assessed before implementation. To reduce development lead time, the UAS will be based on a readily available small electric RC aircraft, "*SIG Rascal 110*", as the platform for the research. Finally, the framework to develop the system architecture will also encompass the regulatory requirements to operate the UAS.

1.1 Problem Statement

New military systems can be acquired either through COTS or developed from new based on requirements. Civil regulation in the United States currently restricts operation of the small UAS to within visual LOS. With no commercial motivation, COTS UASs are consequently not often developed to operate beyond visual LOS. Some military-developed small UASs have operating ranges that exceed visual LOS. However, they are generally more expensive as they have to meet stringent specifications.

The normal mode of system acquisition with design and build cannot fulfill the new operating paradigm of the small UAS requirement in term of cost and functionality. To overcome this shortfall, a modified mode of acquisition to develop small UAS from COTS equipment is studied.

1.2 Objective

This research aims to (1) develop the architecture of a small UAS that is capable of operating up to five times the visual LOS range through the use of COTS equipment, (2) establish a framework and document the development process so that it can be effectively and reliably repeated across other small UAS in AFIT research and (3) validate SOF of the designed architecture and seek airworthiness approval for flight testing. The architecture can potentially be applied to existing or new UAS research such as cooperative flight with multi-UASs or autonomous target recognition with the aim to fulfill the need for small UAS that are economical and expendable in military operations.

1.3 Investigative Questions

The investigative questions for this research are;

i. What are the requirements for a framework to effectively and reliably repeat the capability to operate beyond visual LOS on other small UASs?

ii. What COTS components are required in a small UAS architecture to operate beyond visual LOS and how is the architecture integrated and validated?

iii. What are the hazards associated with beyond visual LOS operation and how can they be mitigated to achieve airworthiness approval?

1.4 Scope and Assumptions

The scope of this research is to establish and demonstrate the system architecture and design a prototype small UAS for the proof of concept to operate beyond visual LOS. This architecture will be portable to other platforms within the Group 1 or 2 UASs. A framework will be used to organize the development so that the process can be effectively and reliably repeated on other small UASs to operate beyond visual LOS.

To reduce development lead time, a readily available "*SIG Rascal 110*" will be used as the platform to seek airworthiness approval. The SOF assessment will be based on the FMECA of potential risk of the architecture and its corresponding mitigations. In the premise of this research, there will be a clear LOS (no blockage) for wireless signal between the UAV and the ground pilot. However, the research will also validate the approach to possible exceedance of transmission range associated with beyond visual LOS operation. This will be simulated by reducing the level of transmission power within the UAV and the GS. The design will be validated through progressive test flight to achieve the desired distance.

1.5 Methodology

The first part of this research focuses on the approach to address the investigative question. The second part of this research proceeds to identify the system specification and functional requirement for a UAS to operate beyond visual LOS. The system architecture will subsequently be integrated through test and validation.

The third part of the research will focus on mitigating the risks identified in the architecture through the use of the FMECA and establish the Bill of Material (BOM). In

the last part, the result from the test architecture will be analyzed and a final hazard assessment will be conducted before seeking acceptance of the residual risk.

1.6 Thesis Overview

Chapter 2 and 3 of the research cover the Literature Review and Methodology. The Literature Review chapter presents the background knowledge essential for this thesis. This includes classification of UAS, regulatory requirement for UAS operation, Budget Link analysis for signal transmission and the FMECA process. The chapter also presents related research on UAS architecture that extends operating range and/or improves flight control and safety. The Methodology chapter explains the approach to address the investigative question. It will also consolidate the requirements and processes to develop the system and build a framework which can be referenced for similar development in the future.

The next two chapters describe how the architecture was developed and how the hazard analysis was conducted. Chapter 4 includes the selection of key components, development of the physical architecture through FMECA and a hazard analysis of the designed system. The chapter will conclude with a BOM of the demonstrated architecture. Testing and verification results will be captured and analyzed in Chapter 5. Chapter 6 concludes this research with proposal for potential future work based on the insights gained.

II. Literature Review

Chapter 2 presents the background knowledge required to complete this thesis. The first portion defines the classification of military UAS and the necessary regulations that prescribes the requirements to operate an UAS beyond visual LOS. This is followed by the explanation on the FMECA process and Budget Link Analysis which was employed to ensure airworthiness of the system architecture. The second portion of this chapter describes research related to UAS architecture that extends operating range and/or improves flight control and safety.

2.1 Classification of Military UAS

The classification of the UAS is related to this research as it defines the system and performance specifications that set the boundary of this research. UAS are generally classified according to their weight and operating profile (Department of Defense, 2013; Ministry of Defence, 2010). However, the structure of classification and quantitative specification differs between different organizations. Figure 1 and Table 1 illustrates the UAS classification between two established Armed Forces, the United States Air Force (USAF) and the United Kingdom Royal Air Force (RAF) respectively. The comparison and application of the two classifications to define the requirements for the system design will be carried out in Chapter 3 of this research.

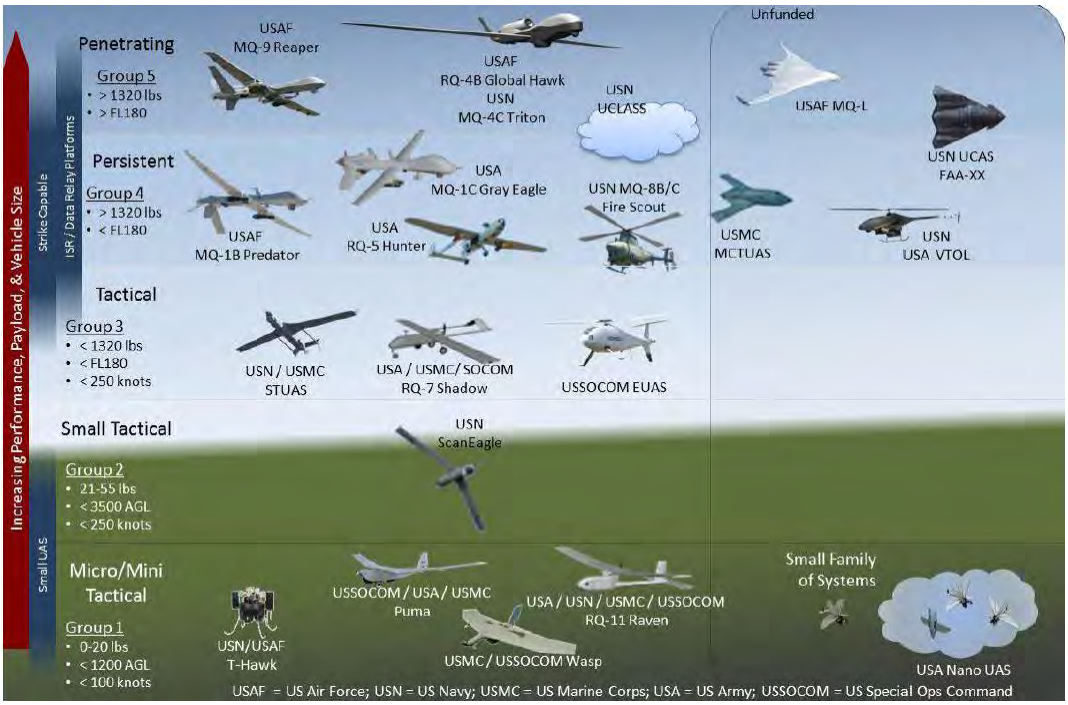

Figure 1. Classification of UAS by USAF (Department of Defense, 2013)

Table 1. Classification of UAS by RAF (Ministry of Defence, 2010)

UNMANNED AIRCRAFT CLASSIFICATION TABLE						
Class	**Category**	**Normal Employment**	**Normal Operating Altitude**	**Normal Mission Radius**	**Civil Category (UK CAA)**	**Example Platform**
Class I < 150 kg	MICRO < 2 kg	Tactical Platoon, Sect, Individual (single operator)	Up to 200 ft AGL	5 km (LOS[23])	Weight Classification Group 1 (WCG) Small Unmanned Aircraft (<20 kg)	Black Widow
	MINI 2-20 kg	Tactical Sub-Unit (manual launch)	Up to 3000' AGL	25 km (LOS)		Scan Eagle, Skylark, Raven, DH3
	SMALL > 20 kg	Tactical Unit (employs launch system)	Up to 5000' AGL	50 km (LOS)	WCG 2 Light UAV (20><150 kg)	Luna, Hermes 90
Class II 150 – 600 kg	TACTICAL	Tactical Formation	Up to 10,000' AGL	200 km (LOS)	WCG 3 UAV (>150 kg)	Sperwer, Iview 250, Hermes 450, Aerostar, Watchkeeper
Class III > 600 kg	MALE[24]	Operational/ Theatre	Up to 45,000' AGL	Unlimited (BLOS)		Predator A & B, Heron, Hermes 900
	HALE	Strategic/ National	Up to 65,000' AGL	Unlimited (BLOS)		Global Hawk
	Strike/ Combat	Strategic/ National	Up to 65,000' AGL	Unlimited (BLOS)		

2.2 Airworthiness Requirement for UAS

This section of the chapter covers the regulatory requirement on airworthiness for the conduct of flight test to validate the designed architecture.

2.2.1 Civil Airworthiness Requirement

The US civil regulatory requirement mandates a documented airworthiness approval by the Federal Aviation Authority (FAA) for an aircraft, manned and unmanned, to ensure that "it conforms to its type design and is in a condition for safe operation" (Code of Federal Regulation, 2011:14.21.1, 124).

The approval document is in the form of an Airworthiness Certificate. However, the existing certification requirement in the Code of Federal Regulation (CFR), Title 14 Chapter 21, was originally published for manned aircraft and the stringent requirements could not be fully complied by UAS (Maddalon et al., 2013:5). The FAA has submitted a proposed regulation with the aim to better integrate UAS into the National Air Space (Department of Transport, 2015). There is a section in the proposal that addresses the current deficiency in UAS certification requirements. Consequently, the research has to reference the proposed regulation to ensure that the system design fulfills relevant ensuing requirements.

Currently, the FAA only issues Special Airworthiness Certificates for UAS conducting 1) Research and Development, 2) Crew Training and 3) Market Survey (Department of Transport, 2015: 2,4). This research is focused on the UAS architecture

and not the development of a specific UAS design. Hence, a special airworthiness certificate from the FAA is not necessary.

To ensure airworthiness of the UAS in general, the FAA has implemented an interim airworthiness approval process. This interim approval process is in the form of a Certification of Approval (COA) and is determined by the UAS's intended use. UAS operated by individuals solely for recreational purposes are termed as model aircraft and will comply with regulations from its community based organization (United State Congress, 2012:77). When the intended use deviates from recreational purpose, such as public or civil applications, a FAA-issued COA is required for any operation within the National Air Space (Department of Transport, 2014). This requirement is also extended to commercial purposes.

The expected flight test to validate the system design is part of the research conducted under the Air Force Institute of Technology (AFIT). This placed the intended use under civil application. Consequently, a COA from the FAA is required for the test flight if it is conducted in the National Air Space. However, in the scope of this research, the test flights will be conducted in military controlled air space. Hence, a military approval instead of a COA is required.

2.2.2 Military Airworthiness Requirement

The Department of Defense (DoD) prescribes it airworthiness requirement in MIL-HDBK-516C, where it defines airworthiness as "the property of a particular air system configuration to safely attain, sustain, and terminate flight in accordance with the approved usage limits" (Department of Defense, 2008).

The USAF acknowledges that not all of its aircraft will be able to fully comply with the stringent airworthiness requirements stipulated in MIL-HDBK-516C (Department of Air Force, 2010). For these aircrafts, airworthiness was ensured through a Flight Release on a case by case basis (Department of Air Force, 2011). Hence, small UASs would normally be operated under a Military Flight Release (MFR).

The MFR is required for all USAF's small UASs prior to any flight regardless if it is to be flown in military controlled airspace or National Air Space. As an institution, AFIT has an internal Technical and Safety Review Board (TRB/SRB) to accept the residual risks associated with the flight test of an UAS with a valid MFR (Air Force Institute of Technology, 2014). Formal acceptance of the residual risk is recorded through the AFIT Document 5028. The TRB/SRB will be convened prior to each test flight.

In summary, to conduct a UAS test flight, regulatory approval must first be sought through a MFR. Thereafter, the residual risk of the system design in a flight test will be approved by the AFIT TRB/SRB. If the flight is conducted outside military controlled airspace, a COA is required.

2.3 Failure Mode Effect and Criticality Analysis

FMECA is a reliability evaluation technique which examines the potential failure modes within a system and its equipment in order to determine the effects on equipment and system performance. Each potential failure mode is classified according to its impact on mission success and personnel/equipment safety. The FMECA is composed of two separate analyses, the Failure Mode and Effect Analysis (FMEA) and the Critical Analysis (CA) (Department of Defense, 1993).

The MIL-STD-1629 (Department of Defense, 1980) that prescribes the FMECA process for the DoD was rescinded in 1984. However, the procedure was generally carried forth and remained widely employed during the development process to ensure reliability of military and industry systems (Department of Defense, 1993). The indicative procedure in MIL-STD-1629 comprised of five major tasks.

i. Perform FMEA to identify effect of item failure on system operation and classify each potential failure according to its severity.
ii. Perform CA to rank each potential failure mode identified in the FMEA according to combined influence of severity classification and its probability of occurrence.
iii. Document procedure for performing FMECA-Maintainability Analysis. This supplies the criteria for Maintenance Planning Analysis, Logistic Support Analysis and identifies maintainability design features that require corrective action.
iv. Document the procedure for performing a Damage Mode and Effects Analysis. This provides early criteria for survivability and vulnerability assessments.

v. Document the procedure for developing a FMECA plan for contractors' compliance.

A comprehensive FMECA would include all five tasks prescribed in MIL-STD-1629. However, the research only seeks to develop the UAS architecture and does not aim to produce a system to be fielded for actual operation. Hence, the focus will only be on the first two tasks which analyze the potential failure modes and its impact to mission success.

2.4 Link Budget Analysis

Similar to manned aircrafts, UAS are operated in three modes, "Manual", "Assisted Fly-By-Wire" (commonly known as "Stabilized") or "Autonomous". The key difference is the presence of an onboard Auto-Pilot (AP) computer in the second and third mode. The majority of UASs use Radio Frequency (RF) to transmit data wirelessly (Gundlach, 1975: 472) for all 3 modes of operation. These data include telemetry on (generally) health and status, payload data, and Command and Control (C2) data. Proper control of the UAS depends on uninterrupted RF communication between the UAV and GS.

The "*SIG Rascal 110*" was designed for operation within visual LOS. Extending the range beyond visual LOS requires an analysis to verify that the RF communication link between the air vehicle and the GS remains uninterrupted. Link budget is the primary communication system analysis tool used to determine whether the communication will be reliable (Gundlach, 1975: 475). The signal strength measured at the receiver is expressed as below (Gundlach, 1975: 476).

$$Si = P_T G_T L_T L_P G_R L_R \left(\frac{\lambda}{4\pi R}\right)^2 \quad (1)$$

Si = Signal Strength
P_T = Transmitter Power
G_T = Transmitter antenna gain
L_T = Transmitter loss
L_p = Propagation loss
G_R = Receiver antenna gain
L_R = Receiver losses
λ = Wavelength of carrier signal
R = Separation distance

Converting the Equation (1) for received signal strength to decibel (dB), and rearranging them based on separation distance, the following equation (Gundlach, 1975: 483) is derived:

$$R < 10^{0.05[\text{EIRP} - \text{Psensitivity} + \text{Lp,Atm} + \text{Lp,Precip} - 20\log10(fMhz) + 20\log10(0.3/4\pi) + G_R + L_R - L_M]} \quad (2)$$

R = Range (Km)

EIRP = Effective Isotropic radiate Power

$$= P_T + G_T + L_T (\text{dBm}) \quad (3)$$

$P_{Sensitivity}$ = Receiver sensitivity (dBm)

$L_{p,Atm}$ = Propagation loss to atmosphere absorption (dB)

$L_{p,Precip}$ = Propagation loss to precipitation absorption (dB)

$20\log10(f\text{Mhz}) + 20\log10\left(\frac{0.3}{4\pi}\right)$ = Free space loss (4)

$G_{R(\text{dbi})}$ = Receiver antenna gain (dBi)

$L_{R(\text{db})}$ = Receiver losses (dB)

L_m = Link margin (dB)

P_T = Transmitter Power (dBm)

G_T = Transmitter antenna gain (dBi)

L_T = Transmitter loss (dB)

The maximum range is determined by four components, 1) Transmission, 2) Propagation, 3) Reception and 4) Link Margin. Transmission is measured in terms of EIRP and is comprised of transmitted power, transmitter antenna gain, and losses within the transmission system. Propagation loss is attributed to the environment and combination of losses due to free space, atmospheric absorption and precipitation absorption. The reception is determined by the sensitivity of the receiver antenna, receiver antenna gain and losses within the receiver system. Lastly, Link Margin is introduced to buffer real-time variation in the signal-to-noise ratio.

2.4.1 Electric Field Strength Conversion

Radiated emission can be described by many means. One of the ways to describe radiated emission is through the electric field strength measured at some distance from the radiators. Understanding of the electric field strength is important as the emission limit in the regulation (Code of Federal Regulation, 2009; 810) is prescribed in this mean. Electric field strength is measured with the following equation (Ghasemi et al., 2012;40);

$$E = \frac{\sqrt{30 * P}}{D} \quad (5)$$

E = Electric field strength (V/m)

P = Transmitted power (W)

= $P_T * G_T$ (6)

D = Distance (m)

2.5 Related Research

This thesis referred to a series of research that are related to the architecture design of a small UAS. Beyond LOS operation of small UAS has been explored using means of relay nodes to maintain the RF communication link around an obstacle (Seibert et al., 2010). Although the aim is not the same as this research, the system architecture from the earlier effort can potentially be adopted to extend the range to safely operate the UAS beyond visual LOS.

In the mentioned research, a second UAS was used to relay the telemetry and image data from the primary UAS to the GS. The relay UAS is configured slightly differently from the primary UAS, such that, it does not have a camera system but is installed with an additional modem and image data receiver. The image data receiver was a modified from the image data transmitter by adding a form factor receiver.

C2 data, including telemetry data, for the AP computer is transmitted in the 915 MHz frequency band with 1 W power. Due to a limitation in the hardware, the relay UAS receives the C2 data link from the primary UAS though one modem and thereafter relays it from another modem that is operating in a different channel. The dual modem on the relay UAS was subsequently reduced to one with availability of new and more capable

modem hardware. The telemetry Image data is transmitted in the 2.4 GHz frequency band and 1 W power. It is similarly received through a receiver and relay through another transmitter operating in a different channel.

Key components in the architecture include the "*Virtual Cockpit*" software which provides the user interface for the operators on the ground with the "*Kestrel™ autopilot*" on board the UAV. The C2 data link is initially transmitted through the "*DIGI XTend®*" modem which was subsequently replaced by the more capable "*MICROHARD*" modem. Image data is received by the "*Yellow Jacket*" receiver on the ground. However, additional detail on the airborne transmitter was not documented.

As a follow-on to the research in 2010, the same architecture was modified to incorporate autonomous cooperative control on the relay UAS (Shuck, 2013). The architecture was also extended from the original UAV platform, "*OWL*", to a larger "*SIG Rascal 110*". The new architecture was developed with changes to several of the key components. The "*Yellow Jacket*" receiver for image data were retained but the user interface software has been changed to "*Mission Planner*". The onboard AP has also been changed to "*Ardupilot Mega autopilot*". The frequency for the C2 data link remained in the 915MHz band using the "*DIGI XBee-Pro® 900*" with 50mW power. The Image data link was transmitted from the UAV through a 600 mW transmitter in 5.8 GHz.

2.5.1 Autopilot Computer

The general working principle of a COTS AP computer was explained in a research where an AP computer was designed for a small UAS (Christiansen. 2004; Seibert et al., 2010). The researcher explained the working principles of the AP in maintaining a stabilized flight towards a set coordinate way point. This mode of operation that does not involve active input of flight control command by the ground operators is called autonomous flight.

Flight heading and profile towards set waypoints are maintained and/or corrected by the AP computer by controlling the motor and servos. Control signals for the servo and motor are generated through the Proportion-Integral-Derivative (PID) feedback controller function in AP computer with inputs from the various sensors and GPS signal. The enhanced understanding on the AP computer board helps to better identify the failure mode and its effect on the system architecture although the same component may not be employed.

In this research, the "*Pixhawk autopilot*" was selected. The aforementioned AP computer shares the same developer as the "*Ardupilot Mega autopilot*" and was based on the firmware and software of the latter (3DR, nd). The "*Pixhawk autopilot*" was selected as it offers more capabilities over its predecessors. These include dual power supply, more accurate position estimation and redundant sensors. At the same time, application knowledge with the "*Ardupilot Mega autopilot*" from earlier research can also be employed due to similarity of firmware and software.

2.5.2 Mission Planning Software

The mission planning software provides user interface and translates mission plans into correct actions to be executed by the Air Vehicle. Basic mission plan are way-points and flight profile that the Ground Operator prescribes for the Air Vehicle. Application and operation knowledge on *"Mission Planner"* has been gained through recent research. In particular, knowledge in integration with flight simulation software and "*Ardupilot Mega autopilot*" has facilitated Hardware in the Loop testing of flight under laboratory condition.

2.5.3 RF Transceivers

The theoretical range of the RF C2 data link with the "*MICROHARD*" modem at 1 W transmission power was calculated to approximately 4.3 km (14,000 ft) (Seibert et al., 2010). With the same transmission power of 1W, the "*RFD 900+*" modem was reviewed for this research. The "*RFD 900+*" possesses several features that were not available on the modems used in earlier research. These include spread spectrum frequency hopping, dual diversity (two antennas) and network capability between multiple modems. The added features may potentially be exploited to enhance the transmission in a given range or increase it beyond what was calculated in earlier research.

2.5.4 Long Range Flights

The "*SIG Rascal 110*" has been successfully flown in an earlier AFIT research to develop autonomous flight (Jodeh, 2006) but was conducted within visual LOS. The tested system architecture of the design will form the basis in this research where it is reviewed and further improved through a FMECA.

Recreational application of Small UAS has been known to transcend visual LOS through First Person View (FPV) operation beyond a range of 40 km (Team BlackSheep, 2010; Montiel, 2011). The system setup for the recreational models that were discussed in online forums was also referenced during the development of the architecture. It is noteworthy to highlight that this research did study if the recreational FPV that operated beyond visual LOS has obtained the relevant regulatory approval.

A key characteristic of long range FPV flights is the use of low frequencies to increase the range. For FPV operation at 43 km, the RC data link was communicated with the "*EzUHF 433MHz*" transceiver system at 600 mW and the Image data link was broadcasted in 2.4 Ghz at 500 mW (Team BlackSheep, 2010). The range of 55 km was achieved with the "*Thomas Scherrer LRS*" transceiver system which also communicates in 433 MHz but at a power of 500 mW. The Image data link was broadcasted at 1.3 GHz frequency with 1.5 W (Montiel, 2011).

2.6 Summary

In this chapter, the background knowledge required to complete this thesis was discussed. The UAS classification which prescribes the performance and system specifications was presented. This was followed by an elaboration of regulatory requirement to test a UAS in flight. Thereafter, the FMECA process and the Link Budget analysis used in the research were explained. Lastly, the research on related efforts to this thesis revealed that previous works shared some common functionality. However, there is no similar work with the aim of developing the architecture of a small UAS that can operate beyond visual LOS using COTS components.

III. Methodology

Chapter 3 delves into the approach to answer the investigative question in the research. The research framework was developed through the use of System Engineering methods. Thereafter, the framework is employed to address the two remaining questions on designing the architecture and analyzing the hazards to validate the SOF of the UAS.

3.1 Research Framework

A Framework is defined as "a document that describes useful methods, practices and procedures for developing Architecture Descriptions. …, it involves a structured tool, methodology, interconnections and standardization that guide what to produce and how to construct them" (Ford, 2014).

The DoD System Engineering Process (SEP) is applied iteratively, adding additional detail and definition with each application (Department of Defense, 2015). In a project development, several SEPs are employed in parallel across the development for each subsystem and thereafter vertically throughout the development to integrate the subsystems. The scale of development for this research is relatively small; hence, a single SEP is adequate. This section of the chapter discusses how the DoD SEP was adopted to create a framework for the conduct of this research. The aim is to document the research process so that it can be reproducible in future applications.

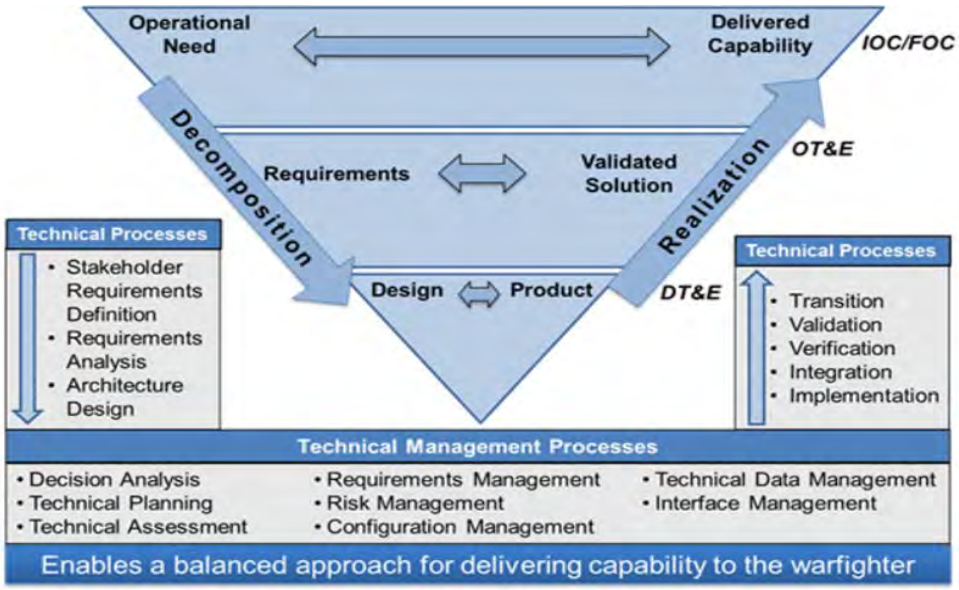

Figure 2. DoD System Engineering Process (Department of Defense, 2015)

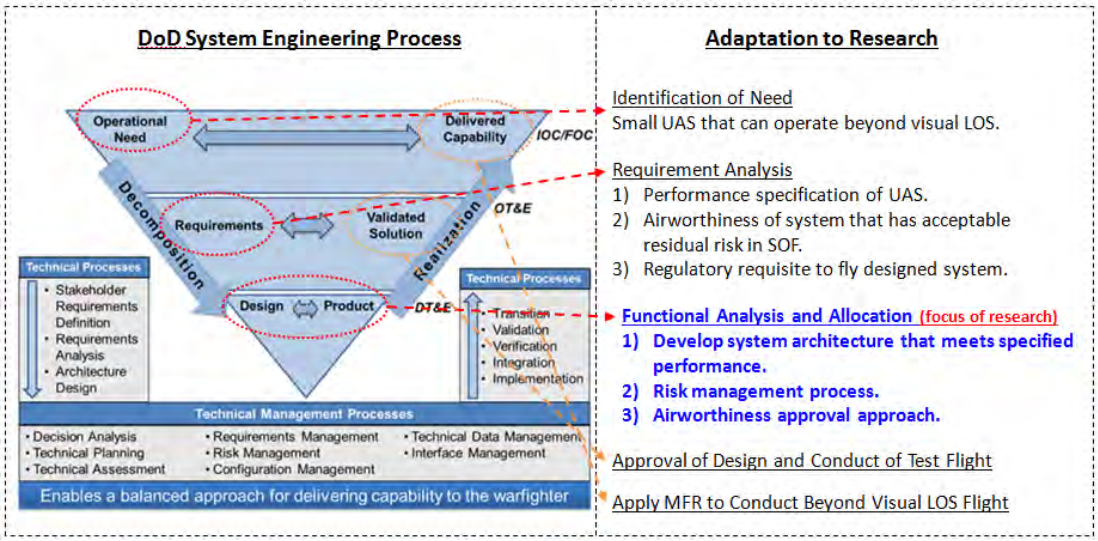

Figure 3. Adaption of DoD System Engineering Process

The process is initiated after the identification of a Need, see Figure 2. In Step 1, an Analysis of Requirement is conducted to define the requirements of the 'solution' system that will fulfill the identified Need. In Step 2, the defined Requirements are translated into functions. This is done through a Functional Analysis on what the

'solution' system needs to carry out. In Step 3, the functional architecture developed from the preceding level is synthesized into a physical system. Step 4 is will seek approval for the design and thereafter validate it though flight test. The process finally ends with the application of a new MFR to operate beyond visual LOS. Figure 3 maps the adaption of the DoD System Engineering Process to this research.

Figure 4 illustrates the complete framework that was used for this research. Development on the system architecture begins after the requirements to fulfill the needs identified in Section 1.1 are defined. The needs are, to develop a UAS that is 1) small in size, 2) operates beyond visual LOS and 3) is low in cost. Objective 1 and 2 will be translated into requirements after the specification are defined in Chapter 4. Objective 3 will be quantified at the end of Chapter 4 and compared against a same size UAV using the empty weight cost of the "*Dragon Eye*".

Specification to the requirement in terms of size and operating profile is based on the classification to military UAS. This will be elaborated in Chapter 4 of the research. The empty weight cost of the designed system will also be compared against the published cost of the "*Dragon Eye*" system to establish the relative affordability in the event that the system is lost in an operation.

The remaining investigative questions of this research are associated with the architecture and air worthiness validation of the system. In the development framework for this research, these correspond to the three elements in the Functional Analysis and Allocation level. Hence, emphasis was placed on the details of the three elements in that level and is documented in the following section of this chapter.

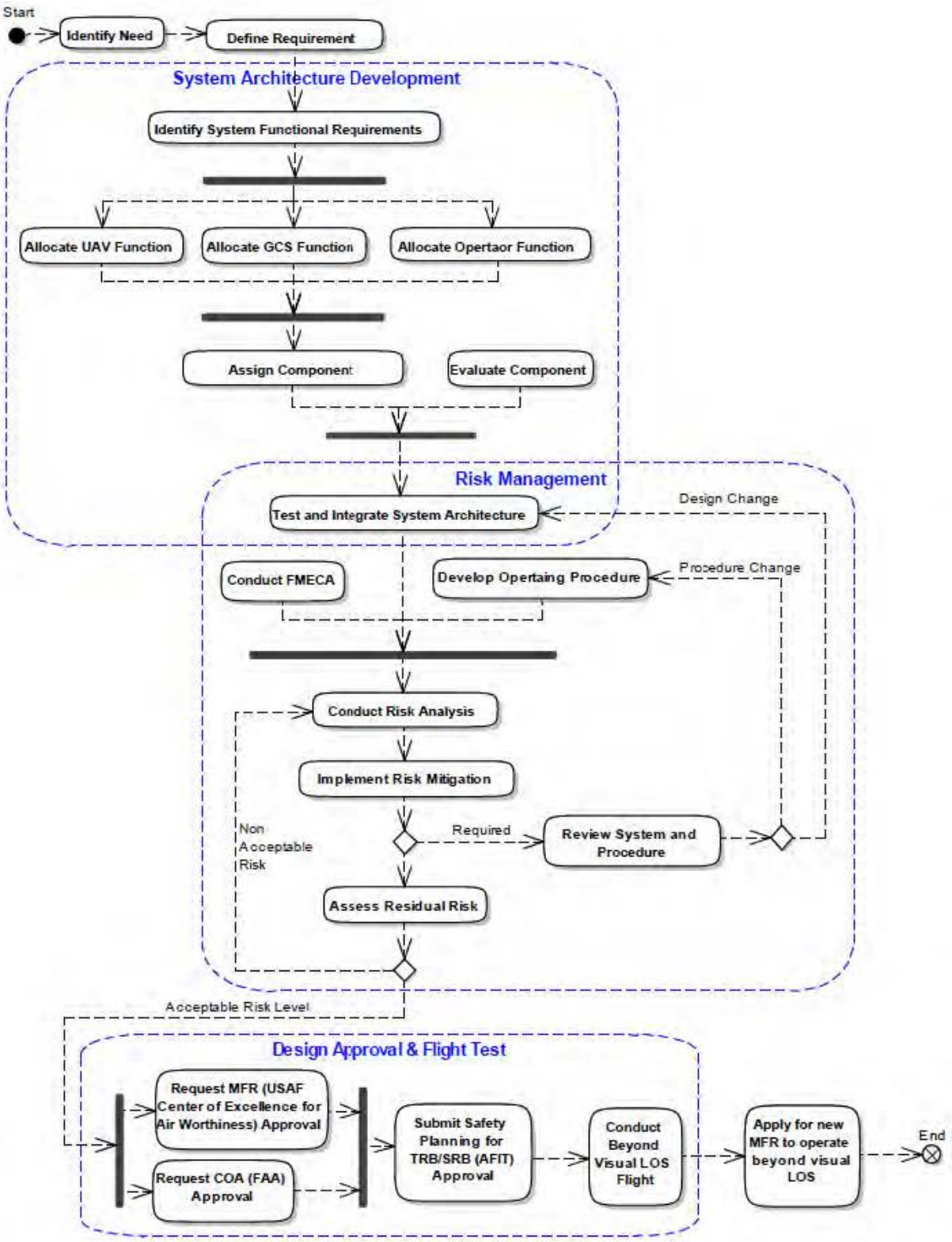

Figure 4: Development Framework for UAS to Operate Beyond Visual LOS

3.2 System Architecture Development

Architecture is defined as "fundamental concepts or properties of a system in its environment embodied in its elements, relationships, and in the principles of its design and evolution" (ISO/IEC/IEEE, nd). Documenting the architecture of the designed system as part of the research framework will facilitate future application or modification.

Development on the system architecture begins after the requirements to fulfill the identified needs have been defined. These requirements are then translated into functions and allocated to the three major sub-systems of the UAS. The allocated functions are subsequently decomposed until it can be performed by a physical component. Thereafter, testing and evaluation are carried out to ensure the multitude of components is properly integrated.

An earlier research effort in AFIT has successfully developed, and autonomously flown a "*SIG Rascal 110*" UAV (Jodeh, 2006). Figure 5 shows the system architecture developed in the previous research effort. However, it is observed that the documented architecture focused only on the communication linkage and was incomplete as a system with key components such as the motor not being included in the diagram. Available fail-safes are also not documented in the architecture definition. Hence, a new architecture has to be designed for this research.

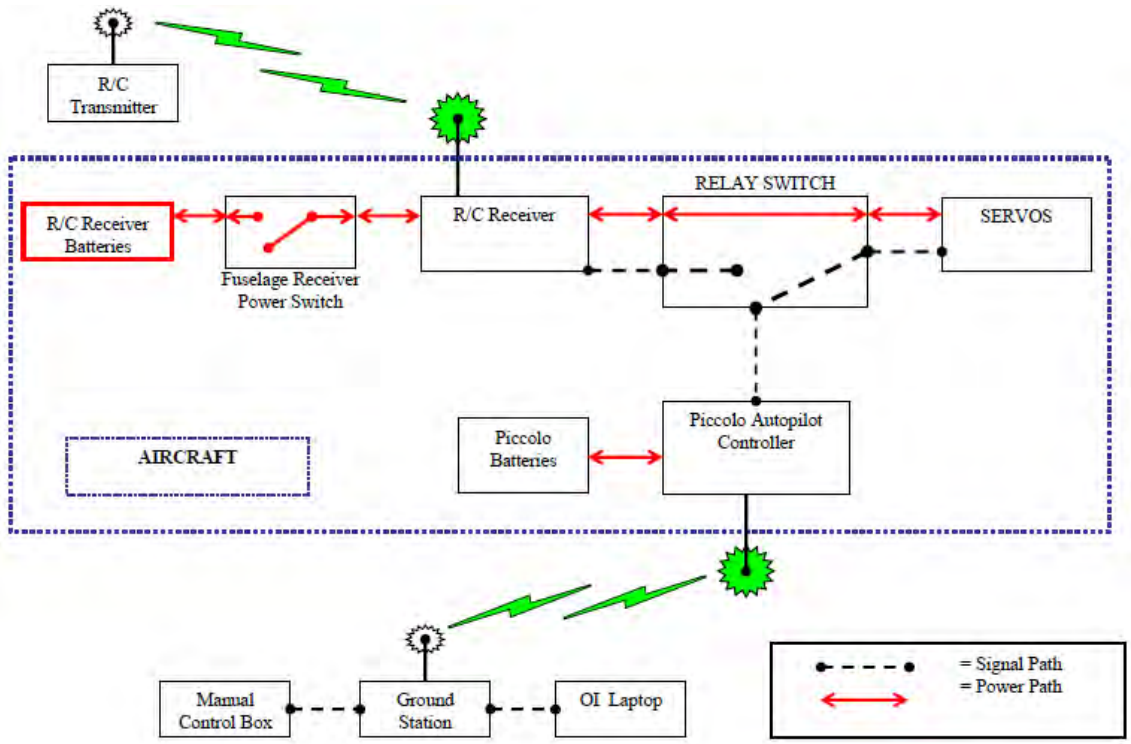

Figure 5. Communication Architecture of Autonomous "*SIG Rascal 110*" (Jodeh, 2006)

The functional requirements of the system are allocated to sub-systems in the designed architecture and progressively decomposed until a physical component can be assigned. This research aims to develop a comprehensive architecture that encapsulates all the components in the design. In addition, it will also document the relationship between the components by indentifying all the information and resource flowing between the component interfaces. Tests will be conducted to verify component capabilities that are critical in fulfilling the defined requirements. One such example is the verification to ensure that the system can operate in an increased range that is beyond visual LOS.

3.3 Risk Management

Risk is the potential for a negative future reality that may or may not happen. It is defined by the probability of occurrence and the consequences of occurrence (Department of Defense, 2001: 133). Risk management is the organized method to identify and measure, thereafter to handle the risk. (Department of Defense, 2001: 134). Similar to the system architecture, documenting the risk management process as part of the research framework will facilitate future application or modification.

Past UAS research efforts in AFIT were focused on the technical development of new capabilities and did not conduct a FMECA for the risk analysis on their systems (Jodeh, 2006; Seibert et al., 2010; Shuck, 2013). In addition, operating beyond visual LOS has considerations that may not be applicable in normal visual LOS operation. The architecture shown in Figure 5 has a dual redundancy on the wireless control input to the aircraft. However, it is evident that the relay switch will be the single point of failure to all the servos in the system. The consequence associated with the relay switch failure has to be analyzed to determine if it is acceptable when the aircraft is operated beyond visual LOS.

The recursive risk management approach carried out in this research to ensure airworthiness of the system is shown in figure 4. The potential hazards of the system architecture are evaluated through the use of FMECA where the outcome of possible failure mode of each component is analyzed. Mitigations through design improvement and contingency procedures were subsequently put in place to reduce the probability or consequence of occurrence. With the design improvement and procedural mitigations in

place, a final risk assessment is conducted to assess if the residual risk is within acceptable level.

3.4 Incremental Flight Testing

As part of the risk management approach, key functions of the designed system are individually validated through flight testing. This is carried out using the existing MFR to operate a "*SIG Rascal 110*" UAS within LOS. After finalizing the design, an initial flight test will be carried out to test the key features. Thereafter, progressive testing will be designed to gradually increase the range of the flight test until it achieves the requirement to operate beyond visual LOS. The latter flight tests will not be carried out due to constraints on the research duration.

3.5 Design Approval

Following the final risk assessment, the system architecture will be compiled with the operating procedures as a part of the Safety Plan which will be reviewed by AFIT's TRB/SRB for approval. Following AFIT's endorsement, the designed system will be submitted for COA and MFR approval.

3.6 Summary

This chapter described the framework that will be used to develop a small UAS that can be operated beyond visual LOS. A risk analysis will be conducted on the system architecture before it is submitted, together with the operating procedures, for approval. The documented framework and system architecture can be applied to facilitate efficient reproducibility of this development for future research.

IV. System Architecture and Risk Management

Following the processes illustrated in Figure 4, Chapter 4 begins by defining the specification that determines the requirements for the system architecture. This is followed by the development of the system architecture together with the risk management process to ensure airworthiness

4.1 Specification of Requirements

The specification of the requirements in terms of weight and operating profile used in the research were referenced to existing UAS classification in USAF and RAF. Adaptations were made to customize the specification from the two classifications.

4.1.1 Weight Requirement

Table 2 summarizes the difference in the weight classification of the UAS between the USAF and RAF that was previously illustrated in Figure 1 and Table 1 respectively.

Table 2. Classification of UAS Weight in USAF and RAF

<table>
<tr><th>Weight [lbs]</th><th colspan="2">USAF</th><th colspan="2">RAF</th></tr>
<tr><td>< 4.4</td><td rowspan="2">Group 1</td><td rowspan="2">Micro/Mini</td><td rowspan="4">Class I</td><td>Micro</td></tr>
<tr><td>< 20</td><td rowspan="2">Mini</td></tr>
<tr><td>< 44</td><td rowspan="2">Group 2</td><td rowspan="2">Small Tactical</td></tr>
<tr><td>< 55</td><td rowspan="2">Small</td></tr>
<tr><td>< 330</td><td rowspan="2">Group 3</td><td rowspan="2">Tactical</td></tr>
<tr><td>< 1,320</td><td>Class II</td><td>Tactical</td></tr>
<tr><td rowspan="3">> 1320</td><td>Group 4</td><td>Persistent</td><td rowspan="3">Class III</td><td>Medium Altitude Long Endurance</td></tr>
<tr><td rowspan="2">Group 5</td><td rowspan="2">Penetrating</td><td>High Altitude Long Endurance</td></tr>
<tr><td>Strike/Combat</td></tr>
</table>

The size of a UAS is associated with its weight in both the USAF and RAF classifications. However, there are notable differences between the two classifications for UAS that weigh below 330 lbs. The USAF classification of a 'small' (tactical) UAS weighs less than 55 lbs while the classification of 'small' UAS in RAF can weigh up to 330 lbs (150 kg).

This research aims to develop a small UAS that can be operated beyond visual LOS, but at the same time, is inexpensive so that it is expendable in an operation. Hence, the comparatively lower weight limit, and its corresponding cost, of the 'small' UAS in the USAF's classification make it more appropriate for the scope of this research. The maximum weight of the USAF's Group 2 Small Tactical UAS is 55 lbs with an estimated empty weight cost up to $550,000. However, the Group 2 Small Tactical UAS in the USAF classification does not adequately differentiate the limit at the lower end of the weight range. The lower weight limit of Group 2 small UAS at 21 lbs is relatively high. Consequently, the minimum weight of 4.4 lbs from the RAF Class I Mini UAS classification was integrated to the USAF Group 2 UAS in the weight specification for this research. This adaptation also recognizes the need of micro technology that is required for miniature UAS which separates its development from the small UAS.

In summary, the applicable weight range for this architecture is between 4.4 to 55 lbs. This weight range is also consistent with the FAA's definition of small UAS (Department of Transport, 2015). The empty weight of "*SIG Rascal 110*" is 11 lbs and is appropriate to serve as the base platform in this research.

4.1.2 Operating Profile Requirement

The UAS classification in the USAF and RAF was previously illustrated in Figure 1 and Table 1 respectively. Table 3 and Table 4 summarized the difference in altitude and operating range of the established Air Forces.

Table 3. Classification of UAS Operating Altitude in USAF and RAF

Altitude [ft]	USAF		RAF	
< 200	Group 1	Micro/Mini	Class I	Micro
< 1,200				Mini
< 3,000	Group 2	Small Tactical		
< 3,500				Small
< 5,000	Group 3 & 4	Tactical/ Persistent		
< 10,000			Class II	Tactical
< 18,000			Class III	Medium altitude Long Endurance
< 45,000	Group 5	Penetrating		
< 65,000				High altitude Long Endurance
				Strike/Combat

Table 4. Classification of UAS Operating Range in RAF

Range [km]		RAF	
5 km (16,400 ft)	LOS[1]	Class I	Micro
25 km (82,000 ft)	LOS		Mini
50 km (164,000 ft)	LOS		Small
200 km (656,000 ft)	LOS	Class II	Tactical
Unlimited	Beyond LOS	Class III	Medium Altitude Long Endurance
Unlimited	Beyond LOS		High Altitude Long Endurance
Unlimited	Beyond LOS		Strike/Combat

From the two tables, it is observed that the operating profile is directly related to the weight of the UAS. From Table 3, the maximum operating altitude, for the identified USAF Group 2 UAS is 3,500 ft above sea level. However, the operating range for the

[1] The definition of LOS in the RAF classification is RF LOS and not visual LOS.

USAF UAS classification was not published. The operating range is published in the RAF classification, but it is referenced to RF LOS and not visual LOS. Hence, it cannot be adopted directly.

From previous research, the "*SIG Rascal 110*" can be safely operated in "Manual mode" at a distance of 1,000 ft (≈ 305 m) at an altitude of 200 ft without visual aid. Visual LOS can be maintained up to a distance of 2,000 ft (≈ 610 m) when operating in "Autonomous mode". The "*SIG Rascal* 110" weighs 11 lbs and has a wing span of 9.2 ft (SIG Rascal Specification, nd). Depending on size, the distance is increased if a larger UAV is employed. For this research, the target was set to extend the range, to five times that of visual LOS, up to 10,000 ft (≈ 3,050 m). A safety factor of 30 % was further added into the target which brings the range to 13,000 ft (≈ 4 km).

4.2 System Architecture Development

In this section, the functional requirements of the system are identified and allocated to various sub-systems of the architecture to be designed. Thereafter, the functional allocation is progressively broken down until physical components can be assigned to fulfill requirements.

4.2.1 Identifying and Allocating System Functional Requirements

A typical UAS setup (Shuck, 2013:32; Diamond et al., 2009:66; Seibert et al., 2010:38) was adopted for the research. This setup includes an Air Vehicle, a Ground Station and Ground Operators. See Figure 6 for typical setup.

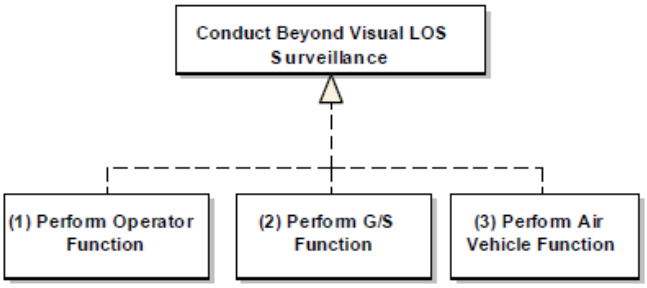

Figure 6: Allocation of System Functional Requirements

In the setup, Ground Operators will conduct mission planning and upload the mission plans into the GS. Thereafter, they will control the UAS from the GS. In addition, the Ground Operators will also be responsible for executing established operating procedures in the event of a contingency.

The GS receives mission plans, processes them into command signals and transmits it to the Air Vehicle. Simultaneously, it receives telemetry data from the Air Vehicle, processes and displays them to the Ground Operators. This data is also stored for future reference. The functional allocation for the GS is decomposed in the Figure 7.

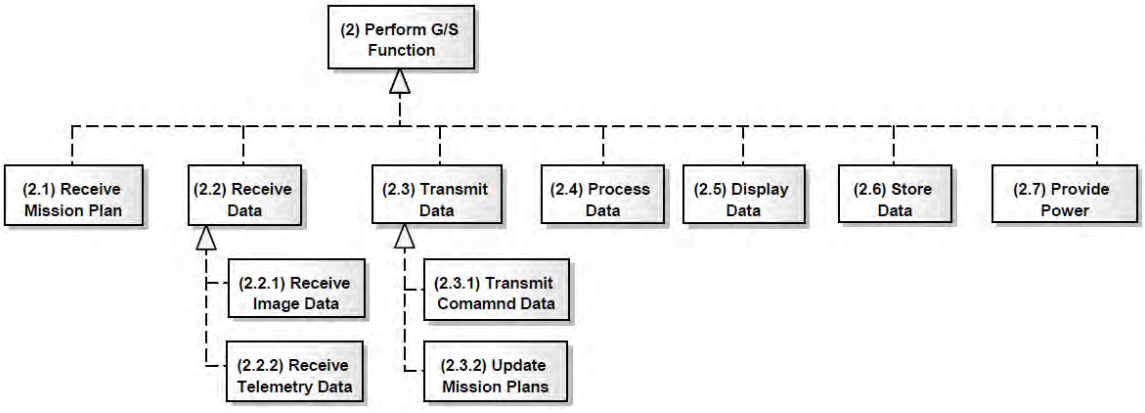

Figure 7: Allocation of System Function for GS

The Air Vehicle will carry the mission payload and fly towards the designated waypoints while monitoring essential onboard data. It transmits telemetry and image data to the GS for monitoring while simultaneously receiving command signals from the GS. Lastly, the Air Vehicle must be capable of receiving GPS signal to establish the system's geographic location. The decomposed functional allocation for the Air Vehicle is illustrated in Figure 8

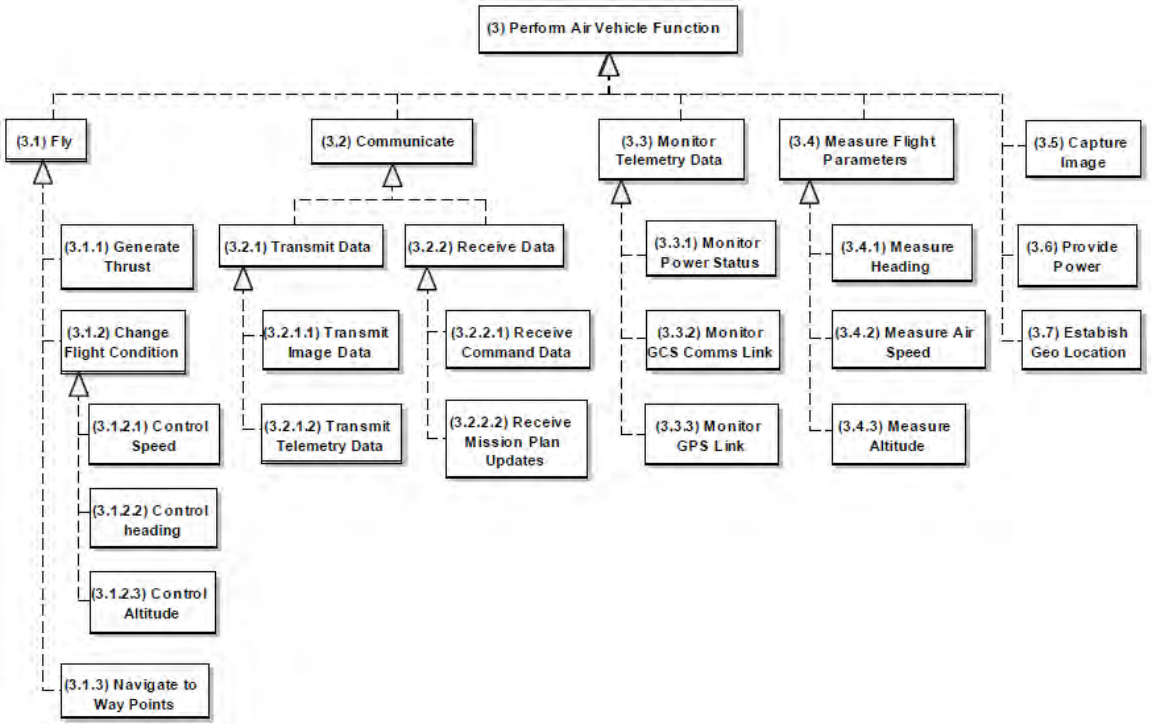

Figure 8: Allocation of System Function for Air Vehicle

4.2.2 Assigning Components to Allocated Function

COTS components were assigned to fulfill the decomposed functions for the subsystems in Figure 7 and Figure 8. See following table for assignment of components to decomposed functional requirement. Key components are evaluated in the next section to ensure that the assigned components can fulfill the allocated functional requirement.

Table 5. Component Assignment for Allocated Functions

Sub System				Functional Requirement	Component Assigned
GS	2.1			Receive Mission Plan	Laptop
	2.2	2.2.1		Receive Image Data	RF Transceiver
		2.2.2		Receive Telemetry Data	RF Transceiver
	2.3	2.3.1		Transmit Command Data	RF Transceiver
		2.3.2		Update Mission Plan	RF Transceiver
	2.4			Process Data	Mission Planning Software
	2.5			Display Data	Laptop
	2.6			Store Data	Laptop
	2.7			Provide Power	Lithium Battery
Air Vehicle	3.1	3.1.1		Generate Thrust	Motor + Propeller
		3.1.2	3.1.2.1	Control Speed	Electronic Speed Controller
			3.1.2.1	Control Heading	Servos to Flight Control Surface
			3.1.2.1	Control Altitude	Servos to Flight Control Surface
		3.1.3		Navigate to Way Points	AP Computer
	3.2	3.2.1	3.2.1.1	Transmit Image Data	RF Transceiver
			3.2.1.2	Transmit Telemetry Data	RF Transceiver
		3.2.2	3.2.2.1	Receive Command Data	RF Transceiver
			3.2.2.2	Receive Mission Plan Updates	RF Transceiver
	3.3	3.3.1		Monitor Power Status	AP Computer
		3.3.2		Monitor GS Comms Link	AP Computer
		3.3.3		Receive GPS Data	AP Computer
		3.3.4		Monitor Flight Parameter	AP Computer
	3.4	3.4.1		Measure Heading	Magnetic Compass
		3.4.2		Measure Air Speed	Pitot-Static Sensor
		3.4.3		Measure Altitude	GPS
	3.5			Capture Image	Camera System
	3.6			Provide Power	Lithium Polymer Battery
	3.7			Establish Geo Location	GPS

4.2.3 Evaluation of Components

Key components for the functional allocation are 1) Mission Planning Software, 2) RF Transceiver, and 3) AP Computer. The mission planning software and AP computer influence the overall system capability while the RF transceiver determines the operating range. Evaluation was conducted on these three components to ensure that the designed system meets the specified requirement in terms of range and SOF.

COTS RC aircraft can be procured at different stages of assembly, ranging from bare fuselage to Ready-to-Fly kit. With a bare fuselage kit, the suppliers would readily recommend the minimum specifications for the basic components on the air vehicle. These recommendations include sizing of the servos (torque requirement), motor (power requirement) and propeller (pitch and diameter requirement). For Ready-to-Fly kit these basic components are packaged with the fuselage. In this research, the basic components were selected based on previously flown "*SIG Rascal 110*" in earlier AFIT research. Consequently, evaluation of these three components was not required.

Battery size is related to voltage and amperage capacity. The required battery size is dependent, in part, on the voltage requirement of the motor and intended duration of the system. This research will only ensure that the selected battery can supply the required voltage to safely drive the motor. Specific amperage capacity of the battery is not established as operating duration may change as different missions require. This will be determined separately after the mission is defined. The research will instead measure the rate of amperage utilization to provide a baseline to scale the battery capacity according to the desired duration for future application. This will be documented in Chapter 5.

GPS, magnetic compass and the pitot-static sensor have singular functions unlike the mission planning software and AP computer. In addition, differences in specifications for these components will only affect the accuracy in the geo-location, air speed and altitude of the air vehicle which do not have a direct impact on the capability, unlike the

RF transceiver. Hence, compatible pitot-static sensor and GPS with integrated magnetic compass are taken from COTS selection without detailed evaluation.

Mission Planning Software

Central to the GS is the software that can translate mission plans into correct actions to be executed by the Air Vehicle. Basic mission plans consists of way-points and flight profiles that the Ground Operators prescribe for the Air Vehicle. Several models of COTS software are available in the market that can fulfill this function. Earlier research conducted in AFIT achieved autonomous UAS flight by employing either "*Mission Planner*" (Shuck, 2013:26; Seibert et al., 2010:164) or "*Virtual Cockpit*" (Diamond et al., 2009:66).

"Mission Planner" will be adopted for this research as it is used in more recent research and more importantly, it is compatible with "*Pixhawk autopilot"*. Care was taken when interfacing the selected software and hardware. "*Mission Planner"* is only compatible with Windows Operating System. Hence, the accompanying laptop in the GS must be running on the Windows Operating System. In addition, configuration management should also be maintained for the software versioning of *"Mission Planner"* as a new version may not be fully backward compatible with the flight firmware in the autopilot computer.

RF Transceiver

Wireless transmission is achieved by modulating the data onto a high frequency carrier signal. A transceiver system is comprised of a modem and an antenna which transmits and receives modulated signals at the same time.

Based on the Link Budget Analysis in Section 2.4, transceiver frequency and power output are two of the factors that determine the transmission range. The spectrum usage for radio frequency is regulated and differs between countries. Considerations have to be taken in selecting the legal frequency spectrum that will be used for various functions on the UAS. In the USA, RF spectrum usage is regulated by the National Telecommunications and Information Administration (NTIA). Prior to selection, the frequency of the intended transceiver should be verified against the Code of Federal Regulation for restrictions (Code of Federal Regulation, 2009: 808) and Spectrum Allocation Chart by NTIA (National Telecommunications and Information Administration, 2011) for possible interference.

Apart from frequency usage, the transmission power is also regulated to reduce interfaces to users of the electromagnetic spectrum (Code of Federal Regulation, 2009: 810). The following table shows the regulated limits to the transmission power at various frequencies.

Table 6: Limits of Transmission Power at Various Frequencies (CFR, 2009: 810)

Frequency (MHz)	Field Strength (μV/m)	Measurement Distance (m)
0.009 – 0.49	2,400/F (kHz)	300
0.49 – 1.705	2,400/F (kHz)	30
1.705 – 30	30	30
30 – 88	100	3
88 – 216	150	3
216 – 960	200	3
Above 960	500	3

Using Equation (5), the corresponding limit to transmission power at 216 to 960 MHz is 12 mW and above 960 MHz is 75 mW. Beyond the regulated limit, additional provisions apply to the transmission device. The Table 7 is an abstract of the additional provisions that are applicable to the various frequencies mentioned in this thesis (Code of Federal Regulation, 2009).

Table 7: Additional Provision on Transmitting Device Beyond Regulated Power Limit

Frequency	Power	Remarks
410 – 470 (MHz)	30 + 6 (dB)	-For intermittent control signals, maximum transmitter power is 30 dBm with antenna gain of 6 dBi. -For continuous transmission, maximum transmission power is 12 mW.
902 – 928 (MHz)	1,000 (mW)	-Applicable to spread spectrum transmitter with minimum of 50 channel hopping capability and digitally modulated transmitter. -Maximum transmission power is reduced to 250 mW if channel hopping is between than 49 to 25 channels.
1.24 – 1.3 (GHz)	40 + 6 (dB)	-For intermittent control signals, maximum transmitter power is 40 dBm with antenna gain of 6 dBi. -For continuous transmission, maximum transmission power is 75 mW.
2.4 – 2.435 (GHz)	1,000 (mW)	-Applicable to spread spectrum transmitter with minimum of 75 channel hopping capability and digitally modulated transmitter. -Maximum transmission power is reduced to 125 mW if channel hopping is less than 75 channels. -At maximum transmission power, use of directional antenna is permitted with power reduction. For every 3dBi gain in antenna, transmission power must be reduced by 1 dB.
5.725 – 5.85 (GHz)	1,000 (mW)	-Applicable to spread spectrum transmitter and digital modulation.

The functional decomposition has identified three categories of data to be transmitted or received; Image, Command and Telemetry. The Command and Telemetry data are commonly categorized together as the Command and Control (C2) data link. This link generally requires lower data transmission rate in the range of 50-200 kbps (Gundlach, 1975:500). Image data on the other hand requires a much higher data transmission rate ranging from 250-450 kbps (Riiser et al., 2012:24,9). Although the C2 data link is less demanding, it is more critical compared to the image data link. To avoid RF interference, the two data links are separated using different frequency spectrums.

From Nyquist's theory, the rate of data transmission is dependent on the available bandwidth which the RF signals are broadcast in. Higher data rate requires larger bandwidth. From Section 2.5, three ranges of transmission frequency were used in earlier research. They were, 915 MHz, 2.4 GHz and 5.8 GHz. The 915 MHz band has consistently been used for the C2 data link in earlier research and will similarly be adopted for this thesis. The allowable bandwidth for spread spectrum transmission in the 2.4 GHz frequency range is 83.5 MHz Federal (Federal Communications Commission, 1996: 20-21). For the 5.8 GHz frequency range, the allowable bandwidth is 125 MHz. Hence, for possible higher data rate, the 5.8 GHz was selected for Image data link (Federal Communications Commission, 1996: 22-23).

From Section 2.5.4, model aircraft that have achieved a range of 40 km operated in lower RF frequency for the C2 data link at 433 MHz. However, it is not necessary to adopt the same frequency as the maximum expected range of the research is not as far. Earlier research has already shown that a 915 MHz modem at 1 W transmission power is capable of reaching 4.3 km (14,000 ft) (Seibert et al., 2010).

For the preliminary architecture, the "*RFD900+*" transceiver and a set of "*Aomway 5.8 GHz*" transmitter and receiver were identified for the C2 and image data link, respectively. The former operates at a mean frequency of 915 Mhz bandwidth with a transmission power of 1,000 mW (RFD 900, nd). The latter operates at a mean frequency of 5.8 Ghz with a transmission power of 1,000 mW (Aomway, nd). Operating range of the transceiver/transmitter was estimated through theoretical analysis with Equation (2)

for the Link Budget Analysis and is shown in Table 8. The system's gains, losses and sensitivity in the table were estimated (Jacques et al., 2015).

$$R < 10^{0.05[\mathrm{EIRP} - \mathrm{Psensitivity} + \mathrm{Lp,Atm} + \mathrm{Lp,Precip} - 20\log10(fMhz) + 20\log10(0.3/4\pi) + G_R + L_R - L_M]} \quad (2)$$

Table 8. Theoretical Range for C2 and Image Data Link

		C2 Data	Image Data
		RFD 900+ (1,000 mW / 915 Mhz)	**Aomway 5.8 GHz (1,000 mW / 5.8 Ghz)**
ERIP	P_{tx} [dBm]	30	30
	G_{tx} [dBi]	2.5	
	L_{tx} [dB]	-1	
$P_{sensitivity}$ [dBm]		(-) -115	
$L_{p,Atm}$ [dB] and $L_{p,Precip}$ [dB]		-5	
$20\log_{10}(f_{Mhz})$		(-) 59.08	(-) 75.27
$20\log_{10}(\frac{0.3}{4\pi})$		-32.44	
G_R [dBi]		2.5	
L_R [dB]		-1.5	
L_M [dB]		-20	
Total [dB]		30.98	11.39
Range [km]	Theoretical	35.4	3.7
	Rated	40	Not rated
	Required	4	

The "*RFD900+*" transceiver was selected as it provides two features that were useful for the architecture. Firstly, it supports dual diversity antenna which reduces chances of RF communication breakdown when the receiver and transmitter antenna are pointing directly at each other. Secondly, it also has a network capability that allows multiple transceivers to communicate at the same time. This capability may be helpful for

future development on cooperative control of multiple UAVs. Both features will be discussed in Section 4.2.4

In general, transmission rate of wireless data depends on the type of transmission techniques and the maximum transmission power. When data packets are lost due to interference or excessive distance, the data transmission rate is reduced to facilitate repeat sending of the lost data packages. Loss of a data package can be reduced with increased transmission power (Roberts, 2012; 160). The "*RFD900+*" transmits at a data rate of 250 kbps. At 40 km, the rated air data rate reduces to 64 kbps (RFD 900, nd). Verification may be required to ensure that the data rate is adequate to support reliable RF communication.

For the Image data link, the theoretical distance with a 20 dB link margin is slightly less than the required range. However, this may be acceptable as the Image data link does not have a direct impact on the SOF. Analysis will be carried out in a later section of the chapter to analyze the adequacy of the selected component.

Onboard Autopilot Computer

Autonomous flight is facilitated out by the AP computer. It controls the motor and servos to maintain and/or correct flight heading and profile towards set waypoints. The servo and motor control signals are generated through the Proportion-Integral-Derivative (PID) feedback controller function in the AP computer (Beard et al., 2012:95) with inputs from the various sensors and GPS signal. In addition, the AP computer also provides programmable built-in fail-safe logic to enhance SOF.

An aircraft's flight is characterized by twelve state variable equations of motion

(Beard et al., 2012). To maintain stabilized flight, an AP computer is required to process and calculate the twelve state motions listed in Table 9. The axis for the state of motions is referenced in Figure 9. The various superscripts indicate the reference frame of the motion state, where '*i*' is the Inertia frame; '*b*' is the Body frame and '*v*' is the Vehicle frame

Table 9. State Variable for Air Vehicle Equations of Motion (Beard et al., 2012:29)

Name	*Description*
p_n	Inertial north position of the MAV along $\mathbf{i}^i$ in $\mathcal{F}^i$
p_e	Inertial east position of the MAV along $\mathbf{j}^i$ in $\mathcal{F}^i$
p_d	Inertial down position (negative of altitude) of the MAV measured along $\mathbf{k}^i$ in $\mathcal{F}^i$
u	Body frame velocity measured along $\mathbf{i}^b$ in $\mathcal{F}^b$
v	Body frame velocity measured along $\mathbf{j}^b$ in $\mathcal{F}^b$
w	Body frame velocity measured along $\mathbf{k}^b$ in $\mathcal{F}^b$
ϕ	Roll angle defined with respect to $\mathcal{F}^{v2}$
θ	Pitch angle defined with respect to $\mathcal{F}^{v1}$
ψ	Heading (yaw) angle defined with respect to $\mathcal{F}^v$
p	Roll rate measured along $\mathbf{i}^b$ in $\mathcal{F}^b$
q	Pitch rate measured along $\mathbf{j}^b$ in $\mathcal{F}^b$
r	Yaw rate measured along $\mathbf{k}^b$ in $\mathcal{F}^b$

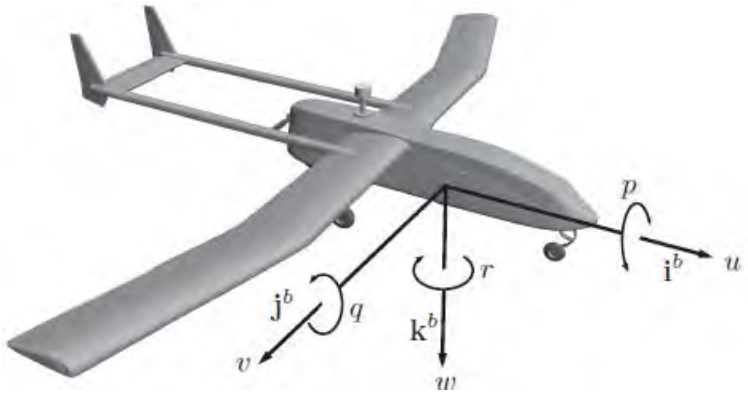

Figure 9: Axes of Motion on UAS (Beard et al., 2012:29)

Several models of AP computers were employed in earlier AFIT research. This was attributed to the emergence of new and more capable products in the COTS market throughout the years. The evolution of AP computers used at AFIT began with "*Piccolo II autopilot*" (Jodeh, 2006: 11) and progressed to "*Kestrel™ autopilot*" (Diamond et al., 2009:30; Seibert et al., 2010:15) with the "*Ardupilot Mega autopilot*" (Shuck 2013:19) being used most recently.

In this research, the "*Pixhawk autopilot*" was selected. The aforementioned AP computer shares the same developer as the "*Ardupilot Mega autopilot*" and was based on the firmware and software of the latter (3DR, nd). The "*Pixhawk autopilot*" was selected as it offers more capabilities over its predecessor. These include separate power supply, more accurate position estimation and dual sensors. At the same time, application knowledge with the "*Ardupilot Mega autopilot*" from earlier research can also be employed due to similarity of firmware and software. The following table compares the key features that are available on the two AP computers.

Table 10: Comparison of "*Pixhawk autopilot*" and "*Ardupilot Mega autopilot*"

Features and Fail-safes for "*Pixhawk autopilot*" and "*Ardupilot Mega autopilot*"	
Description	**Function**
Multi Mode of Control	The AP computer supports numerous modes of flight control input. The three relevant modes are listed below; -"Manual Mode" the AP will relay the input from the RC transceiver to the servos and motor. - "Stabilized mode". The AP computer will stabilize the RC inputs by damping out the servos' close loop response to reduce oscillation in flight and maintain a straight and level flight. -"Autonomous mode" the AP computer will fly the UAV based on the waypoints and flight profile (mission plans) input by operator at the GS computer.
Return to Home	This function can be setup to be initiated from either the RC controller or "Mission Planner" on the GS laptop. Upon reaching the launch site (home), the AP computer will maintain the UAV in a loitering pattern and waits for further command. This facilities immediate contingency response in the event of a "Mission Planner" of RC controller failure.
GS Fail-Safe	This only applicable in the "Autonomous mode". In the event that RF communication between the UAV and GS is loss, the AP computer will automatically return the UAV back to the launch site.
Battery Fail-Safe	The battery voltage and current is measured by the AP computer. A lower limit can be set to initiate a return to launch site when the measured value falls below the threshold.
Geo-Fencing	Permits setting up of a 3 dimensional flying boundary for the UAS. A 2 dimensional polygonal shaped boundary can be set up through "Mission Planner" to restrict the UAS operation within a desired area. A maximum and minimum altitude prescribed by the operator will bound the height of the polygon. When the virtual fence-line is breeched, the AP computer will take over and the UAV will be flown autonomously to a pre-defined rally point within the geo-fencing boundary.
Features and Fail-safes for "*Pixhawk autopilot*"	
Description	**Function**
Separate Power Supply	Built with second input interface at servo rail for secondary power supply. The AP computer will switch over to servo rail power in the event of a failure with the main power bus.
Dual Sensors	Built-in with 2 accelerometer and gyroscope. Internal magnetometer works together with external magnetic compass for more reliable accurate positioning.
GPS Fail-Safe	In the event of a GPS failure, the AP computer has the ability to return to the launch site based on dead reckoning.

Relating to autonomous control, the "*Pixhawk autopilot*" is integrated with a gyroscope, accelerometer, magnetometer and barometer (Pixhawk Specification, nd), see

Figure 10. The first three sensors provide the parameter data required to measure the pitch, roll and yaw movement of the air vehicle. The barometer is attached to a pitot-static sensor that measures pressure and air speed. The altitude, latitude and longitude were derived by the "*Pixhawk autopilot*" from data provided by the external GPS and magnetic compass.

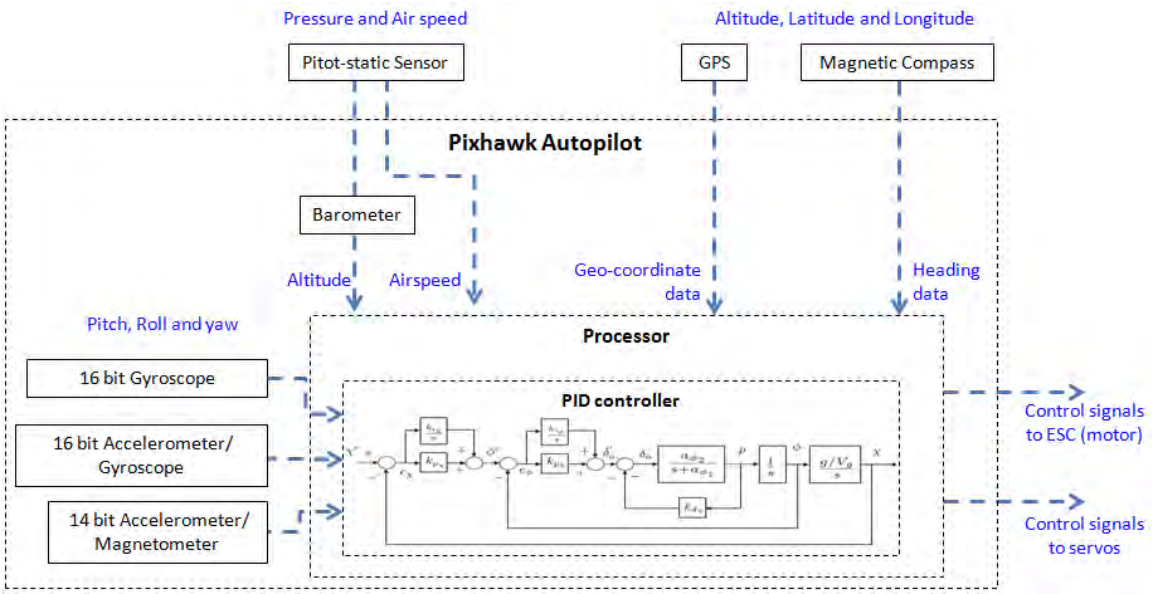

Figure 10: Schematic of "*Pixhawk Autopilot*" for State Variable of Motion

4.2.4 Integration of Preliminary Architecture

With the key components evaluated, a preliminary architecture was developed by integrating the identified components listed in Table 6 and is illustrated in the Figure 11. Tests were conducted on the key components in the next section to verify that the assigned components can fulfill the allocated functional requirement.

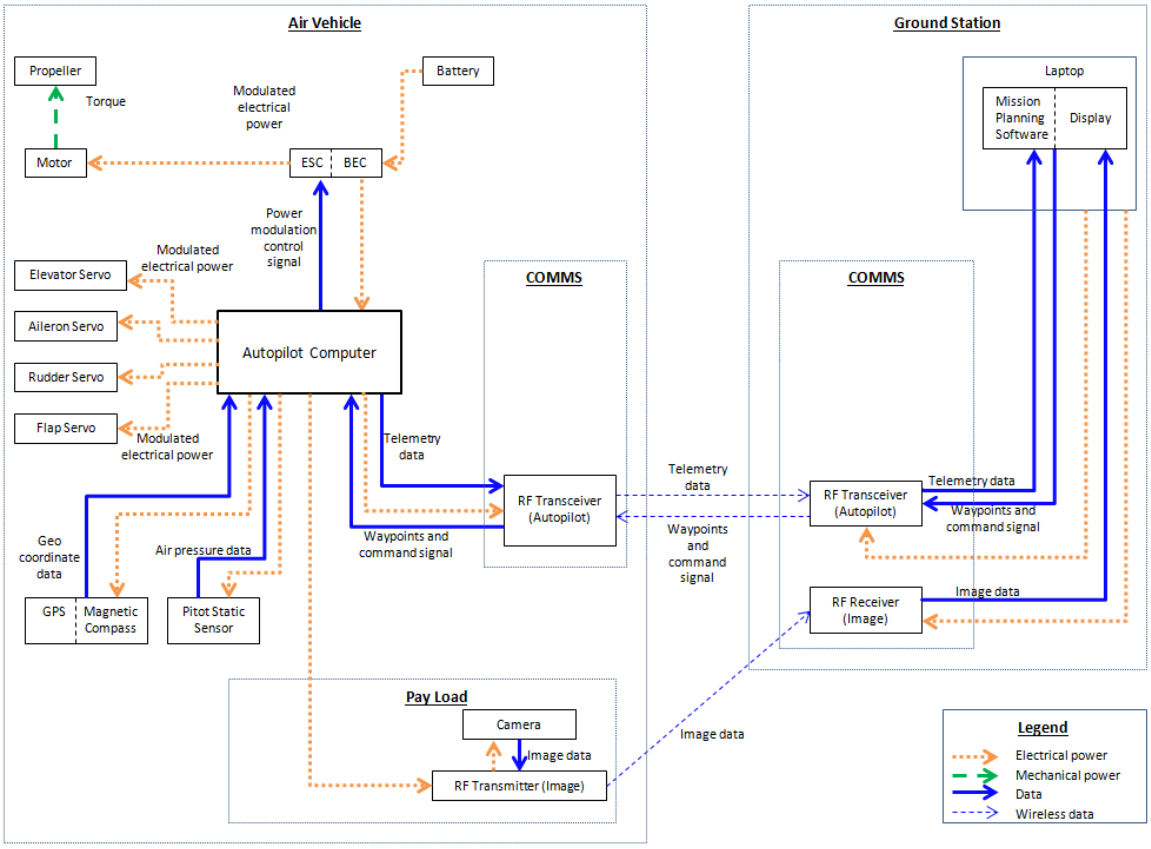

Figure 11: Preliminary Architecture of "*SIG Racal 110*"

4.2.5 Testing of Preliminary Architecture

Network Capable Modems

The "*RFD 900+*" transceiver can be implemented either as a pair or multi-point network, up to 29 nodes. Multi-point network can only be configured with Version 2.5 firmware. The implementation is differentiated through the configuration setting of the modems and defining the number of nodes in the network. When a modem is identified as 'Node ID' '0' with 'Node Destination' '65535', it functions as a base node and broadcasts to all the nodes in the network. 'Node ID' from '1' to '29'with 'Node

Destination' '0' functions as network nodes which communicate through the base node. The 'Node Count' determines the maximum of nodes permissible in the network.

The multi point network can be exploited by setting up a second GS some distance away from the first GS. With the second GS maintaining visual LOS and control of the UAV, the UAV can safely transit beyond the visual range of the first GS. This can be used in incremental flight testing before progressing to beyond visual LOS operation with a single GS. The multi network capability was verified in a test through the use of a ground RC vehicle. See Figure 12 for test set up.

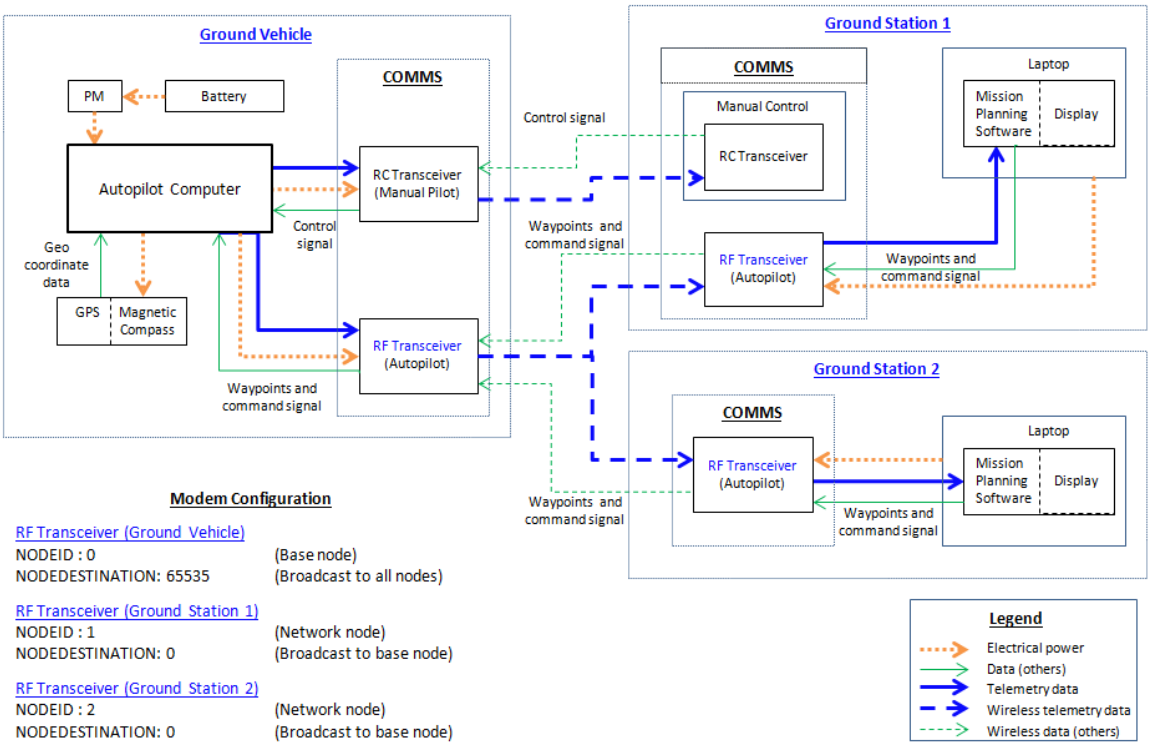

Figure 12: Ground Test Setup for "*RFD 900+*" Network Capability

Two setups were tested with a three node network, two GS and one vehicle, to better understand the response of the network capability. The first test was setup with

default configuration of the modem with 'Node Count' '3', 'Node ID '2' and 'Node Destination' '65535'. No interference was observed when the three operating nodes were placed next to each other. Subsequently, the transmission power was adjusted to the minimum (1 dBm). The two GSs were placed some distance away from each other and a ground vehicle was operated from GS_1 to GS_2 in 'Manual mode', see Figure 13. When the GSs were placed at a distance where there was no transmission overlap, the AP computer will stop the vehicle when it exceeds the transmission range of the GS 1. By reducing the separation to allow for some transmission overlap, the vehicle was successfully operated between the two GSs.

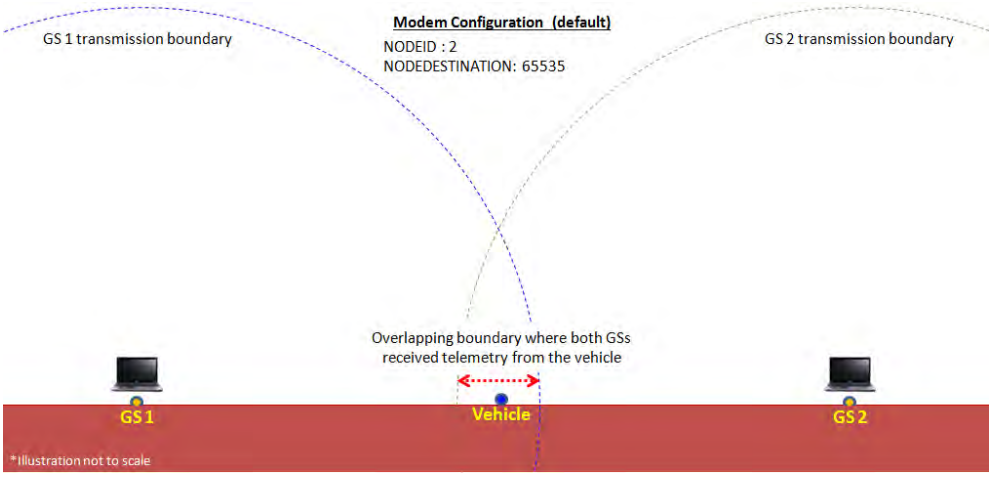

Figure 13: Ground Testing for "*RFD 900+*" Default Setting in Manual Mode

The second test was setup with a base node. Similarly, no interference was observed when the three operating nodes were placed next to each other. It was verified that new mission plans could be updated to the ground vehicle through either GS. Mission plans are essentially a sequence of waypoints set in "*Mission Planner*" that the vehicle will travel to in the "Autonomous mode". The latest update would be cached in

the AP computer and the ground vehicle executed the latest mission plan without anomaly when the "Autonomous mode" was selected.

However, it is to note that the latest mission plan will only be reflected on the GS that provided the update and was not automatically reflected on the remaining GS in the network. Hence, the operator at the remaining GS observed that the autonomous movement of the vehicle did not correspond to their outdated mission plan. The latest mission plan will only be reflected when the operator at the remaining GS refreshes their mission plan on "*Mission Planner*".

Standard operating procedures can be implemented to prevent misunderstanding by the remaining GS that the AP computer is not working properly. Firstly, the operator that is updating a new mission plan must inform the other operators prior to uploading the waypoint. Next, in the event when an operator sees that the UAV is not heading towards the waypoint in his mission plan, the immediate respond shall be to refresh the mission plan and verify that it is not outdated.

The ground test concludes that two GSs and a single vehicle can be safely operated in a network with the "Autonomous mode" at an extended distance as long as it maintains in the transmission range of at least one GS.

Dual Diversity Antenna

In Section 4.2.3, it was highlighted that the *"RFD 900+*" transceiver supports dual diversity antenna. A RF system will minimally require a pair of antennas, one to transmit, the other to receive. The 'Rubber Ducky' antenna used in the research is an omni directional antenna, and has an estimated gain of 5.5 dBi (Jacques et al., 2015). RF

signal propagate spherically from the side of an omni directional antenna with a null spot at the top antenna (Jacques et al., 2015), see following figure. Based on propagation direction of the RF signal, optimal reception is achieved when the length of the receiving antenna is parallel with the transmitting antenna. In the event where the two antennas are pointing at each other, the reception strength will be reduced. This situation may arise as the UAV banks and turns in flight.

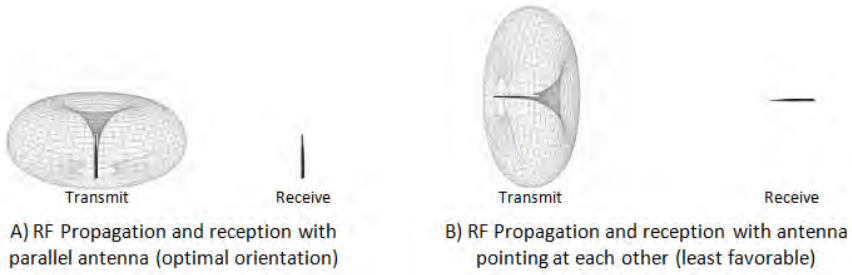

Figure 14: RF Propagation and Reception of RF Signals

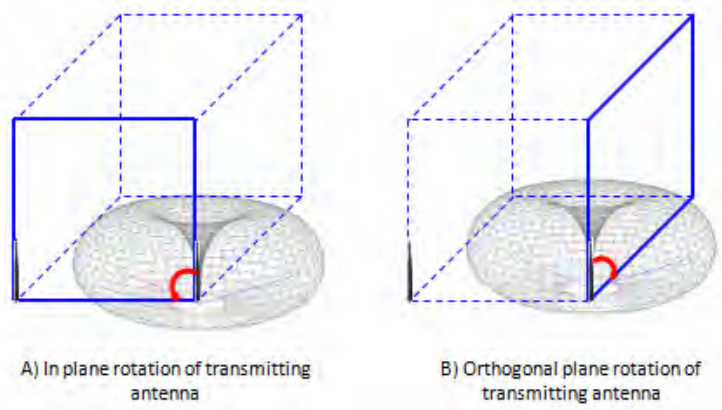

Figure 15: Orientation of RF Transmitting Antenna

A test was conducted to measure the effect of the relative antenna position to the received signal strength. The "*3DR-915 MHz*" transceiver (3DR modem, nd) that supports only s single antenna was used for the test with the transmission power reduced

to 1 dBm. The two transceivers were separated by 30 m and the received signal strength was measured with the direction of the antenna placed at different orientations. The transmitting antenna was first orientated in plane with the receiving antenna by three angles (0^0, 45^0 and 90^0). This was repeated in the orthogonal plane; see the following figure for result.

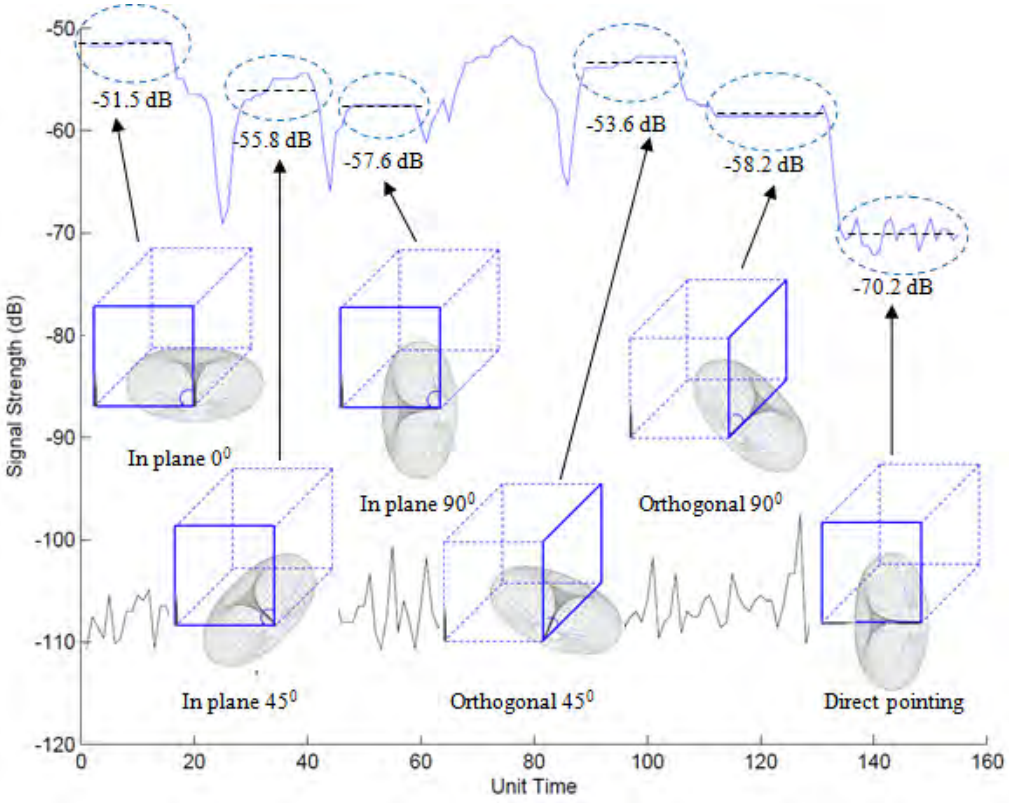

Figure 16: Received Signal Strength at Different Antenna Orientation

It is observed that the received signal strength will be reduced when the orientation of antennas are not parallel. The least favorable orientation is when the two antennas are pointed directly at each other with a measured reduction of 18.7 dB. This is followed by a 90^0 orientation in the orthogonal plane with a 6.7 dB reduction. The orientations of the antennas were arranged in order from the highest received signal strength to the least in the following table.

Table 11: Results of Single Antenna Orientation Test

S/N	Antenna orientation	Received signal strength (dB)	Relative drop in signal strength (dB)
1	Parallel	-51.5	-
2	45^0 in orthogonal plane	-53.6	2.1
3	45^0 in plane	-55.8	4.3
4	90^0 in plane	-57.6	6.1
5	90^0 in orthogonal plane	-58.2	6.7
6	Direct pointing	-70.2	18.7

Dual diversity permits two antennas to be installed orthogonally on the same transceiver. With orthogonal antennas, there is no instance when the receiving antennas are pointing directly at the transmitting antenna. Hence, the least favorable arrangement is a 90^0 in-plane rotation, see Figure 17. This mitigates the loss in signal strength to 6.1 dB from 18.7 dB and brings about an improvement to the reliability of the RF communication as the UAV maneuvers in air.

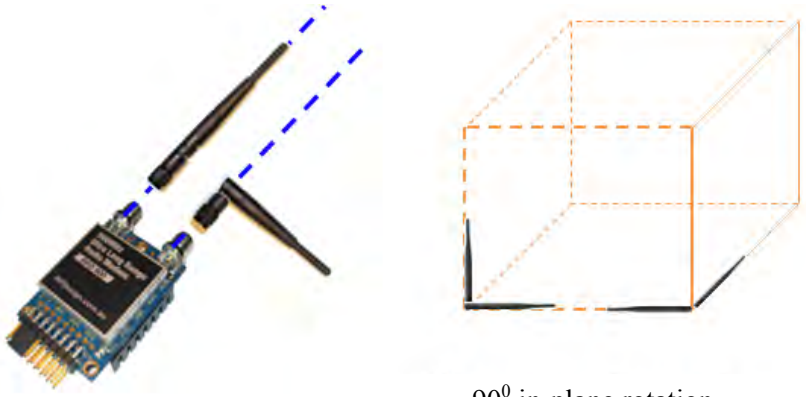

90^0 in-plane rotation

Figure 17: Least Favorable Dual Diversity Antenna Orientation

The ground test concludes that selecting a transceiver with dual diversity antenna would improve the performance and range of the UAS compared to an exact transceiver that only has single antenna.

Characterizing C2 Data Link ("RFD 900+")

A ground test was conducted to verify the transmission range of the *"RFD 900+"* transceiver which was installed with a half wavelength "rubber ducky" antenna. The degradation of signal strength between two *"RFD 900+"* transceivers when one was gradually moved apart from the other was measured using the *"3DR Radio Configuration Utility"* software. The software measures the received signal and noise level for both stationary and mobile transceivers at a frequency of 2 Hz. The test was conducted with a maximum separation of 200 m and repeated at different transmission power. The following figure illustrates the measurements from the ground test with a transmitted power of 1dBm (1.26 mW).

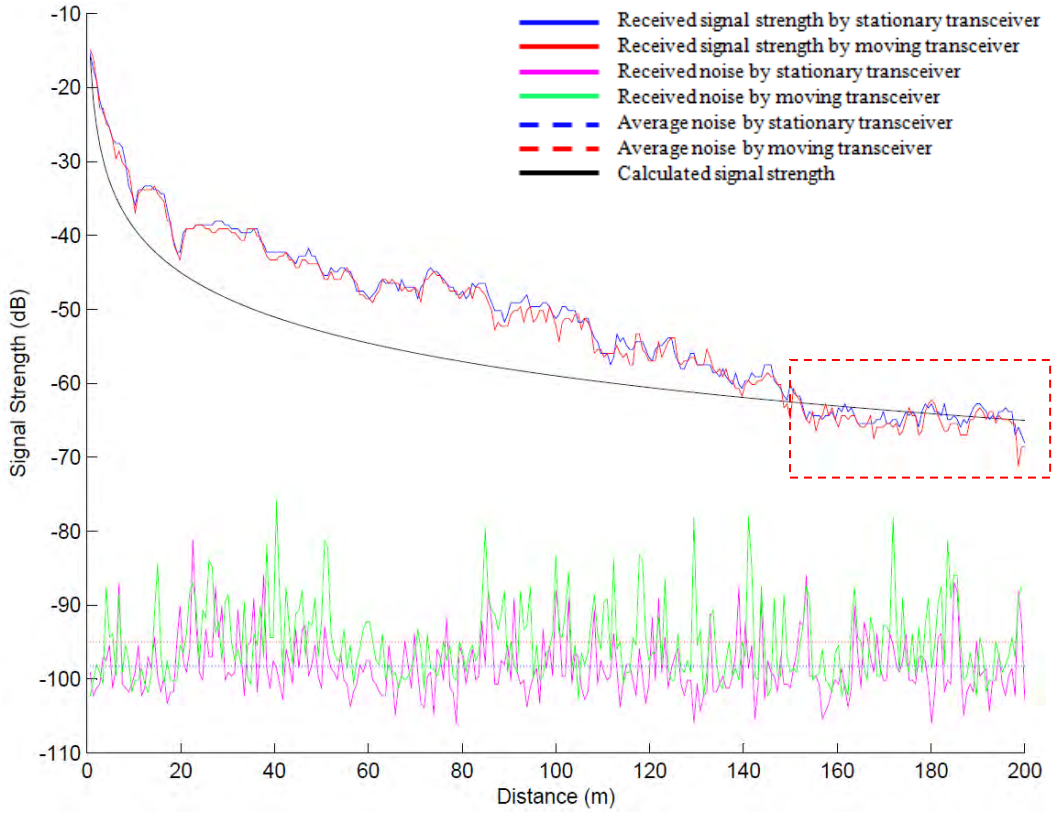

Figure 18: Signal Measurement at 1 dBm Transmitted Power (*"RFD 900+"*)

The signals measured in time were translated to distance base on a uniform speed to travel the separation of 200 m. The average noise level in the figure was calculated directly from the measured data while the calculated signal strength was derived through a series of manipulations on Equation (1). The equation was first converted to decibel and then rearranged based on the separation distance. Thereafter, the various parameters were condensed into a constant *k* that results in the equation shown below.

$$Si = P_T G_T L_T L_P G_R L_R \left(\frac{\lambda}{4\pi R}\right)^2$$

$$Si = P_T + k \text{ -20*log}(R) \tag{7}$$

$$\text{Where } k = 10 \log (G_T L_T L_P G_R L_R) + 20\log \left(\frac{\lambda}{4\pi}\right)$$

Equation (7) was mapped onto the preceding figure by assigning a value to the condensed constant *k* that forms a line of best fit which normalizes the measured received signal strength. For the "*RFD 900+*" that is used for the C2 data link, the value of k_{C2} for the test conducted at 1dBm transmitted power was -80 dB. This is represented by the line titled "Calculated Signal Strength". The normalized line was not fit to the entire range of measured signal strength. Instead, emphasis was placed at the end of the separation distance as the UAV is not expected to operate near the GS.

The value of k_{C2} was also extended to normalize the measured signal strength at the transmission power of 2 dBm (1.58 mW) and 5 dBm (3.16mW). The results are illustrated in the two following figures. The table after the figures summarizes the measurements and results for all three tests.

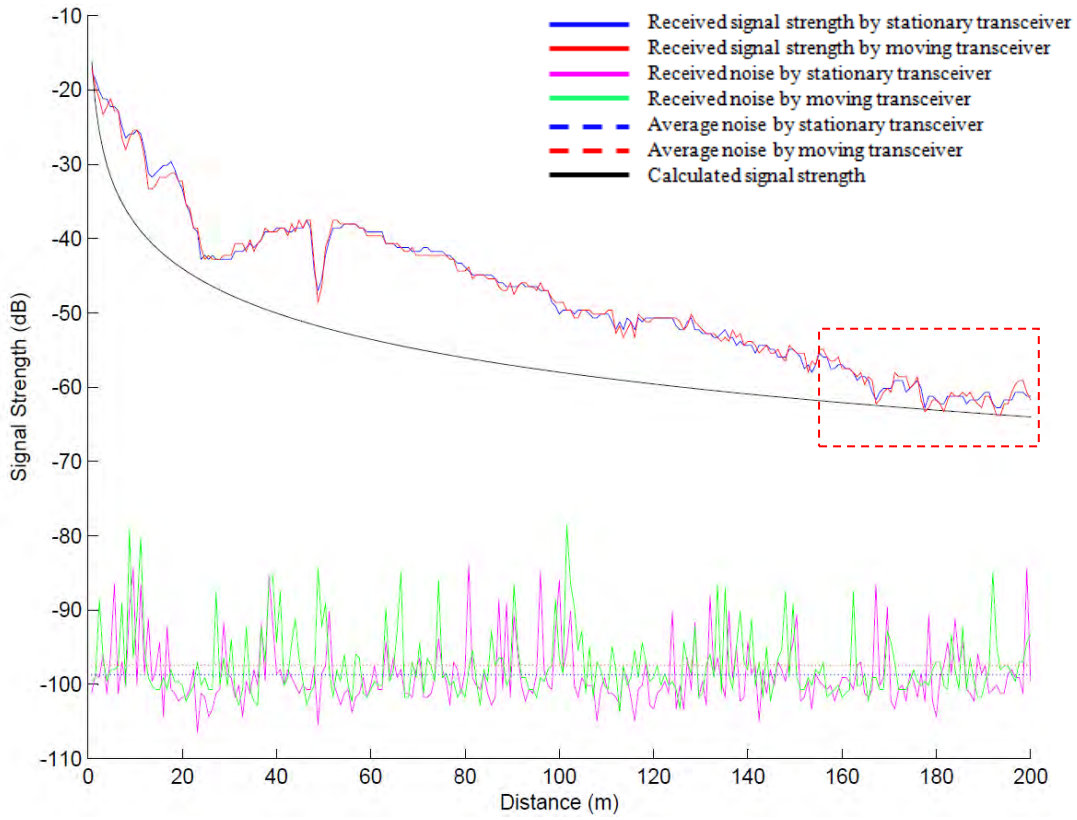

Figure 19: Signal Measurement at 2 dBm Transmitted Power (“*RFD 900+*”)

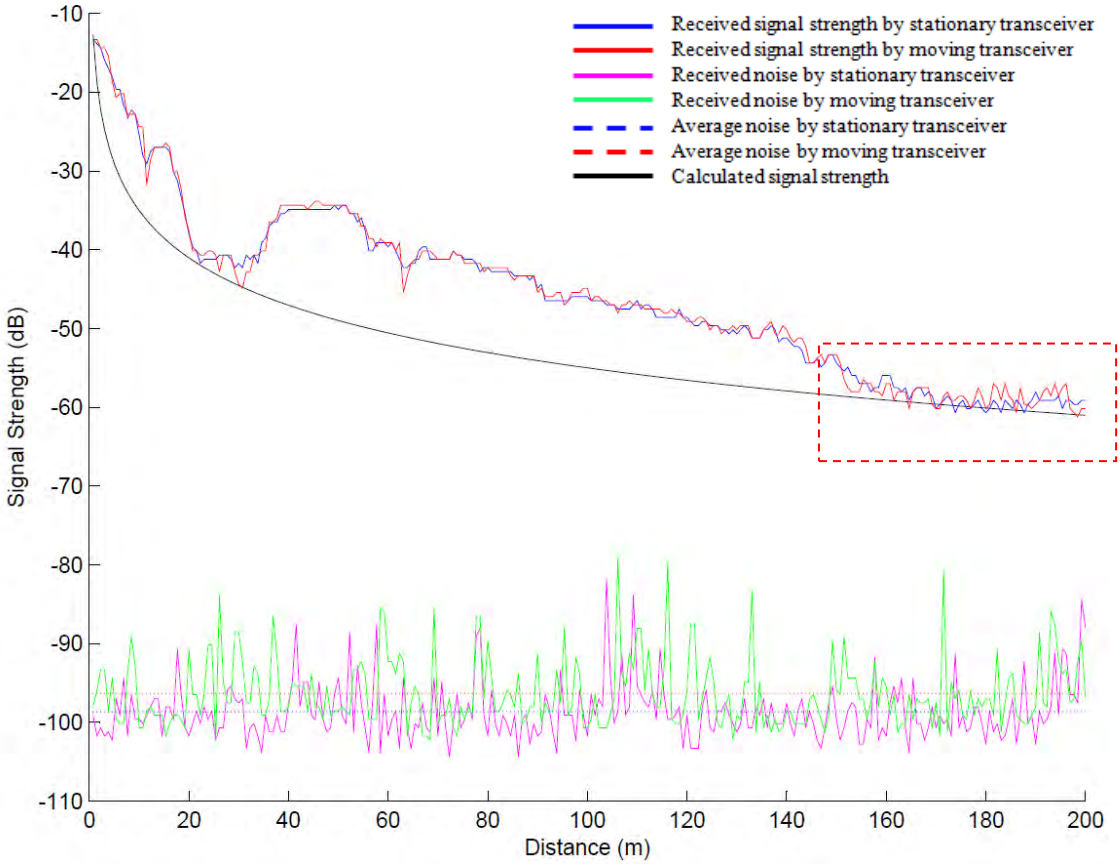

Figure 20: Signal Measurement at 5 dBm Transmitted Power (“*RFD 900+”*)

Table 12: Summary of Measurements on “RFD 900+” Transceiver

TX Power (dBm)	Noise at stationary transceiver (dB)			Noise at mobile transceiver (dB)		
	Peak	Trough	Mean	Peak	Trough	Mean
1	-81.21	-105.95	-98.28	-75.95	-102.79	-94.97
2	-83.34	-106.47	-98.72	-78.58	-103.84	-97.41
5	-81.74	-104.37	-98.67	-79.12	-102.26	-96.30
Average	-82.10	-105.60	-98.56	-77.88	-102.96	-96.23
$Peak_{Average} - Mean_{Average}$			16.46			18.34

From the preceding table, it is observed that the measured noise level at the mobile transceiver was consistently higher than the stationary transceiver across at all three power settings. For design margin, the noise level of -96.23 dB at the mobile transceiver was adopted. The difference between the 'Average Peak' and 'Average Mean' noise level at the mobile transceiver was 18.34 dB. This is within the expected link margin of 20 dBm that was applied in Table 8.

At full transmitted power of 30 dBm (1 Watt), the degradation of signal strength with increasing distance was extrapolated using Equation (7), with k_{C2} at -80 dB. The 'Mean Average' noise level at the mobile transceiver together with a 20 dB link margin were both imposed on the signal strength plot to calculate the maximum range of the system. The figure below illustrates the calculated range.

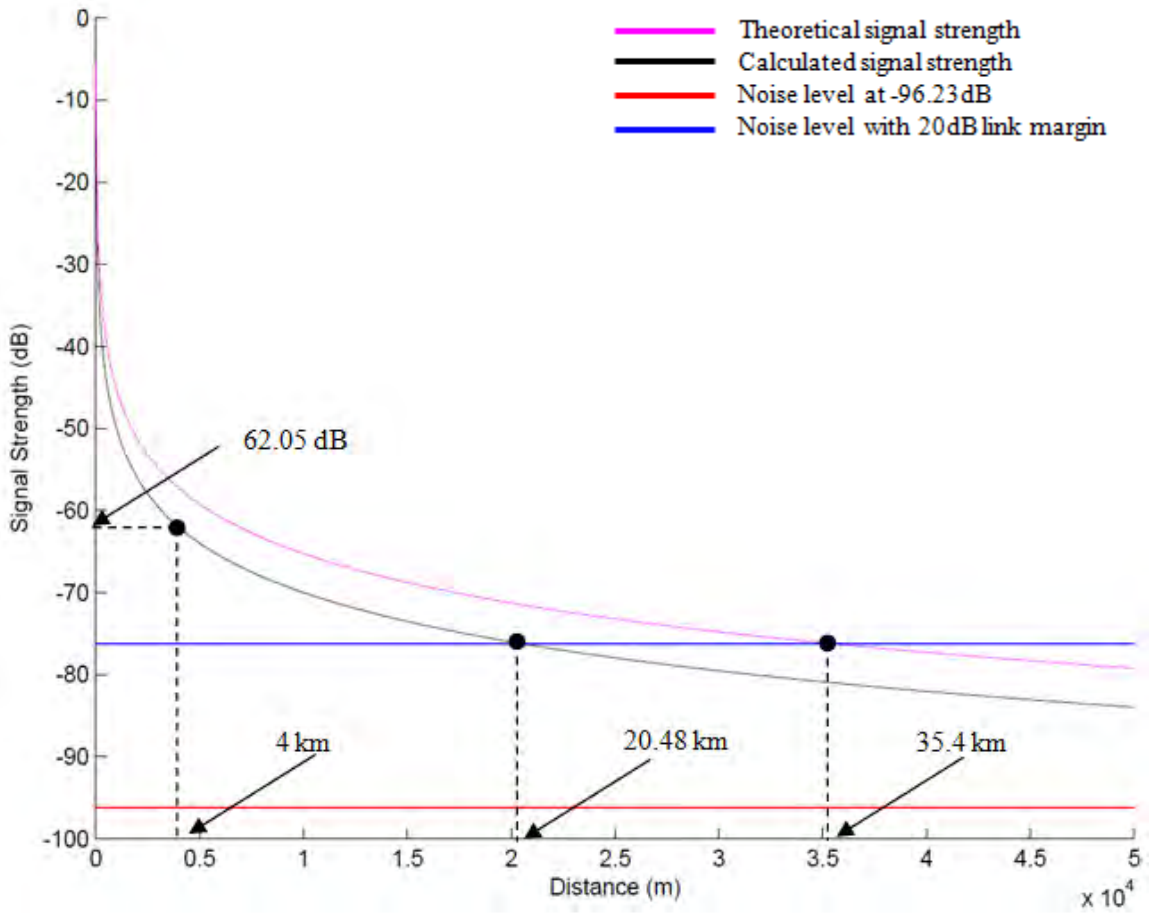

Figure 21: Calculated Range at 30 dBm Transmitted Power (*"RFD 900+"*)

The calculated range (20.48 km) from the ground test was 42.1% lower than the theoretical range (35.4 km) from Table 8, but was nevertheless above the required range of 4 km that was specified in Section 4.1. The calculated link margin available at 4 km is 34.18 dB. It is noted that the expected range will vary as ambient RF noise will not be the same at different operating locations. In the presence of frequency interference, the maximum range will decrease significantly. In addition, the ground test was conducted with zero elevation difference between the two transceivers. Signal strength at the same

distance is expected to improve when the UAV is in the air as there will be less physical obstacles along the RF LOS between the two transceivers.

Characterizing Image Data Link ("Aomway 5.8 GHz")

A similar approach to verify the range for the Image data link was attempted on the "*Aomway 5.8 GHz*". However, this was not feasible due to hardware requirements incompatible with the "*3DR Radio Configuration Utility*". An alternative was explored by using a spectrum analyzer to directly measure the received signal strength and overlay it on the noise signal from the *"RFD 900+"* test. However, this was also not adopted as the unknown internal gains and losses of the spectrum analyzer will be introduced as additional variables to the analysis.

Hence, an analogous calculation was made using the value of k_{C2}. This is based on the assumption that the net transmission gain, reception loss and transceiver sensitivity of the Image data link is approximately the same as the C2 data link. The value of was k_{C2} was adjusted to k_{image} by accounting for the higher transmission frequency.

For a more comprehensive analogous calculation, the ground test for C2 data link was repeated with the single antenna "*3DR-915 MHz*" transceiver, to obtain an average value for the constant k_{C2}. The "*3DR-915 MHz*" transceiver operates with a maximum of 20 dBm (100 mW) in the frequency of 915 MHz (3DR modem, nd). The test was conducted with the stationary transceiver set to 20 dBm and the mobile transceiver at 1 dBm (1.3 mw). It was observed that data link was lost when the mobile transceiver was at a distance of 260 m from the stationary.

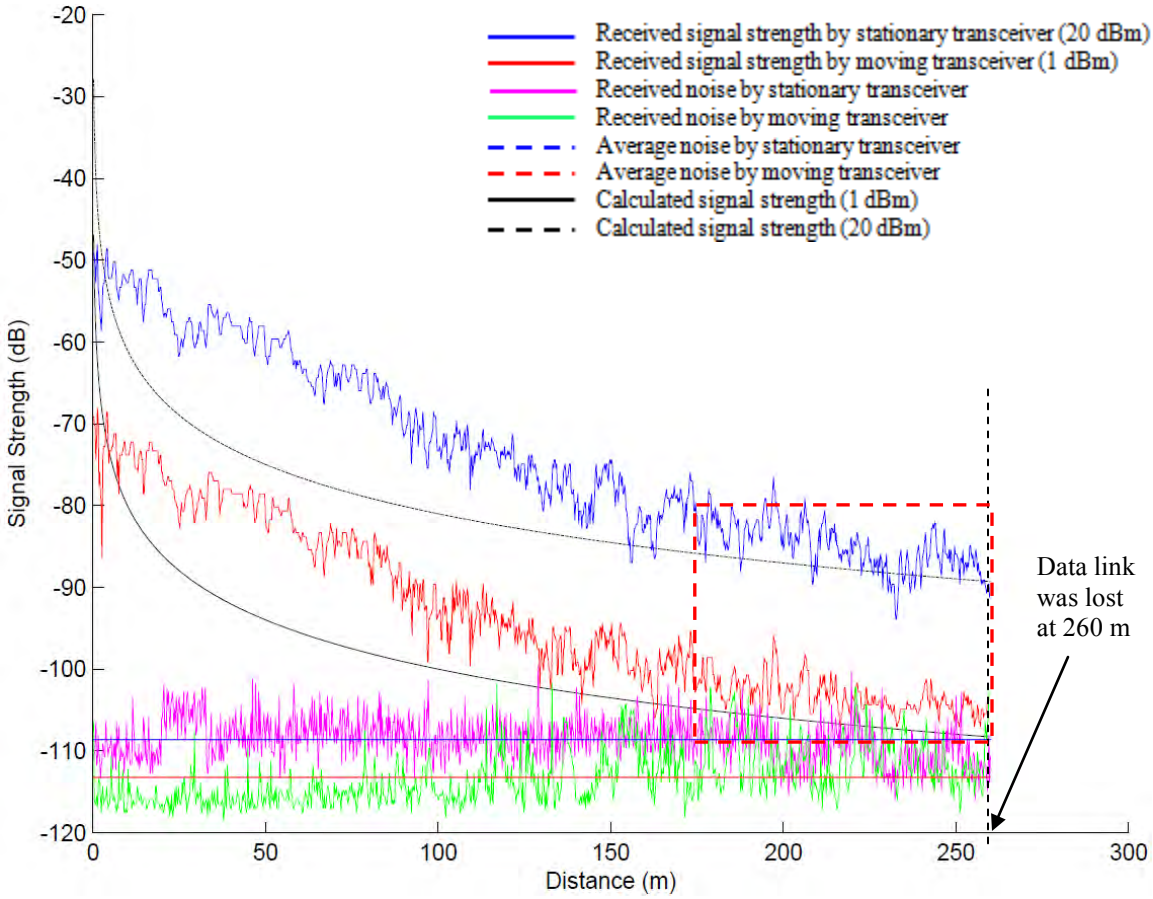

Figure 22: Signal Measurement for *"3DR Radio 915MHz"*

From the preceding figure, the value of k_{C2} that has a line of best fit onto the signal strength is -121 dB. Between the mobile and stationary transceivers, the higher of the two average noise received was at -108.63 dB. This measurement varied from the first C2 data link ground test using the "*RFD 900+*" (-96.23 dB) as the location was different. The following table summarizes the measurements for the two C2 data link ground tests. Calculation of the expected range of the Image data link was based on the average k_{image} and noise level from the two tests.

Table 13: Comparison of Measurements from C2 Data Link Tests

	"RFD 900" Setup	**"3DR-915 MHz" Setup**	**Average**
k_{C2} @ 915 MHz (dB)	-80	-121	-100.5
Relative k_{image} @ 5.8 GHz (dB)	-96.19	-137.19	-116.69
Noise level (dB)	-96.23	-108.63	-102.43

$$Si = P_T + k - 20*\log(R)$$

$$Noise\ Level + Link\ Margin = P_T + (k_{image} - Freq\ increase) - 20*\log(R)$$

$$-102.43 + Link\ Margin = 30 + (-116.69) - 20*\log(4)$$

$$Link\ Margin = 3.7\ \text{dB}$$

From the following figure, it was observed that, the calculated transmission range with a 20 dB link margin is only 0.61 km. Operation beyond 0.61 km may result in occasional loss of image when the transient spikes of noise exceed the received signal strength. At a transmission range of 4 km, the allowable link margin is reduced from 20 dB to 3.7 dB.

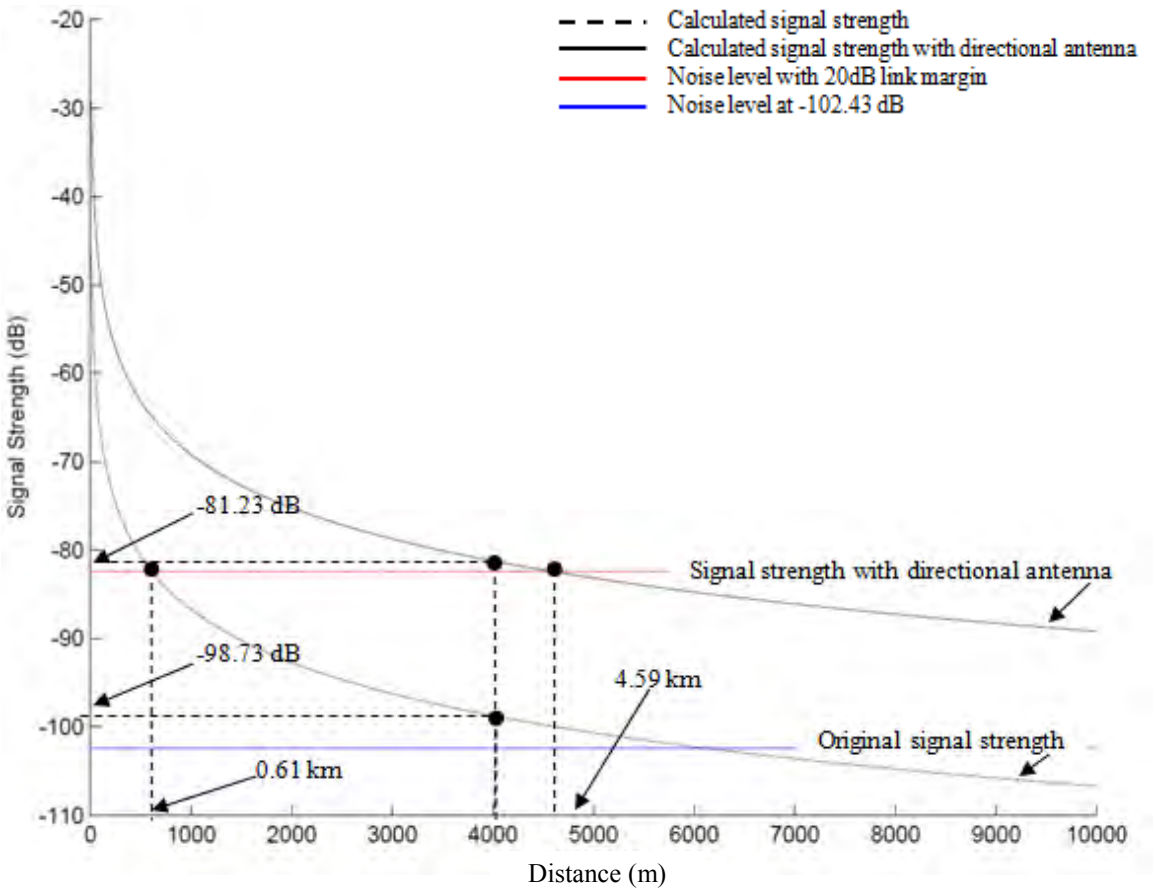

Figure 23: Analogous Range Calculation for Image Data Link

To achieve undisrupted Image data link, a 23 dBi direction antenna (MyFlyDream, nd) was added to increase the reception gain. The original rubber ducky has an estimated gain of 5.5 dBi (Jacques et al., 2015). With a net gain of 17.5 dBi from the directional antenna, the calculated range is extended to 4.59 km. At the required range of 4 km there is an available link margin of 21.2 dB, see Figure 23.

4.3 Risk Management

This section starts with the definition on risk classification. Subsequently, it proceeds to examine the preliminary architecture and contingency procedures to identify potential risks and is followed by an analysis of its impact on SOF. Thereafter, mitigations are implemented to reduce the residual risk of the final architecture to an acceptable level.

4.3.1 Risk Classification

Risk is defined as a product of mishap severity and mishap probability. The severity and probability can be measured quantitatively or qualitatively. It is noteworthy that quantitative data on the reliability of UAS are limited (Cline, 2008:5), in particular, reliability data for small UAS is generally not available (Murtha, 2009:1). The categorization of risk severity and probability specified by AFIT's TRB/SRB are shown in the following two tables (Air Force Institute of Technology, 2014). The qualitative assessment on the probability of failure used in this research was based on experiences from past UAS research effort in AFIT.

Table 14. Categorization of Mishap Probability (Air Force Institute of Technology, 2014)

PROBABILITY DESCRIPTORS	LEVEL	DESCRIPTION
Very Likely	A	Highly expected to occur - Many significant concerns even after mitigation applied
Likely	B	Expected - Significant concerns remain even after mitigation applied
Less Likely	C	Not expected but possible – Some concern exists even with mitigation applied
Unlikely	D	Unexpected - Minor concerns after mitigation applied
Very Unlikely	E	Highly unexpected – Little or no concern after mitigation applied

Table 15. Categorization of Mishap Severity (Air Force Institute of Technology, 2014)

MISHAP SEVERITY	CATEGORY	CONSEQUENCE OF MISHAP
Catastrophic	I	Death, system loss, or severe environmental damage. System loss or equipment damage exceeding $2,000,000 (i.e. Aircraft Class A Mishap).
Critical	II	Severe injury, severe occupational illness, or major system/facility/ environmental damage. For personnel, severe injury or illness equates to lengthy hospital stays and/or permanent injury. Major system/facility/ environmental damage equates to equipment or property damage loss exceeding $500,000 but less than $2,000,000 (i.e. Aircraft Class B Mishap).
Marginal	III	Minor injury, occupational illness, or minor system/ facility/ environmental damage. For personnel, minor injury or illness requires medical treatment resulting in lost work days but no permanent injury. Minor damage equates to losses exceeding $10,000 but less than $500,000 (i.e. Aircraft Class C Mishap).
Negligible	IV	Less than minor injury or system damage. For personnel, the impact of the injury or illness equates to no work days lost. For equipment or facilities, less than minor damage equates to losses less than $10,000.

Severity is related to the consequence of mishap which includes two aspects, safety to human and cost of damage to system and property. The risk assessment and acceptance by the TRB/SRB is a comprehensive process which also covers possible accidents during preparation and pre-flight check. An example of such an accident is the inadvertent contact of the fingers with a spinning propeller.

The focus of the research is on airworthiness of the UAV. Hence, the assessment is centered on the UAV when it is in flight and is derived from the consequence of individual component failure. The risk to personnel safety during handling of the system will be addressed separately during the TRB/SRB process.

4.3.2 FMECA

Risk identification and analysis were conducted inductively (bottom-up) through the use of FMECA. The different modes of failure that can occur on each component were identified and its consequential effect on the system was analyzed to establish the

level of risk it poses to SOF. To optimize the architecture, the components were grouped based on their functional domain in the FMECA to facilitate possible development of mitigating solutions that are applicable to more than one component or failure mode.

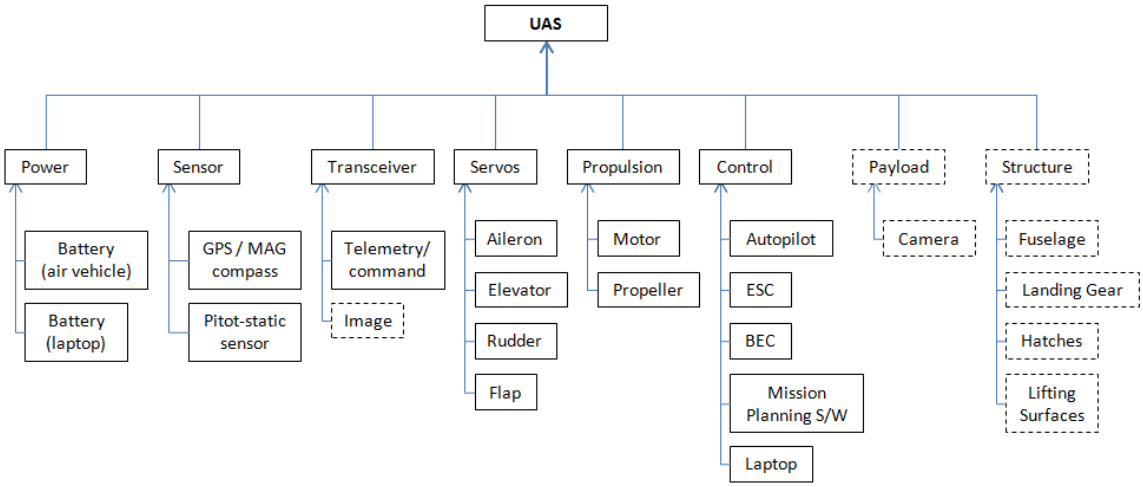

Figure 24: Functional Grouping of Components in FMECA

Two functional domains, Payload and Structure, were not covered in the FMECA. Depending on the nature of operation, different missions require different payloads. Therefore, FMECA on the payload will be conducted separately in the future upon clarification of mission requirements. The structural design of COTS RC model aircraft have been validated by a large base of recreational users. Hence, FMECA is not conducted for this domain unless the original structure was modified.

Mitigations in the form of hardware redundancy for low-cost UAS are typically constrained by size, weight, power and budget (Freeman et al., 2014:1). Hence, careful consideration was taken to ensure that redundancy was not excessively introduced for the mitigations in the FMECA. In total, there are 34 risks attributing to the various failure

modes from the 16 components in the preliminary architecture. The detailed analysis on the risk of each failure mode and its mitigation is documented in Appendix A. The results of the FMECA and its risk mitigation are summarized in Table 16.

Table 16. Summary of Design Improvements and Contingency Procedures

S/N	Component	Mitigation		Probability	Severity
		Design	Procedure		
1	Primary Battery	-Dual power supply for AP computer -Separate power supply between motor, avionics and payload -Connector clips -Parallel battery arrangement	-Battery fail-safe	E	IV
2	GPS/ Magnetic Compass	-Backup flight mode (Manual)	-GPS fail-safe	D	IV
3	Pitot-static Sensor	-Backup flight mode (Manual)	NA	E	IV
4	Telemetry/ Command Transceiver	-Separate frequency spectrum -Frequency hopping capability	-GS fail-safe -Geo fence	E	IV
5	Aileron Servo	-Individual power supply for servo, avionics and motor -Connector clips	-Battery fail-safe	E	IV
6	Elevator Servo				
7	Rudder Servo				
8	Flap Servo				
9	Motor	-Retain manual flight control for non-powered landing	NA	E	III
10	Propeller				
11	AP Computer	-Backup flight mode (Manual) - Separate power supply between motor, avionics and payload -Dual power supply for AP computer	NA	E	III
12	ESC	-Retain manual flight control for non-powered landing -Power module to limit maximum current	NA	E	III
13	BEC	-Dual power supply	NA	E	IV
14	Mission Planning S/W	NA	-Return to launch site from RC controller	E	IV
15	RC controller	NA	-Return to launch site from laptop	E	IV
16	Laptop	- Backup flight mode (Manual) -Separate display for FPV image -OSD to impose telemetry on FPV image	NA	E	IV

Among the risks of all the failure modes on a component, the rating with the highest probability and worst severity was taken and listed in the last two columns of the table. Details for the various fail-safes mentioned in the table can be found in Appendix B.

There are a total of one hundred and twenty ($\binom{16}{2} = 120$) permutations in which two out of the sixteen components can fail. This is compounded with variation of multiple failure modes for each permutation. The FMECA did not consider dual components failure as a simultaneous occurrence which individually has 'very unlikely' probability is extremely remote. An exhaustive analysis for such remote probability of occurrence will yield minimal value in improving the design of the architecture.

4.3.3 Risk Analysis

Risk acceptance by AFIT's TRB/SRB is based on an integrated assessment matrix, of severity and probability. Risks residing in the region of 'Medium Risk' will not be accepted (Air Force Institute of Technology, 2014:7) and thus require further mitigation. The risks associated with each component failure listed in the preceding table are mapped onto the assessment matrix in the Figure 25.

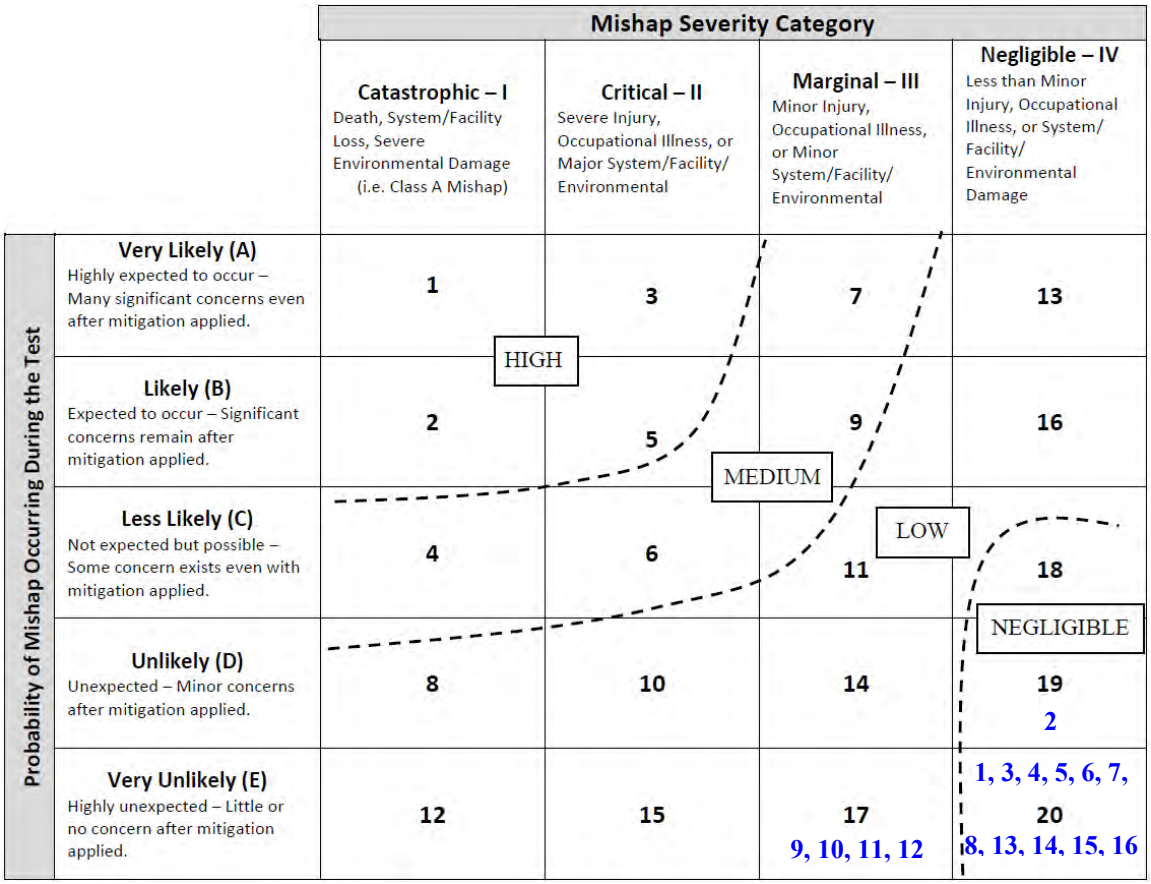

Figure 25: Risk Mapping on Assessment Matrix (AFIT, 2014)

Post mitigation, the risks associated with the failures of most components has been reduced to the region of 'Negligible Risk'. Those that remained in the region of 'Low Risk' are associated with the possibility when unaware personnel did not move out of the landing path of the UAV during a non-powered landing.

For Risk #9 (Motor failure) and #10 (Propeller failure), further mitigation could not be implemented without a change in fuselage design to a twin engine platform. Mitigation to Risk #12 (ESC failure) may be implemented through parallel ESC operation. However, this is restricted by the capability of the AP computers. The

"*Pixhawk autopilot*" has the ability to control multiple motors each with its individual ESC. However, it does not have the ability to control a motor through two parallel ESCs.

For Risk #11 (AP computer failure), a complete AP computer failure is defined as a situation where no data or power is passed through or processed by the *"Pixhawk Autopilot"*. Further mitigation for this risk is possible with a second AP computer that shares the same input and has either 1) an independent output or 2) a parallel output. The prior would require a switch to select which AP computer to be in control. However, the switch would present itself as a single point of failure. If the reliability of the switch is lower than the AP computer, it would increase the overall probability of a loss in AP control.

The second option with parallel output could not be achieved as the firmware for "*Pixhawk autopilot*" does not support parallel operation of two AP computers. Furthermore, it does not permit one in backup mode. Literature review has also revealed that there is no known COTS AP computer that possesses the required capability to support dual auto pilot operation. Hence, the residual risk is retained in the Low Risk region which is acceptable by the TRB/SRB.

4.4 Intermediate Architecture

The next figure shows the integrated architecture of the UAS post mitigation from the FMECA. Iterative testing was conducted to verify the new features that were added and are documented in the next section.

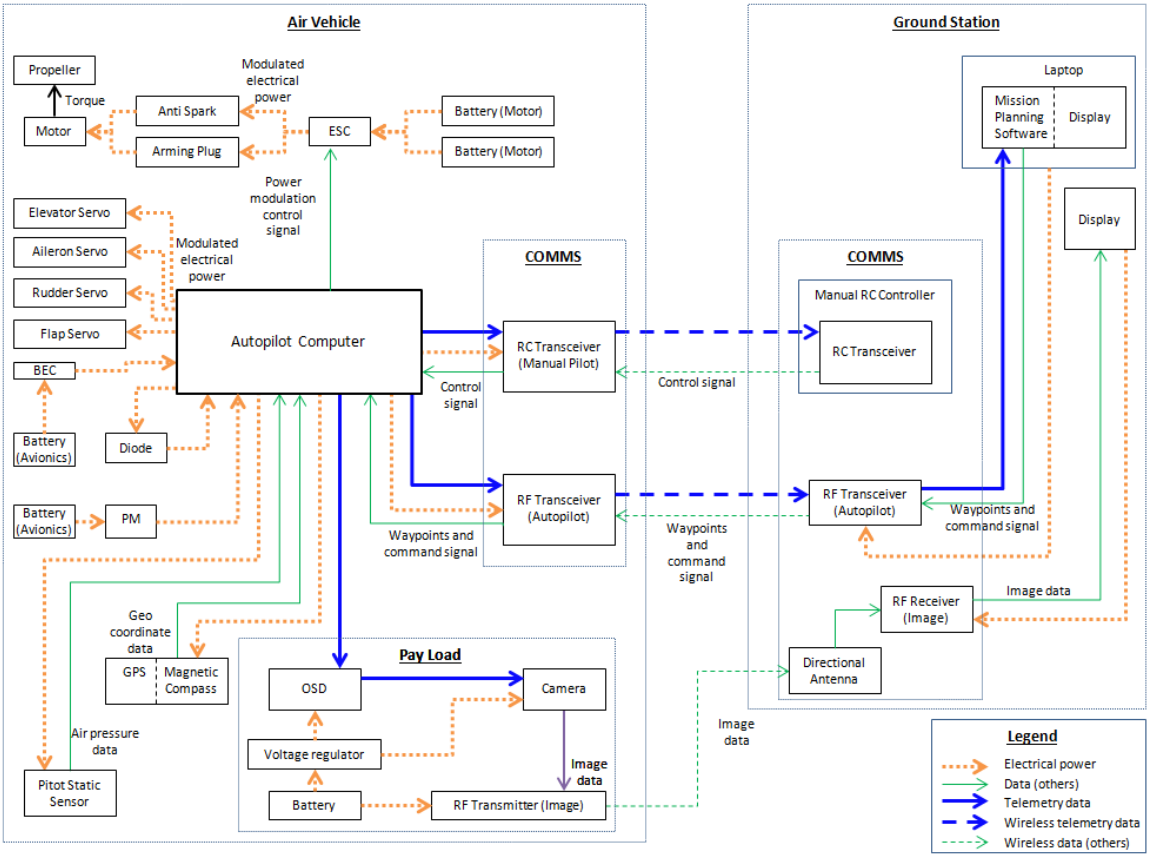

Figure 25: Intermediate Architecture of UAS Post FMECA

4.5 Iterative Testing of Intermediate Architecture

Manual RC control and Geo-Fencing are the two key features added in the intermediate architecture. The manual RC control serves as a back-up mode to the AP computer. The Geo-Fencing feature in the *"Pixhawk autopilot"* is programmed to prevent the UAV from flying beyond the transmission range of the transceivers.

Characterizing RC Data Link ("Taranis" and "FrSky L9R")

Manual RC flight is a common mode of control used by recreational users and is regularly integrated with a COTS AP computer for stabilized or autonomous flight.

Verification on the transmission range of the RC transceiver is necessary to ensure that it can accommodate the specified distance. The RC controller manufactured by "*Taranis*" was used in earlier research. To maintain familiarity by the Ground Operator, the "*Taranis*" RC controller was retained. Familiarity with the RC controller during flight testing is essential as the Ground Operator functions as the safety pilot and responses to contingency through the "Manual mode".

The operating frequency of the RC data link is 2.4 GHz and uses digital modulation which does not conflict with the C2 and Image data link. The RC commands are input through the *"Taranis"* controller by the Ground Operator and received by the *"FrSky L9R"* transceiver on board the Air vehicle. In return, the transceiver would send regular signals to the controller which informs the Ground Operator that communication link between the transceivers is still intact.

Adopting the same approach used for the Image data link, the range of the RC Data link was calculated using Equation (7). For undisrupted transmission, the RC Signal Strength (*Si*) received by the UAV must be equal to or greater than the combined noise level and allocated link margin. From *"Taranis"* manual (Taranis, nd), the transmitted power is 100 mW (20 dBm). Similar to the Image data link, the average noise level measured from the two C2 data link test was used. Compensating for the lower transmission frequency, the range of the RC data link is shown with the following calculation.

$$Si = \quad P_T + k \text{ -}20*\log(R)$$

$$\textit{Noise Level +Link Margin} = \quad P_T + (k_{C2} \text{ - } \textit{Freq increase)} \text{ - } 20*\log(R)$$

$$-102.43 + 20 = \quad 20 + (-100.5 - 7.67) - 20*\log(R)$$

$$20*\log \textit{(R)} = \quad -5.74$$

$$R = \quad 0.52 \text{ km}$$

The calculated transmission range with a 20 dB link margin is 0.52 km. Without the link margin, the range increases to 5.16 km. At 4 km, the link margin is reduced from 20 dB to 2.22 dB. The distance rated for *"FrSky L9R"* receiver with a "*Taranis*" controller is 3 km to 5 km (Frsky L9R, nd). The comparable value between calculated and rated range provided further assurance on the assumptions for the *k* factor and noise level.

To reduce disruption to the RC data link within the 4 km range, the link margin is compensated with an increase in transmission power. However, amplification of RF power is limited to 1,000 mW (30 dBm) for a carrier signal at 2.4 GHz (Code of Federal Regulation, 2009: 824; Federal Communications Commission, 1996: 20). With an increase of 10 dB, the undisrupted range is increased to 1.6 km. Without the 20 dB link margin, the range is extended to 16.3 km. When operating at the 4 km range, the permissible link margin is reduced to 12.22 dB. The rated range for a 1,000 mW amplifier with 2.4 GHz is 4 to 8 miles (6.4 -12.9 km) (3DR Amplifier, nd).

The regulatory limit on the amplification of the transmitted power was attributed to the cap of 36 dBm on the EIRP when the antenna gain is specified at 6 dBi. However,

there is provision in the regulation to increase the antenna gain by reducing the transmitted power. At 30 dBm (1,000 mW) transmitted power, for every 3 dBi increase in antenna gain, the transmission power must be reduced by 1 dBm (Code of Federal Regulation, 2009: 825).

$$Si = P_T + k - 20*\log(R)$$

$$Noise\ Level + Link\ Margin = P_T + (k_{C2} - Freq\ increase + gain\ increase) - 20*\log(R)$$

$$-102.43 + 20 = 24.77 + (-100.5 - 7.67 + 13.5) - 20*\log(R)$$

$$R = 4.23 \text{ km}$$

If the transmission power is boosted to 300 mW (24.77 dBm) and a directional antenna with 19 dBi gain was used, there will be an overall increase of 18.27 dB in the range calculation in Equation (7). Recalling Section 2.4.5, the net gain in the *k* factor with the directional antenna will be reduced to 13.5 dBi. These modifications will ensure that there will be adequate link margin for the RC data link within the 4.23 km.

Table 17. Summary of Results for Different RC Data Link Configuration

Configuration	Range (km)			Link Margin at 4 km (dB)
	With 20 dB Link Margin	Without 20 dB Link Margin	Rated	
Normal	0.52	5.16	3 - 5	2.22
Antenna Gain (24 dBi)	4.35	43.45	NA	20.7
Increase Power (300mW)	1.6	16.33	6.4 - 12.9	12.22
Increase Power & Antenna Gain (19dBi)	4..23	42.32	NA	20.5

Geo-Fencing

Geo-Fencing is a feature on the *"Pixhawk autopilot"* that was not employed in previous AFIT research. This feature is adapted in the architecture to restrict the flight

profile of the UAS within a desired location and altitude range. The Geo-fence is set up on the geo-map in the "Mission Planner" with a polygon of maximum 18 points. The maximum and minimum altitude are also defined as part of the setup.

Ground tests were conducted to familiarize with the feature and to verify the response when the fence is breached. The details on the Geo-Fencing feature of "*Pixhawk autopilot*" are documented in Appendix B. Hardware in the Loop testing was carried out in the laboratory. The airborne sub-system was simulated through the software called "*Flight Gear*" which generates the necessary flight data to the "*Pixhawk autopilot*" though the "*Mission Planner*". However, due to compatibility issues between the versions of software that were available in the laboratory the desired response could not be simulated. Consequently, a ground test was setup.

The ground test was conducted with a partial setup of the system as shown in Figure 28. Without the propulsion subsystem, the "Air Vehicle" was carried and moved towards the Geo-fence line with the system set in "Manual flight" mode. Upon passing the fence line, the "*Pixhawk autopilot*" immediately switches itself into "Guide flight" mode with the direction of the UAV's intended heading aligning to the rally point in "*Mission Planner*".

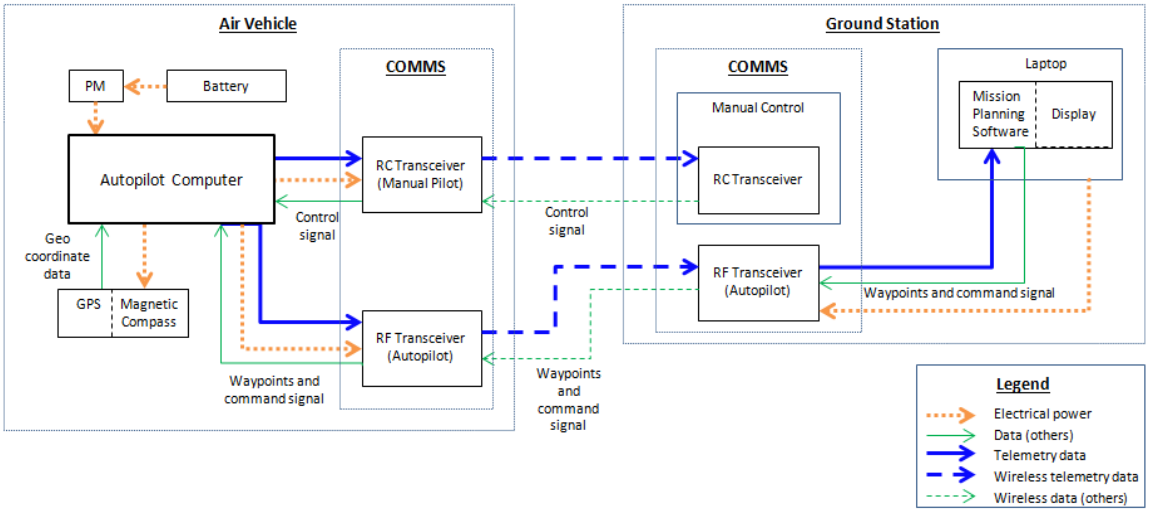

Figure 26: Setup for Geo-Fencing Ground Test

It must be highlighted that in flight, the Air Vehicle will require some time to change its flight profile and turn back to the rally point. Hence, some distance must be buffered for the Geo-fence. This distance will depend on the flight characteristics of the Air Vehicle, maximum prescribed bank angle and turning radius. Test flights within visual LOS will be conducted to verify the buffer distance required by the "*SIG Rascal 110*" to turn back to the rally point upon a breech in Geo-fence.

4.6 Final Architecture

The final architecture of the small UAS and the range of the various data links are shown in the following figure and table. The concept to operate the UAS beyond visual LOS is depicted in Figure 28. Progressing from bench tests, the architecture is incrementally tested in visual LOS flight to verify the various functions. The conduct of the test flights and its results will be discussed in the next chapter.

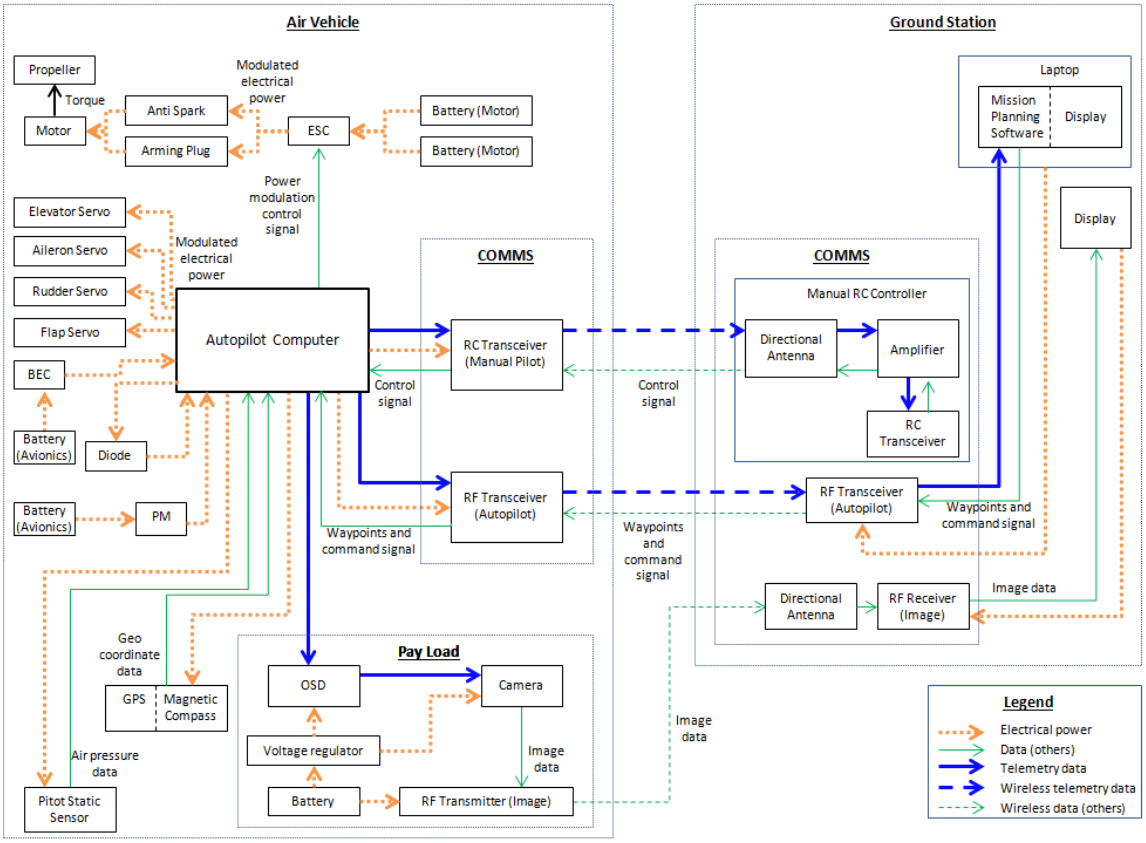

Figure 27: Final Architecture of UAS

Table 18. Summary of Transmission Range for Individual Data Links

Data link type	Frequency Range	Max. Range with 20 dB link margin	Link Margin at 4 km (dB)	Remark
C2	915 Mhz	20.48 km	34.18	Nil
RC	2.4 GHz	4.23 km	20.5	300 mW amplification and 19 dBi directional antenna
Image	5.8 Ghz	4.59 km	21.2	23 dBi directional antenna

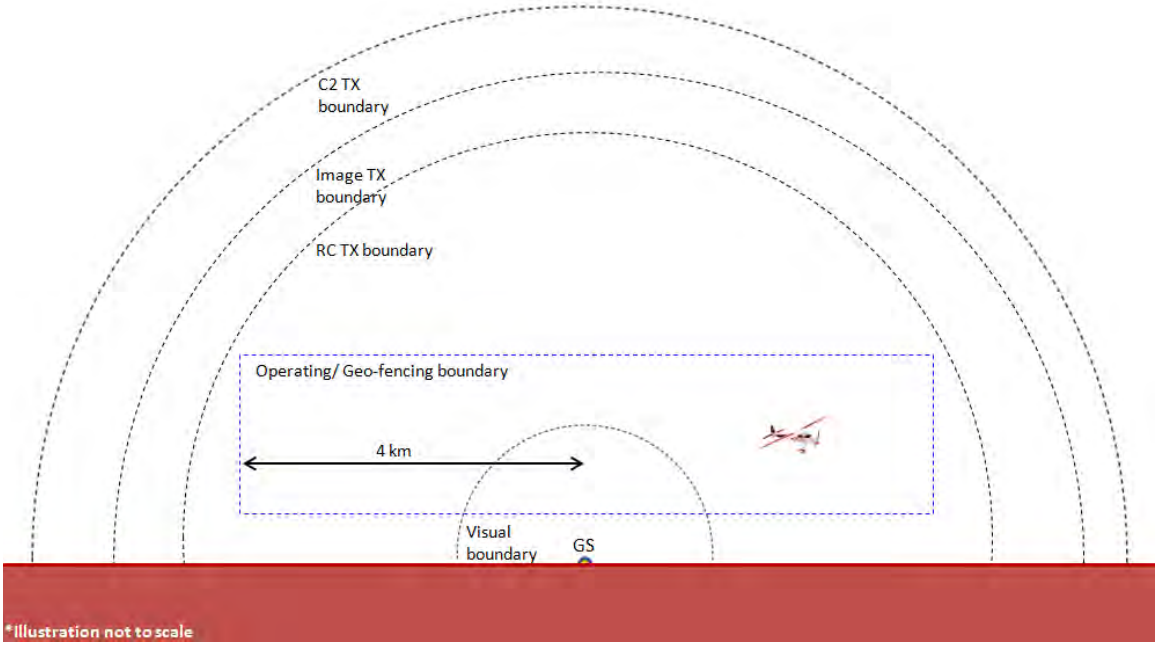

Figure 28: Concept for Beyond LOS Operation

4.7 Bill of Material

Using the empty weight cost of $10,000/lbs for the "*Dragon Eye*", the 11 lbs "*SIG Rascal 110*" would cost $110,000. Table 19 shows the BOM and the corresponding cost for the design. Base on the architecture with COTs component, the total cost is $2,094.24. Comparatively, a loss of a COTS based UAV will only cost 2% of an UAV that meets military specifications. The empty weight cost is calculated from the UAV and does not include the equipment and components at the GS. Refer to Appendix C for source reference on cost of product.

Table 19. Bill of Material for Final Architecture

Description	Qty	Unit Cost	Cost
Sig Rascal 110	1	$549.99	$549.99
Servo	7	$0.00	$0.00
Motor (HimaxHC6332-230 Brushless Electric Motor)	1	$199.99	$199.99
Propeller (APC 19x10E)	1	$12.99	$12.99
Anti Spark (50 Ohm resistor)	1	$0.00	$0.00
Arming Switch	1	$12.99	$12.99
ESC (120 A)	1	$265.95	$265.95
PM (45 V)	1	$21.28	$21.28
Pixhawk Autopilot computer	1	$199.99	$199.99
Telemetry Transmitter (RFD 900+ modem)	1	$89.50	$89.50
Telemetry Antenna (900MHz)	2	$7.95	$15.90
RC Transceiver	1	$38.95	$38.95
Video transmitter (Aomway 5.8 GHz TX 1000)	1	$84.90	$84.90
BEC	1	$24.99	$24.99
Diode	1	$0.00	$0.00
GPS/Magnetic Compass	1	$89.99	$89.99
Pitot-static Sensor	1	$54.99	$54.99
OSD	1	$16.32	$16.32
Camera (Hack HD camera PCB)	1	$164.95	$164.95
Voltage regulator (5 V)	1	$6.65	$6.65
Battery (Primary - 6 cell 8,000mAh)	4	$40.43	$161.72
Battery (Backup - 3 cell 1,300mAh)	2	$11.90	$23.80
Battery (Payload - 3 cell 1,300mAh)	1	$11.90	$11.90
	Total	$2,047.74	

4.8 Summary

This chapter began by defining the system specification for the requirements and the evaluation of key components. Thereafter, the iterative development for the physical architecture through the use of FMECA as a risk management approach was documented. A bill of material at the end of the chapter tabulates the cost of the UAV in the final architecture and compares it to the cost of a similar size UAV based on the empty weight cost of the "*Dragon Eye*". Incremental flight testing will be conducted within visual LOS

to progressively verify key aspects of the architecture to garner confidence before an actual flight beyond visual LOS. This progressive testing will be elaborated in the next chapter.

V. Test Results and Post Test Hazard Analysis

The MFR for the "*SIG Rascal 110*" prescribes that the UAV must always be maintained within visual LOS during operation, either by the operator or ground observers. This means that the UAV can fly beyond the visual LOS of the operator provided that a forward deployed observer maintains visual contact and has means of communication with the GS. Incremental flights test will be designed on this principle to progressively verify key aspects of the architecture.

5.1 Incremental Test Flights

A series of tests was designed to incrementally verify the capability of the architecture in order to garner confidence for an actual flight that is beyond visual LOS. The first series of flight tests is aimed at verifying the features in the architecture that were not present in previous research, namely the network capability of the "*RFD 900+*" and the Geo-fencing of the "*Pixhawk autopilot*".

The first series of flight tests was conducted within visual LOS from the operator and scaled down transmission power of the "*RFD 900+*" to simulate operation in a farther range. As the payload is not required for the test, the corresponding components were not installed. See the following figure for the tested architecture.

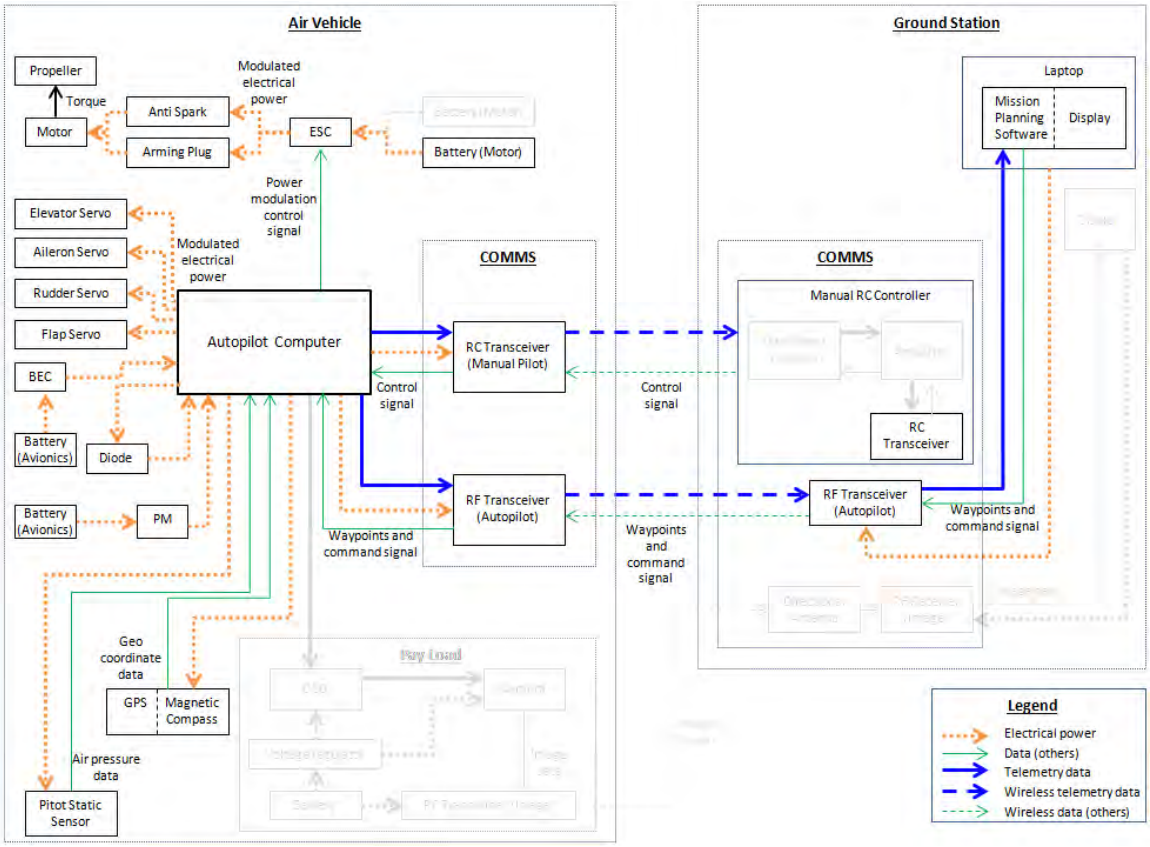

Figure 29: Architecture of Flight Tested UAS

In Section 4.3.1, it was discussed that the risk assessment for personnel safety during handling of the system will be addressed separately during the TRB/SRB process. The details on the aforementioned assessment, together with the test procedures, can be referenced to the approved TRB/SRB document (Seah, 2015).

5.1.1 Network Capability Test

Discussed in Section 4.2.5, the network capability of the "*RFD 900+*" transceiver can be used to gain confidence on the architecture so as to incrementally extend the operating range to beyond visual LOS. At the lowest transmission power (1 dBm) of the "*RFD 900+*" transceivers, the maximum allowable separation distance between the GS

and UAV was calculated. From Section 4.2.5 the measure k_{C2} is -80 dB. Using the average noise of -96.23 dB and factoring a 20 dB link margin, the calculated range from Equation (7) is 0.727 km

$$Si = P_T + k \text{ -20*log}(R) \quad (7)$$

$$\text{-96.23 + 20} = 1 \text{ -80 -20*log } (R)$$

$$R = 0.727 \text{ km}$$

From section 4.1.2, the range for visual LOS operation with "*SIG Rascal 110*"" is approximately 300 m and 600 m in "Manual mode" and "Autonomous mode", respectively. From section 4.5, the transmission range of the RC transceiver, with 20 dB link margin, is 520 m. To safely conduct a flight test that is permissible by the MFR, the two GSs were separated by approximately 200 m, a distance which the safety pilot can safely control the UAV in "Manual mode" from GS_1 in the event of an emergency.

A total of three tests were designed and conducted to verify the network capability of the UAS. This was carried out with the two GSs co-located next to each other. The capabilities tested were 1) updating of mission plan in the network, 2) network redundancy with one ground node disconnected and 3) network fail-safe with all ground nodes disconnected. These tests were conducted with a mission plan that is created between the two GS, and within the permitted flight altitude. The test flight envelope is reflected by the non-shaded area in the following figure.

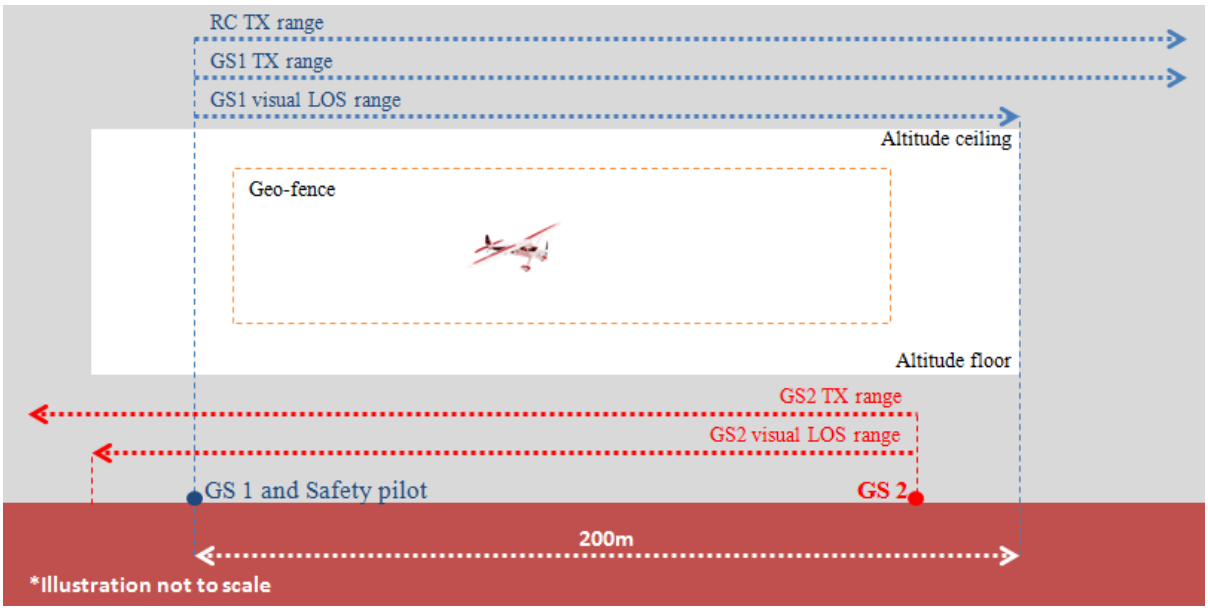

Figure 30: Airspace Envelope for Flight Test

Network Update

A flight test similar to the ground test conducted in Section 4.2.5 was replicated. While the UAV was loitering above a prescribed location in "Autonomous mode", a new waypoint was updated to the mission plan from GS_1, with GS_2 intentionally maintained with the outdated plan. No anomaly was observed when the UAV received the new mission plan and preceded flying towards the new waypoint. The telemetry and flight path of the UAV for the new mission plan was correctly reflected in both GSs. However, as the mission plan at GS_2 was not updated, the new flight path did not correspond to the outdated plan to loiter at the initial location. Nonetheless, this does not have any adverse effect on the UAS.

Network Redundancy

A second test was conducted to verify the robustness of the network. In a repetition of the first test, while the UAV is flying towards the new way point, the transceiver at GS_1 was disconnected. At the same time, the mission plan at GS_2 was refreshed. The test was successfully conducted with no anomaly observed on the UAS and the current mission plan.

Network Fail-Safe

The third test began with the UAV loitering above a prescribed location in "Autonomous mode". A new mission plan was updated from GS_1. While the UAV was executing the mission plan both GSs were disconnected and reconnected immediately. Reconnection took less than the allocated Fail-safe duration of 20 sec. During this period, no anomaly was observed on the UAV as it continues with its current mission plan.

The test was repeated, but this time, the two GSs were intentionally left disconnected beyond the 20 sec Fail-safe duration. It was observed that the UAV responded accordingly to the Fail-safe sequence and return to the launch site after 20 sec. Thereafter, the connection was reestablished and the UAV promptly resumed its last mission plan.

The three set of tests concluded that there will be no anomaly to the UAS as long as one GS remains in transmission with the UAV. It also demonstrated that the UAV will respond to the latest mission plan that is cached in its AP computer. Outdated mission plan reflected in the remaining ground nodes will not have an adverse effect to the UAS.

In the event of a GS reconnection after a complete loss of network transmission, the UAV will resume its current mission plan after it recovers from the fail-safe action.

5.1.2 Geo-Fencing Test

The Geo-fence was manually activated with a Pulse Width Modulation (PWM) signal from the RC console that was set above 1,750. The fence will remain activated as long as the AP computer receives a PWM signal that is above 1,750. The response to a breach in Geo-fence was verified for operations in the three commonly employed modes "Autonomous mode", "Stabilized mode" and "Manual mode". A Geo-fence was set around the GS with its boundary within visual LOS and the permissible flight altitude, refer to Figure 30. A rally point (location and altitude) was identified within the boundary for the UAV to return and loiter around when the fence is breached. This test was carried out with intentional breaches to the Geo-fence boundary.

The original intent was to activate the Geo-fence through "*Mission Planner*" from the GS. However, it was realized during the flight test that this approach was not feasible as PWM signal can only be transmitted from the RC console. The last available PWM switch on the RC console for the *Sig Rascal 110* was configured for a separate geo-mapping test and decision was made not alter the setup. The test was eventually carried out with a *Super Sky Surfer* UAS that was installed with the "*ArduPilot Mega*" AP computer instead. There is no difference in the Geo-fence feature for the "*Pixhawk*" and "*ArduPilot Mega*" AP computer as they share the same firmware and software.

From the GS, it was observed that the AP computer responded immediately upon a breach in the fence boundary. In all three modes, the UAV switched over to "Guided-

mode" and returned to the rally point when it breached the fence boundary. Once inside the boundary, the "Guided-mode" can be switched out through a cycle of the mode switch on the RC console to regain control of the UAV. Due to inertia, the UAV requires some response distance to change its flight heading and return back to the fence boundary. The turn radius will depend on the aerodynamic capability and the control setting of the UAV. For the *SIG Rascal 110*, a response distance of 30 m is recommended and should be factored in as part of the area where the UAV is not permitted to operate outside.

No anomaly was observed on the function of the Geo-fence feature. However, two operational concerns were noted during the test. Firstly, the flight path overlay on the map and Geo-fence boundary is only visible from the GS console. During "Manual mode" or "Stabilized mode" the safety pilot can only estimate the boundary and may not be aware that the UAV has breached the fence which result a switch to "Guided-mode". There is no indication of "Guide-mode" on the safety pilot's RC console. Without active communication from the GS to signal a breech in fence boundary, the safety pilot may misinterpret that there is a failure in the RC console as the UAV is not responding to the manual controls, resulting to unwarranted distress.

The second concern is on switching out from "Guided mode" after a breach in boundary. To toggle out of "Guided mode", the safety pilot will cycle the mode switch on the RC console. This however will not have any effect if the UAV is still outside the boundary. To regain control of the UAV while it is outside the fence, the safety pilot will

first have to de-activate the Geo-fence before toggling the mode switch. The safety pilot will similarly be subjected to unwarranted distress without familiarity to this response.

5.1.3 UAV Setting

The setting on the UAV was documented in Table 20 to facilitate replication of the system.

Table 20: Flight Setting of Autopilot Computer

Servo Gains	Roll Servo	Pitch Servo	Yaw servo
Proportional	1.5	1.5	1
Integral	0.04	0.07	0.1
Derivative	0.1	0.1	0.05
Max Integrator	15	15	15

Total Energy Control System	Max Climb	Min Sink	Max Sink	Pitch Dampening	Tine Constant
	5 (m/s)	2 (m/s)	5 (m/s)	0	5

Airspeed (m/s)	Cruise	Min Fly-by-wire	Max Fly-by-wire	Ratio
	20	12	40	1.994

Throttle (0-100%)	Cruise	Min	Max	Slew Rate
	50	20	60	100

Navigation Angle	Max Bank	Pitch Max	Pitch Min
	45	15	-25

L1 Control – Turn Control	Period	Damping
	25	0.75

Other Max	P to T	Rudder Mix
	-	0.5

5.1.4 Battery Consumption

The battery consumption for the motor and the avionics/servo were characterized to facilitate endurance planning for future research. When applying the consumption rate, a 10% safety factor is recommended as the flight condition and profile will not be the same for all operation.

- Average consumption rate for the avionics/servos bus was 2,700 mA per hour.
- Average consumption rate for the motor bus was 10,982 mA per hour.

5.2 Post Fight Test Hazard Analysis

Results from the flight test have verified the robustness of the network capability and the dependability of the Geo-fencing feature. No new or unforeseen hazard was observed during the test. The successful flight test provided assurance on the designed capability and paves the way for the next sequences of flight tests which will progressively and incrementally test the architecture's capability to extend the operating range beyond visual LOS. The subsequent sequence of flight tests is discussed in the next section.

5.3 Proposed Approach for Sequential Flight Test

The following sequence of flight tests is proposed to progressively test the architecture capability with incremental range. The aim is to collect test points at increased range for the application of a new MFR to operate beyond visual LOS.

Sequence Two Flight Test

The second sequence will test the full architecture of the UAS which includes the payload that was not installed during the first flight test. This test will be conducted within visual LOS at full transmission power, but with an increased separation distance between the two GS to 400 m which is twice that of the first sequence. A safety pilot will be positioned between the two GSs to retain the ability to control the UAV in "Manual

mode". This will facilitate as a backup in the event of an unforeseen failure with the architectural integration.

Seamless RF transmission is assured through the characterization of the various transceivers in Chapter 4. The separation distance of 400 m between the two GS will be within the 4 km designed transmission range (with 20 dB link margin). In addition, the flight boundary of the test envelope will also be contained by the Geo-fence. This is illustrated with the non-shaded area in the following figure.

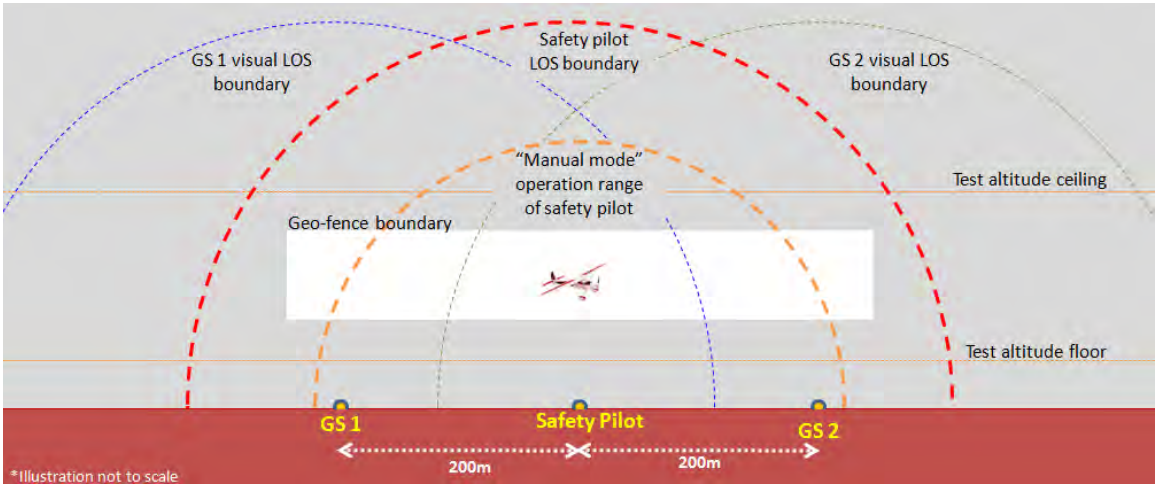

Figure 31: Concept for Second Sequence of Flight Test

Sequence Three Flight Test

A successful test flight on the second sequence would be the final verification to the integration of the full architecture and will provide assurance that the architecture will perform as designed. The third sequence of test flight will increase the separation distance between the two GSs to 1.4 km which exceed the visual LOS from the individual GS. This distance would also be the furthest operating range for past and current AFIT research on small UAS.

Complying with the MFR's requirement, the safety pilot will be positioned between the two GS to provide overlap and maintain visual LOS throughout the entire separation. From Chapter 4, the separation distance of 1.4 km between the two GS will be within the 4 km designed transmission range (with link margin). Hence, RF link for the C2 data and image data between the individual GS and the UAV would be maintained throughout the test boundary. This will be the same for the RC data link between the UAV and RC console of the safety pilot. Refer to the following figure for the concept of the third sequence of test flight.

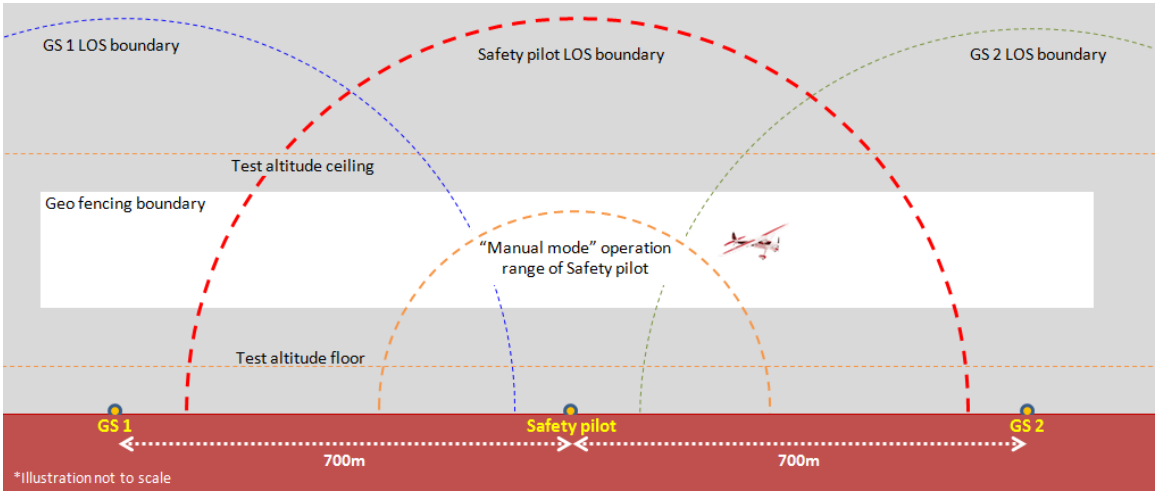

Figure 32: Concept for Third Sequence of Flight Test

Incremental testing with the three aforementioned sequences will provide the data points required to verify that the designed UAS can successfully operate over a distance of 1.4 km. The successful test points where GS_1 still has RF link with the UAV when it is flying above GS_2 can then be used to seek an approval for a second MFR to operate the UAS over the tested range of 1.4 km with a single GS. Thereafter, Sequence Three of

the flight test can be iterated to build upon the data points for an operating distance of 2.8 km between two GSs.

With the concluded test point, a third MFR will be sought to operate an UAV up to the range of 2.8 km with a single GS. The designed range of 4 km will finally be tested at the third iteration of Sequence Three flight test. Alternatively, with the second MFR to operate at a range of 1.4 km, four GSs can be arranged in a line with a total separation distance of 4.2 km between the first and last GS.

5.4 Summary

The flight test conducted for this research demonstrated the capability and robustness of the new features in the designed architecture that were not employed in previous AFIT research. The responses of the UAS to these features were also documented in the chapter to facilitate application of the architecture for possible future research efforts. Finally the achievement of the flight test with no new hazard observed reflects the level of comprehensiveness in the risk assessment and iterative designing process that was carried out in Chapter 4 of the research.

VI. Conclusions and Recommendations

This chapter concludes the research and highlights its significance. Thereafter, recommendations are also made for future work.

6.1 Conclusions of Research

The research has achieved two of the three objectives that were established in Section 1.2. The first objective is to develop the architecture for a small UAS, based on COTS components, which is capable of operating at a distance five times that of the visual LOS range. This was achieved through parametric analysis and ground testing.

The second objective is to establish a framework and document the development process to facilitate effective and reliable replication on other AFIT small UAS for future research. The effectiveness of the framework was demonstrated with the successful designing and testing of the UAS in a short period of nine months. The reliability of the UAS architecture developed through the framework was vindicated by the successful flight tests. Finally, the characterization data, test procedures and the results were documented to facilitate future replication.

The last objective to validate the designed architecture and to seek air worthiness to operate beyond visual LOS was not fully achieved. This was attributed to the incremental approach of flight testing and MFR revisions discussed in Chapter 5. This process required considerable lead time which extended beyond the duration of the research. Hence, a proposed sequence of flight testing was documented in Section 5.3 as a continuation to complete the remaining objective.

With the completion of this research, the three investigative questions identified in Section 1.3 were addressed as below.

i. *What are the requirements for a framework to effectively and reliably repeat the capability on other small UASs?*

A structured framework to repeat the development of the architecture and apply them on other UAS was adapted from the DoD System Engineering Process. The requirements were documented in Section 3.1 of this research.

ii. *What COTS components are required in a small UAS architecture to operate beyond visual LOS and how is the architecture integrated and validated?*

From the framework established for the previous question, the architecture of the small UAS to operate beyond visual LOS was developed through an iterative designing process. Integration and validation of the architecture was demonstrated by the successful conduct of flight test and documented in Chapter 4 and Chapter 5. The final architecture employed for the UAS is documented in Section 4.6. The COTS components required for the architecture can be found in Section 4.7 of this thesis.

iii. *What are the hazards associated with beyond visual LOS operation and how can they be mitigated to achieve airworthiness approval?*

The hazards associated with beyond LOS operation were identified and mitigated through the FMECA process. The outcome is summarized in Section 4.3.2 and the details can be found in Appendix A of the document.

The COTS based UAS architecture offered an economical alternative that required a shorter development time compared to conventional design and build approach. As a comparison to the empty weight cost of a conventional UAS with components that meets military specification, the COTS based "*SIG Rascal 110*" cost 98% less. The total development time from design and prototyping, including documentation, for the UAS took nine months.

6.2 Significance of Research

Two significant issues were drawn from the research. Firstly, the legally available COTS transceivers for the RC and Image data links selected to achieve a range of 4 km for the "*Sig Rascal 110*" is at the edge of current technological limits. To further increase the range, an improvement in technology to economically increase the sensitivity to the transceivers is required. This will increase the overall system gain in the link budget without exceeding the legal limit on the transmission power.

Alternatively, a change in transmitting frequency can be adopted. Indicated in Equation (2), a reduction in frequency will increase the transmission range at the same power. From the research on long range flights in Section 2.5.3, the following frequencies may be used as an alternative to increase the operating range with current technological limits.

Table 21: Comparison of Current and Alternate Transmission Frequencies

	C2 data link	RC data link	Image data link
Current	915 MHz	2.4 GHz	5.8 GHz
Alternative	No change	433 MHz	2.4 GHz or 1.3 GHz

To adopt the alternate frequencies, new considerations have to be addressed. In particular, license is required to transmit beyond 12 mW and 75 mW in the 433 MHz band and 1.3 GHz respectively.

Secondly, the use of COTS component has its inherent challenges in dealing with rapid changes in technology. The components identified for the architecture may be replaced by new and better alternatives and will no longer be available after a short span of time. The interface and relationship between the individual components architecture illustrated in the architecture will facilitate the selection and integration of new replacement components to the existing system.

6.3 Recommendations for Future Research

As a continuation to achieve a MFR to operate at the designed range of 4 km, the incremental testing proposed in Section 5.3 is recommended. In addition, the network capability of the C2 transceiver may be explored for multiple UAV control from a single GS. This can theoretically be achieved by configuring the GS as the base node instead of its current arrangement as a network node.

.

Bibliography

"3DR " (nd)
http://3drobotics.com/about/

“3DR Amplifier for 2.4 GHz” (nd)
https://store.3drobotics.com/products/2-4ghz-amplifier-1000mw

"3DR Modem Technical specification" (nd)
https://store.3drobotics.com/products/3dr-radio-915_mhz?taxon_id=40

Abatti James M. "Small power: the Role of Micro and Small UAVs in the Future". Research report, Air Command and Staff College, Air University, Maxwell Air Force Base. November 2005

Air Force Institute of Technology. *UAS Test Safety Review Process*. EN Operating Instruction 91-6. Ohio: Wright Patterson Air Force Base, 05 May 2014.

“Aomway 5.8GHz 1,000mW Video Transmitter” (nd)
http://www.fpvmodel.com/aomway-5-8g-1000mw-a-v-1w-transmitter-5-8g-32ch-receiver-for-fpv-_g509.html

"ArduPilot Firmware" (nd)
http://plane.ardupilot.com/wiki/arduplane-setup/apms-failsafe-function/

Beard Randal W. and Timothy W. Mclain. *Small Unmanned Aircraft; Theory and Practice*. Oxfordshire: Princeton University Press, 2012.

Christiansen Reed S. *Design of an Autopilot for Small Unmanned Aerial Vehicle.* MS thesis. Department of Electrical and Computer Engineering, Brigham Young University, August 2004.

Cline Charles Benjamin. *Method For Improving Airworthiness of Small UAS.* MS thesis. North Carolina State University, Raleigh North Carolina, 2008.

Code of Federal Regulation. *Telecommunication*. Title 47 Part 15, CFR: GPO 2009.

Code of Federal Regulation. *Aeronautics and Space*. Title 14 Part 21, CFR: GPO 2011.

“ISO/IEC/IEEE Definition of Architecture” (nd)
http://www.iso-architecture.org/ieee-1471/defining-architecture.html

Department of Air Force. *USAF Airworthiness*. Air Force Policy Directive 62-6. Washington: HQ USAF, 11 June 2010.

Department of Air Force. *USAF Airworthiness*. Air Force Instruction 62-601. Washington: HQ USAF, 12 May 2011.

Department of Defense. *MIL-STD-1629A.* DoD MIL_STD. Washington: GPO, 24 November 1980.

Department of Defense. *Failure Mode, Effect and Criticality Analysis (FMECA).* CRTA-FMECA; F30602-91-C-0002. Washington: GPO, April 1993.

Department of Defense. *Systems Engineering Fundamentals.* Washington: GPO, January 2001

Department of Defense. *Unmanned System Integrated Roadmap 2002-2027.* DoD Unmanned System Roadmap. Washington: GPO, December 2002

Department of Defense. *Airworthiness Certification Handbook.* DoD MIL-HDBK-516C. Washington: GPO, 2008.

Department of Defense. *Unmanned System Integrated Roadmap 2013-2038.* DoD Unmanned System Roadmap. Washington: GPO, 2013.

Department of Defense. *Defense Acquisition Guidebook.* Washington: GPO, 2015.

Department of Transport. *Unmanned Aircraft Operation in the National Air Space*. JO 7210.873. Washington: FAA, 11 July 2014.

Department of Transport. *Proposed New Rules for Small Unmanned Aircraft Systems*. Press Release. Washington: FAA, 15 Feburary 2015.

Department of Transport. *Operation and Certification of Small Unmanned Aircraft System*. Docket No.: FAA-2015-0150. Washington: FAA, 2015.

Diamond Theodore T, Adam L. Rutherford and Jonathan B. Taylor. *Cooperative Unmanned Aerial Surveillance Control System Architecture* MS thesis, AFIT/GSE/ENV/09-M07. School of Engineering and Management, Air Force Institute of Technology (AU), Wright-Patterson AFB OH, March 2009.
Federal Communications Commission. Understanding the FCC Regulations for Low-Power, Non-Licensed Transmitter. Bulletin No. 63. Maryland: Office of Engineering and Technology, February 1996.

"Economist, Joining the Drone Club" 15 August 2011
http://www.economist.com/node/21526053

Ford Thomas C. Class Lecture, SENG 640, Systems Architecture. School of Engineering and Management, Air Force Insititute of Technology, Wright-Patterson AFB OH, March 2014.

Freeman Paul and Gary J. Balas. "Actuation Failure Modes and Effects Analysis for a Small UAV," *America Control Conference* (Jun 2014).

"FrSky L9R 2.4 GHz Reciever Specification" (nd)
http://www.multiwiicopter.com/products/frsky-l9r-long-range-taranis-rx

Gertler Jeremiah. "US Unmanned Aerial Systems". Congressional Research Service, 03 January 2012.

Ghasemi Abdollah, Ali Abedi, farshid Ghasemi. *Propagation Engineering in Wireless Communications.* Springer-Verlag New York. 2012.

Gundlach Jay. *Designing Unmanned Aircraft System: A Comprehensive Approach.* Reston: American Institution of Aeronautics and Astronautics, Inc. 1975.

Jodeh Nidal M. *Development of Autonomous Unmanned Aerial Vehicle Research Platform: Modeling, Simulating, and Flight Testing.* MS thesis, AFIT/GAE/ENY/06-M18. School of Engineering and Management, Air Force Institute of Technology (AU), Wright-Patterson AFB OH, March 2006.

Jacques David, John Colombi. Class Lecture, SENG 650, Small UAS Design. School of Engineering and Management, Air Force Institute of Technology, Wright-Patterson AFB OH, March 2015.

Kwee Siam Seah. "Test Project Technical And Safety Review." TRB/SRB document ENV 1505, Air Force Institute of Technology (AU), Wright-Patterson AFB OH, August 2015.

Long Di, Yang Quan Chen, "Autonomous Flying Under 500 USD Based on RC Aircraft", *In Proceedings of 2011 ASME/IEEE International Conference on Mechatronic and Embedded Systems and Applications (MESA 2011)*, 28-31 (August 2011)

Maddalon Jeffrey M., Kelly J. Hayhurst, Daniel M. Koppen, Jason M. Upchurch, Harry A. Verstynen and A. Terry Morris. "*Perspectives on Unmanned Aircraft Classification for Civil Airworthiness Standard."* NASA/TM–2013-217969, National Aeronautics and Space Administration, Virginia. February 2013.

Miller, Jack."Strategic Significance of Drone Operation for Warfare," E-International Relations Students, 19 Aug 2013.
http://www.e-ir.info/2013/08/19/strategic-significance-of-drone-operations-for-warfare/

Ministry of Defence. *Unmanned Aircraft Systems: Terminology, Definitions and Classification*. MOD Joint Doctrine note 3/10: Swindon: Development, Concepts and Doctrine Centre, May 2010.

"Montiel Roberto Long Range FPV Flight – 55 km" 26 May 2011
http://planet-soaring.blogspot.com/2011/05/fpv-new-round-trip-record-flight-from.html

Murtha Justin Fortna. *An Evidence theoretic Approach To design Of Reliable Low-Cost UAVs.* MS thesis, Virginia Polytechnic Institute and State University, Blacksburg VA, July 2009.

"MyFlyDream Directional Antenna Specifications" (nd)
http://www.myflydream.com/index.php?main_page=product_info&cPath=1&products_id=5

"National Telecommunications and Information Administration - United States radio Frequency Allocation" August 2011
http://www.ntia.doc.gov/files/ntia/publications/spectrum_wall_chart_aug2011.pdf

Office of Management and Budget. *Budget of the United States Government, Fiscal Year 2015 Historical Tables* Washington: GPO, 2015

"Pixhawk Specification" (nd)
https://store.3drobotics.com/products/3dr-pixhawk?taxon_id=42

"RFD 900 Data Sheet" (nd)
http://rfdesign.com.au/downloads/RFD900%20DataSheet.pdf

Riiser Haakon, Tore Endestad, Paul Vigmostad, Carsten Griwood and Pal Halvon "Video Streaming Using a Location-based Bandwidth-lookup Service for Bitrate Planning." *ACM Transactions on Multimedia Computing, Communications, and Applications"*, Volume 8 Issue 3 Article 24:1-19 (July 2014)

Roberts Richard M. *Networking Fundamentals*. The Goodheart-Willcox Company Inc, 2012.

Sam Perlo-Freeman, Aude Fleurant, Pieter D. Wezeman and Siemon T. Wezeman. *Trends In World Military Expenditure, 2014*. SIPRI Fact Sheet. Solna Sweden, Stockholm International Peace Research Institute, April 2014.

Seibert Matthew T., Andrew J. Stryker, Jill R. Ward, Chris T. Wellbaum. *System Analysis and Prototyping for Single Operator Management of Multiple Unmanned Aerial Vehicles operating Beyond Visual Line of Sight*. MS thesis, AFIT/GSE/ENV/10-M01. School of Engineering and Management, Air Force Institute of Technology (AU), Wright-Patterson AFB OH, March 2010.

Shuck Timothy J. *Development of Autonomous Optimal Cooperative Control in relay Rover Configured Small Unmanned Aerial System.* MS thesis, AFIT/ENV-13M-27. School of Engineering and Management, Air Force Institute of Technology (AU), Wright-Patterson AFB OH, March 2013.

"Team BlackSheep Long Range FPV flight – 43.54 km" 20 October 2010 http://www.rcgroups.com/forums/showthread.php?t=1326375

"Taranis Instruction Manual"(nd) http://www.hobbyking.com/hobbyking/store/uploads/610533161X407442X46.pdf

United States Congress, *FAA Modernization and Reform Act of 2012.* Public Law No 95, 112th Congress. Washington: GPO, 14 February 2012

Appendix A: Failure Mode Effect and Criticality Analysis

1. Power Supply Sub-system

Component: Battery (Primary)							
Hazard		Effect		Mitigation	Prob	Severity	
Mode	Causal factor	Immediate	System			Health	Cost
Loss of component function	Component failure	-Loss of power to motor -Loss of power AP computer	-Loss of thrust -Aircraft enters into a controlled non-power descend	Design -**Separate power supply from avionics and payload** -**Dual power supply to AP computer** to maintain power to servo and transceivers -**Parallel battery arrangement** to maintain adequate voltage supply when one series of battery fails	E	IV	IV
Depleted capacity	Exceed planned duration			Procedure -*Pixhawk* has a configurable **Battery fail-safe** logic to initiate return to launch site when battery reached a set minimum voltage and/or battery capacity level.	E	IV	IV
	Insufficient Charge			Procedure -Labels to identify expended battery from charged ones	E	IV	IV
Loss connection	Connector failure			Procedure -Full-functional check prior to launch	E	IV	IV
	Loose connectors			Design -Used of **connector clips** to ensure security between wire connectors	E	IV	IV
				Overall	E	IV	

Component: Battery (laptop)							
Hazard		Effect		Mitigation	Prob	Severity	
Mode	Causal factor	Immediate	System			Health	Cost
Loss of component function	Component failure	-Loss of power to GS transceivers, *Mission Planner* and monitor display	-Loss of telemetry monitoring and capability to amend mission plan in flight	<u>Design</u> -Redundancy of power supply from generator	E	IV	IV
Depleted capacity	Exceed planned duration						
	Insufficient Charge						
Loss connection	Connector failure						
	Loose connectors						
				Overall	E	IV	

2. Sensor Sub-system

Component: GPS / Magnetic Compass							
Hazard		Effect		Mitigation	Prob	Severity	
Mode	Causal factor	Immediate	System			Health	Cost
Loss of GPS Link (Unable to be re-established)	Inadequate number of satellite signal	-AP loses orientation	-Uncontrolled flight heading and altitude. -Loss of autonomous capability, air vehicle is unable to proceed to way point	<u>Procedure</u> -In autonomous mode, *Pixhawk* has a configurable **GPS fail-safe** logic that initiate circling at location when GPS signal is loss for more than 3 seconds. Return to launch site via dead reckoning will be initiated if loss in GPS link exceeds 20 sec <u>Design</u> -Switch to **manual backup mode** and land air vehicle via FPV	D	IV	IV
Loss of component function	Component failure				E	IV	IV
				Overall	D	IV	

Component: Pitot-static Sensor							
Hazard		Effect		Mitigation	Prob	Severity	
Mode	Causal factor	Immediate	System			Health	Cost
Leak in air tube	Damage during installation/handling	-Lower air pressure to sensor	-Lower air speed perceived by AP.	-Latent failure. Non observable unless sever leak resulted to perceived airspeed is lower than minimum airspeed limit.	E	IV	IV
Erratic air pressure data output	Intermittent failure of sensor	-Fluctuating air pressure from sensor	-Fluctuating air speed perceived by AP.	-Latent failure. Non observable unless fluctuation is significant and noticed by the ground operator.	E	IV	IV
Loss of component function	Component failure	-Loss of air pressure data	-Loss of air speed data	<u>Procedure</u> -Unverified effect in autonomous mode <u>Design</u> -Switch to **manual backup mode** and fly air vehicle back manually via FPV	E	IV	IV
				Overall	E	IV	

3. Transceiver Sub-system

<table>
<tr><th colspan="6">Component: Telemetry/command transceiver</th></tr>
<tr><th colspan="2">Hazard</th><th colspan="2">Effect</th><th rowspan="2">Mitigation</th><th rowspan="2">Prob</th><th colspan="2">Severity</th></tr>
<tr><th>Mode</th><th>Causal factor</th><th>Immediate</th><th>System</th><th>Health</th><th>Cost</th></tr>
<tr><td>Loss of component function</td><td>Component failure</td><td rowspan="3">-Loss of telemetry data</td><td rowspan="3">-Air vehicle performance cannot be monitored from the GS

-New mission plan cannot be updated to the air vehicle</td><td><u>Procedure</u>
-Pixhawk has a configurable GS fail-safe logic to initiate circling at location when telemetry link is lost for more than 1.5. A return to launch site will be initiated when loss of telemetry link exceeds 20 sec</td><td>E</td><td>IV</td><td>IV</td></tr>
<tr><td rowspan="2">Loss of transmission data</td><td>Exceed transmission range</td><td><u>Procedure</u>
-Geo-fence can be programmed into the AP computer to initiate a return to launch site when the air vehicle fly beyond the set boundary</td><td>E</td><td>IV</td><td>IV</td></tr>
<tr><td>Signal interference</td><td><u>Design</u>
-Separate frequency spectrum between different transceiver in the UAS

-Select modem with frequency hopping capability</td><td>E</td><td>IV</td><td>IV</td></tr>
<tr><td colspan="5">Overall</td><td>E</td><td colspan="2">IV</td></tr>
</table>

Component: RC transceiver							
Hazard		Effect		Mitigation	Prob	Severity	
Mode	Causal factor	Immediate	System			Health	Cost
Loss of component function	Component failure	-Loss RC communication link	-Loss of backup manual capability by UAS	Procedure -*Pixhawk* has a configurable **Throttle fail-safe** logic to initiate circling at location when RC link is lost for more than 1.5 sec. If link lost exceeds 20 sec, a return to launch site will be enabled	E	IV	IV
Loss of transmission data	Exceed transmission range			Procedure -**Geo-fence** can be programmed into the AP computer to initiate a return to launch site when the air vehicle fly beyond the set boundary	E	IV	IV
	Signal interference			Design -**Separate frequency spectrum** between different transceiver in the UAS -Select modem with **frequency hopping capability**	E	IV	IV
				Overall	E	IV	

4. Servo Sub-system

Component: Aileron							
Hazard		Effect		Mitigation	Prob	Severity	
Mode	Causal factor	Immediate	System			Health	Cost
Loss of component function	Component failure	-Loss of servo movement	- Loss of rolling capability by air vehicle	Procedure -Unverified effect in autonomous mode Design -Switch to **manual backup mode** and fly air vehicle back manually via FPV without affected servo	E	IV	IV
Erratic servo response	Intermittent failure of servos	-Servo does not respond according to input command	- Chattering of control surface as AP constantly corrects for the servo deflection	Design -Switch to **manual backup mode** and fly air vehicle back manually via FPV without affected servo	E	IV	IV
				Overall	E	IV	

Component: Elevator							
Hazard		Effect		Mitigation	Prob	Severity	
Mode	Causal factor	Immediate	System			Health	Cost
Loss of component function	Component failure	-Loss of servo movement	-Loss of pitching capability by air vehicle	Design -Unverified effect in autonomous mode -Switch to **manual backup mode** and fly air vehicle back manually via FPV without affected servo	E	IV	IV
Erratic servo response	Intermittent failure of servos	-Servo does not respond according to input command	- Chattering of control surface as AP constantly corrects for the servo deflection	Design -Switch to **manual backup mode** and fly air vehicle back manually via FPV without affected servo	E	IV	IV
				Overall	E	IV	

Component: Rudder							
Hazard		Effect		Mitigation	Prob	Severity	
Mode	Causal factor	Immediate	System			Health	Cost
Loss of component function	Component failure	-Loss of servo movement	-Loss of yawing capability by air vehicle	Design -Unverified effect in autonomous mode -Switch to **manual backup mode** and fly air vehicle back manually via FPV without affected servo	E	IV	IV
Erratic servo response	Intermittent failure of servos	-Servo does not respond according to input command	-Chattering of control surface as AP constantly corrects for the servo deflection	Design -Switch to **manual backup mode** and fly air vehicle back manually via FPV without affected servo	E	IV	IV
				Overall	E	IV	

Component: Flap							
Hazard		Effect		Mitigation	Prob	Severity	
Mode	Causal factor	Immediate	System			Health	Cost
Loss of component function	Component failure	-Loss of servo movement	-Loss in additional lift and braking capability by air vehicle	Design -Unverified effect in autonomous mode -Switch to **manual backup mode** and fly air vehicle back manually via FPV without affected servo	E	IV	IV
Erratic servo response	Intermittent failure of servos	-Servo does not respond according to input command	- Chattering of control surface as AP constantly corrects for the servo deflection	Design -Switch to **manual backup mode** and fly air vehicle back manually via FPV without affected servo	E	IV	IV
				Overall	E	IV	

5. Propulsion Sub-system

Component: Motor							
Hazard		Effect		Mitigation	Prob	Severity	
Mode	Causal factor	Immediate	System			Health	Cost
Loss of component function	Component failure	-Loss of torque to propeller	-Loss of lift to wings	Design -Switch to **manual backup mode** for controlled non power manual landing via FPV	E	III	IV
				Overall	E	III	

Component: Propeller							
Hazard		Effect		Mitigation	Prob	Severity	
Mode	Causal factor	Immediate	System			Health	Cost
Loss of component function	Component failure Mid air collision with birds	-Loss of thrust from propeller	-Loss of lift to wings	Design -Switch to **manual backup mode** for controlled non power manual landing via FPV	E	III	IV
				Overall	E	III	

Severity for failure of motor or propeller is accorded as category III due to possible risk to personnel safety if unaware personnel did not get out of the landing path of the UAV.

6. Control Sub-system

Component: Autopilot Computer							
Hazard		Effect		Mitigation	Prob	Severity	
Mode	Causal factor	Immediate	System			Health	Cost
Complete loss of component function (lose bypass logic to manual mode)	Component failure	-Loss of power to motor, servo and transceiver	-Aircraft enters into an non-power and un-controlled descend with servos fixed in the last position prior to loss of AP	Procedure -Announce loss of control and inform personnel to stay clear of the air vehicle's descend path	E	III	III
Partial loss of component function (minimally retains bypass logic to manual mode and power supply to servo)		-Loss of power to motor and transceiver	-Loss of lift and telemetry link	Design -Switch to **manual backup mode** for controlled non power manual landing via FPV -**Separate power supply to payload subsystem** to maintain FPV	E	IV	IV
				Overall	E	III	

Severity for complete failure of AP computer is accorded as category III due to possible risk to personnel safety if unaware personnel did not get out of the landing path of the UAV. The severity to cost was also accorded as category III attributing to the potential cost of property damage that the air vehicle may crash into as there is no mean to control the directions during the gliding descend.

Component: ESC							
Hazard		Effect		Mitigation	Prob	Severity	
Mode	Causal factor	Immediate	System			Health	Cost
Loss of component function	Component failure	-Loss of power to motor	-Aircraft enters into an non-power and un-controlled descend	Design -Switch to **manual backup mode** for controlled non power manual landing via FPV	E	III	IV
Erratic power supply	Intermittent failure	-ESC does not send correct power to motor	-Fluctuating air speed resulting to fluctuating lift as AP constantly corrects for prescribed altitude	Design -Switch to **manual backup mode** for controlled non power manual landing via FPV	E	IV	IV
Run away power supply	ESC internal short circuit	-Surge in power supply exceed motor rated limit and melts magnetic coil	-Loss of motor resulting to loss of lift	Design -**Power module to limit maximum current** to ESC	E	IV	IV
				Overall	E	III	

Severity for complete failure of ESC is accorded as category III due to possible risk to personnel safety if unaware personnel did not get out of the landing path of the UAV.

Component: BEC							
Hazard		Effect		Mitigation	Prob	Severity	
Mode	Causal factor	Immediate	System			Health	Cost
Loss of component function	Component failure	-Loss of power to AP computer	-Aircraft enters into an non-power and un-controlled descend with servos fixed in the last position prior to loss of AP	Design -**Dual power supply** to AP computer	E	IV	IV
				Overall	E	IV	

Component: Mission Planning Software							
Hazard		Effect		Mitigation	Prob	Severity	
Mode	Causal factor	Immediate	System			Health	Cost
Loss of component function	Component failure	-Loss of mission planning capability, telemetry	-Loss of mission planning capability and telemetry display at GS	Procedure -Program switch **to initiate return to launch site on manual RC controller**	E	IV	IV
				Overall	E	IV	

Component: Manual RC Controller							
Hazard		Effect		Mitigation	Prob	Severity	
Mode	Causal factor	Immediate	System			Health	Cost
Loss of component function	Component failure	-Manual backup mode	-No effect in autonomous mode	Procedure **-Initiate return to launch site in autonomous mode**	E	IV	IV
				Overall	E	IV	

Component: Laptop							
Hazard		Effect		Mitigation	Prob	Severity	
Mode	Causal factor	Immediate	System			Health	Cost
Loss of component function	Component failure	-Loss of mission planning capability, telemetry and image display at GS	-Loss of mission planning capability, telemetry and image display at GS	Design -Switch to **manual backup mode** for controlled non power manual landing via FPV **-Separate monitor to display FPV image** **-OSD to provide telemetry display on FPV image**	E	IV	IV
				Overall	E	IV	

Appendix B: Setup for Pixhawk Autopilot Computer (ArduPilot, nd)

Several features and fail-safe functions on the *"Pixhawk Autopilot"* were utilized to mitigate the risks identified in the FMECA. The fail-safes applied were 1) Throttle Fail-Safe, 2) GS Fail-Safe, 3) Battery Fail-Safe and 4) GPS Fail-Safe. Features of *"Pixhawk Autopilot"* employed in the architecture include geo-fence and dual power capability.

The fail-safes were invoked by setting the necessary parameters in the configuration through the *"Mission Planner"*. Configuration setting of the fail-safe is carried out in the "Advance Params" function found under "Configuration" in the toolbar. It is to note that different versioning of the *"Mission Planner"* has different Graphic User Interface. In this research, *"Mission Planner"* version 1.3.24 was used.

1. Fail-Safe Action

The various types of fail-safe mention above will conclude into different predefined actions after it has been triggered. The actions for the individual fail-safe differs from each other, some only have a single action, while others may have a series of actions depending on how the parameters are configured.

Fail-safes that have a series of action have two modes of responses. These are configured into the *"Pixhawk Autopilot"* as "FS_SHORT_ACTN" (Short Fail-Safe Response) and "FS_LONG_ACTN" (Long Fail-Safe Response). Each mode of response will maintain a duration based on the value specified in "FS_SHORT_TIMEOUT" and

"FS_LONG_TIMEOUT" before concluding its predefined action. The table below summaries the description of the two modes of responses used in the architecture.

Table 22: Summary of Fail-Safe Response

Mode	Parameter Name	Value	Action Description
Short Fail-Safe Response	FS_SHORT_TIMEOUT	"1.5"	-Duration of failure associated with mode of fail-safe before "Short Fail-Safe Response" is initiated. -Default 1.5 second is used for the architecture
	FS_SHORT_ACTN	"0"	Nil (Disabled)
		"1"	Circle in current location
		"2"	Glide Landing with zero throttle setting and servo deflection
Long Fail-Safe Response	FS_LONG_TIMEOUT	"20"	-Duration of failure associated with mode of fail-safe before "Long Fail-Safe Response" is initiated. -Default 20 second is reduced for the architecture
	FS_LONG-ACTN	"0"	Nil (Disabled)
		"1"	Return to launch location
		"2"	Glide Landing with zero throttle setting and servo deflection

2. Throttle Fail-Safe

Throttle input controls the rotational speed of the electrical motor which in turn determines the amount of thrust generated by the propeller. This input is sent from the RC console to the onboard AP computer as a Pulse Width Modulation (PWM) signal where higher throttle input relates to higher PWM frequency. On board the air vehicle, the AP computer interprets the PWM frequency and translates it into corresponding current amperage for the motor.

Throttle Fail-Safe is activated when the received PWM frequency by the AP computer is lower than the predefined frequency at the minimum throttle input. This situation occurs when there is a component failure in the RC subsystem or when the air vehicle exceeded the transmission range of the RC transceivers. It is to note that the RC controller will generate an audio warning when the received signal strength reached the

preset low threshold as the air vehicle operates near its maximum transmission range or in the presence of interference.

Throttle fail-Safe is enabled when the "THR_FAILSAFE" parameter is set as "1" and is triggered when the PWM frequency drops below the "THR_FS_VALUE" parameter. The value input for the "THR_FS_VALUE" parameter must be lower than the frequency when the throttle is at the minimum position. For the *"Taranis"* RC controller used in this research, the associated "THR_FS_VALUE" value is set below 925.

The fail-safe action will depend on how the two modes of response are configured; see previous section on Fail Safe Action. Depending on the configured parameter, "FS_SHORT_ACTN' (Short Fail-Safe Response) will be invoked when the duration of the associated fault exceeds the value for "FS_SHORT_TIMEOUT". As the fault persists beyond the value set for "FS_LONG_TIMEOUT", the "FS_LONG_ACTN' (Long Fail-Safe Response) will be initiated. See Figure 33 for the sequence of the Throttle Fail-Safe Response.

The contingency procedure mentioned Figure 33 is to initiate "Autonomous mode" through the GS and input a command to launch return the UAV back to the launch site. With a loss in function of the RC console, the safety pilot cannot land the UAV manually. This will be replaced by an autonomous landing that is activated through the GS.

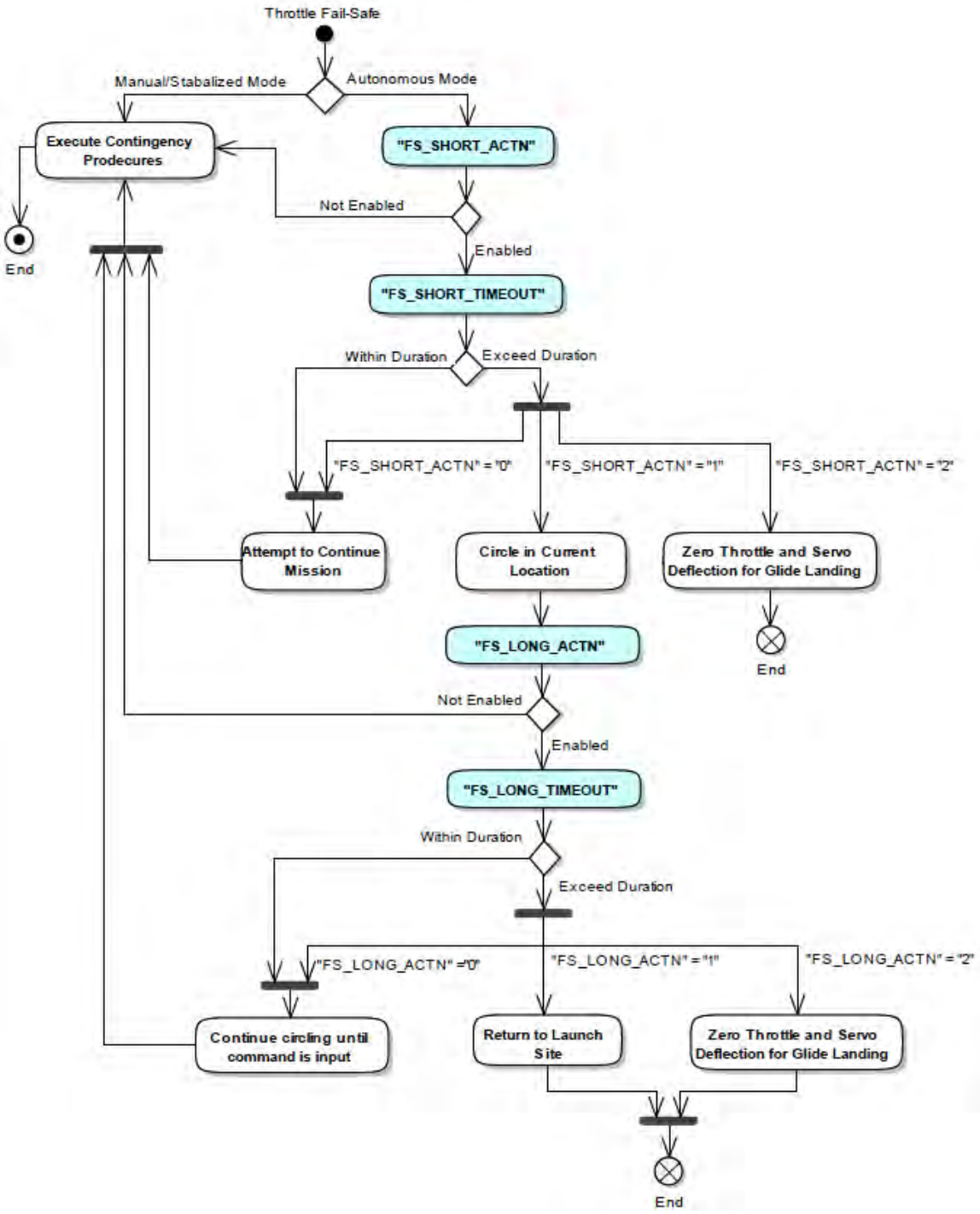

Figure 33: Sequence of Throttle Fail-Safe Response

3. GS Fail-Safe

Telemetry protocol message is continuously transmitted from the GS to the air vehicle. The AP computer will interpret a loss of communication link with the GS if there is protocol message is not received. When the value of "FS_GCS_ENABLE" parameter is set to "1", GS Fail-Safe is enabled. The response of the GS Fail-safe is similar to the Throttle Fail-safe and will depend on the Fail-safe action defined in Section 1 of this appendix. However, the contingency procedure for the GS Fail-safe is different from the Throttle Fail-safe. For GS Fail-safe, the Safety pilot will select "Manual mode" or "Stabilized mode" from the RC console and land the aircraft manually.

4. Battery Fail-Safe

Battery Fail-Safe triggers a return to launch site when the voltage or current drops below the values specified in the parameter configuration for the main power bus to the AP computer. The parameters associated with this function are "FS_BATT_VOLTAGE" and "FS_BATT_MAH" with default values set as "0" which disable the fail-safes. Changing the parameter to the desired values will enable the fail-safe function. The unit of measure associated with "FS_BATT_VOLTAGE" is in volt and "FS_BATT_MAH" is in mAH.

5. GPS Fail-Safe

GPS Fail-Safe can only be set up after enabling the Advance Fail Safe function of the "*Pixhawk* autopilot". The Advance Fail Safe is enabled by setting the "AFS_ENABLE" parameter to '1'. The GPS fail safe will be triggered if GPS lock is loss

for more than 3 seconds and will return to the waypoint number that was specified in the "AFS_WP_GPS_LOSS" parameter. For example, when the parameter is set to '5' the UAV will return to the number 5 waypoint that was set in the mission plan.

Thereafter, the UAV will loiter above the way point. If GPS link is restored, the UAV will resume its mission. However if the GPS link is not restored after 30 second, the AP computer will stop the mission and return the UAV to the launch site.

It is to note that the GPS Fail-safe has an association with GS Fail-safe. In the event that GS link with the UAV is loss together with the GPS link, the AP computer will terminate the operation by setting the throttle to zero and deflects all control surface to maximum. This will result to the UAV spiraling to the ground.

6. Geo-fencing

There are two modes of activation for the Geo-fence. The first mode is via a RC channel input with a PWM value above 1,750. This PWM signal must be maintain throughout the entire duration when the fence is activated. The second mode of activation is via the parameter "FENCE_AUTOENABLE". When set to the value of '1', the Geo-fence will be automatically enabled after an autonomous take-off.

Appendix C: Source Reference for Components in Architecture

Battery Sizing

Preliminary sizing of the battery for a system endurance of 0.5 hr was conducted to allocate suitable costing for the various power supplies for the sub-systems. The 'Usable Energy' of a battery will depend on the 'Battery Efficiency' and 'Usable Factor' which are typically 0.8 (Gundlach, 1975:72).

$$Energy_{battery} = Capacity * Voltage * n_{battery} * f_{usable} \quad (8)$$

Payload Battery

Table 23: Calculated Payload Battery Consumption

Component	Voltage (V)	Current (mA)	Power Required = Voltage * Current (mW)
Transmitter	3.7 – 5	500	2,500
Camera	5 - 12	700	8,400
OSD	5	500	2,500
		Total	13,400 mW

$$\begin{aligned} Battery_{usable} &= Capacity * n_{battery} * f_{usable} \quad (9) \\ &= 1{,}300 * 0.8 * 0.8 \\ &= 832 \text{ mAhr} \end{aligned}$$

From Equation (8), the usable battery capacity is derived to give Equation (9). A 3 cell Lithium Polymer (LiPo) battery with output voltage of 11.1 V and capacity of 1,300 mAhr was selected. From Equation (9), the battery 'Usable Capacity' is derived at 832 mAhr. The total capacity current required by the payload sub-system from the battery is

1,207 mA $\left(\frac{13{,}400\ \text{W}}{11.1\ \text{V}}\right)$. Hence, with 832 mAh 'Usable Capacity', the endurance for the Payload sub-system is 0.69 hr.

Motor Battery

The capacity of the primary battery is determined by numerous factors. These include duration of the mission, motor size, flight profile of the UAV, take-off weight, transceiver transmission power and wind condition. From earlier research efforts, four 6 cell batteries were arranged in parallel, each with a pair of battery in series was used to power the "*SIG rascal 110*". Each battery is 22.2 V and carries a capacity of 5,000 mA. A 20 minutes flight was achieved with 10,000 mA at 44.4 V at the end of the test. However, the specific utilization rate was not documented. The same battery configuration was retained but in the new architecture, it is only powering the motor and not the entire UAV. From Chapter 5, the average consumption rate for the motor bus was 10,982 mA per hour. The selected battery configuration is expected to have an excess of 45% capacity to support a 0.5 hr flight. Factoring for battery usable capacity, the configuration would still have an excess of 9% capacity after a 0.5 hr flight.

Avionics Battery

The avionics battery supplies power the AP computer, which in turn powers the servos, transceivers and GPS. In the event of a loss in propulsion, the operator will switch to 'Manual Mode' and glide the UAV to a clear location for landing. The current consumption of the avionics is relatively small compared to the motor. To reduce diversity in parts, the same 3 cell LiPo battery (11.1 V, 1,300 mAhr) selected for the

payload sub-system were used to power the avionics system. Similar to the motor battery, the utilization rate will be measured in Chapter 5 to verify adequacy of the capacity.

Table 24: Source Reference for Components in Architecture

S/N	Description	Reference website
1	Sig Rascal 110	http://www.sigplanes.com/SIG-Rascal-110-EG-ARF_p_232.html
2	Servo	comes with air vehicle
3	Motor (HimaxHC6332-230 Brushless Electric Motor)	http://www.sigplanes.com/SIG-Rascal-110-EG-ARF_p_232.html
4	Propeller (APC 19x10E)	http://www.sigplanes.com/SIG-Rascal-110-EG-ARF_p_232.html
5	Anti Spark (50 Ohm resistor)	Consumable hardware - negligible cost
6	Arming Switch	http://www.sigplanes.com/SIG-Rascal-110-EG-ARF_p_232.html
7	ESC (120 A)	http://www.castlecreations.com/products/phoenix-edge-lite-hv.html
8	PM (45 V)	http://www.hobbyking.com/hobbyking/store/__56855__HKPilot_Mega_10s_Power_Module_With_XT60_Connectors.html
9	Pixhawk Autopilot computer	https://store.3drobotics.com/products/3dr-pixhawk/?utm_source=google&utm_medium=cpc&utm_term=branded&utm_campaign=branded&gclid=CPWikYGcuMYCFVU6gQodTpkJUg
10	Telemetry Transmitter (RFD 900+ modem)	http://store.jdrones.com/RDF900_Telemetry_Modem_p/rdf900mdm1.htm
11	Telemetry Antenna (900MHz)	https://store.3drobotics.com/products/antenna-900mhz-rp-sma-2dbi?taxon_id=34
12	RC Transceiver (2.4 GHz)	http://www.multiwiicopter.com/products/frsky-l9r-long-range-taranis-rx
13	Video transmitter (Aomway 5.8 GHz TX 1000)	http://www.fpvmodel.com/aomway-5-8g-1000mw-a-v-1w-transmitter-5-8g-32ch-receiver-built-in-dvr-for-fpv_g602.html
14	BEC	https://store.3drobotics.com/products/apm-power-module-with-xt60-connectors?taxon_id=34
15	Diode	Consumable hardware - negligible cost
16	GPS/Magnetic Compass	https://store.3drobotics.com/products/3dr-gps-ublox-with-compass
17	Pitot-static Sensor	https://store.3drobotics.com/products/pixhawk-airspeed-sensor-kit?taxon_id=34
18	OSD	http://www.hobbyking.com/hobbyking/store/__80102__Minim_OSD_for_APM_or_Pixhawk_Flight_Controllers.html
19	Camera (Hack HD camera PCB)	http://hackhd.com/

S/N	Description	Reference website
20	Voltage regulator (5 V)	http://www.hobbyking.com/hobbyking/store/__41922__Blue_Arrow_Ultra_Micro_Automatic_Voltage_Regulator_5V_1A_DC_Output.html
21	Battery (Motor - 6 cell 5,000mAh)	http://www.hobbyking.com/hobbyking/store/__9176__Turnigy_5000mAh_6S_20C_Lipo_Pack.html
22	Battery (Avionics - 3 cell 1,300mAh)	http://www.hobbyking.com/hobbyking/store/__11903__Turnigy_nano_tech_1300mah_3S_25_50C_Lipo_Pack.html
23	Battery (Payload - 3 cell 1,300mAh)	http://www.hobbyking.com/hobbyking/store/__11903__Turnigy_nano_tech_1300mah_3S_25_50C_Lipo_Pack.html

REPORT DOCUMENTATION PAGE

Form Approved
OMB No. 0704-0188

PLEASE DO NOT RETURN YOUR FORM TO THE ABOVE ADDRESS.

1. REPORT DATE *(DD-MM-YYYY)*	2. REPORT TYPE	3. DATES COVERED (From – To)
09-17-2015	Master's Thesis	Sep 2014 – Sep 2015

4. TITLE AND SUBTITLE

System Architecture of Small Unmanned Aerial System for Flight Beyond Visual Line-of-Sight

5a. CONTRACT NUMBER

5b. GRANT NUMBER

5c. PROGRAM ELEMENT NUMBER

6. AUTHOR(S)

Kwee Siam, Seah. Military Expert 5 (Major), Republic of Singapore Air Force

5d. PROJECT NUMBER

5e. TASK NUMBER

5f. WORK UNIT NUMBER

7. PERFORMING ORGANIZATION NAMES(S) AND ADDRESS(S)

Air Force Institute of Technology
Graduate School of Engineering and Management (AFIT/EN)
2950 Hobson Way
WPAFB OH 45433-7765

8. PERFORMING ORGANIZATION REPORT NUMBER

AFIT-ENV-MS-15-S-047

9. SPONSORING/MONITORING AGENCY NAME(S) AND ADDRESS(ES) AGENCY (spelled out)

AFRL/RQQA
2210 8th Street Bldg 146, Room 300 Wright-Patterson AFB, OH 45433 COMM 937-713-7038
Email: derek.kingston@us.af.mil

10. SPONSOR/MONITOR'S ACRONYM(S)

AFPL/RQQA

11. SPONSOR/MONITOR'S REPORT NUMBER(S)

12. DISTRIBUTION/AVAILABILITY STATEMENT

DISTRIBUTION STATEMENT A. APPROVED FOR PUBLIC RELEASE; DISTRIBUTION UNLIMITED.

13. SUPPLEMENTARY NOTES

14. ABSTRACT

Small Unmanned Aerial Systems (UAS) have increasingly been used in military application. The application in expanding scope of operations has pushed existing small UAS beyond its designed capabilities. This resulted in frequent modifications or new designs. A common requirement in modification or new design of small UAS is to operate beyond visual Line-Of-Sight (LOS) of the ground pilot. Conventional military development for small UAS adopts a design and built approach. Modification of small Remote Control (RC) aircraft, using Commercial-Off-The Shelf (COTS) equipment, offers a more economical alternative with the prospect of shorter development time compared to conventional approach. This research seeks to establish and demonstrate an architecture framework and design a prototype small UAS for operation beyond visual LOS. The aim is to achieve an effective and reliable development approach that is relevant to the military's evolving requirements for small UASs. Key elements of the architecture include Failure Mode Effect and Criticality Analysis (FMECA), fail safe design for loss of control or communication, power management, interface definition, and configuration control to support varying onboard payloads. Flight test was conducted which successfully demonstrated a control handoff between local and remote Ground Station (GS) for beyond visual LOS operation.

15. SUBJECT TERMS

Small UAS Architecture. Small UAS Development Framework. Beyond Visual LOS Operation. FMECA

16. SECURITY CLASSIFICATION OF:			17. LIMITATION OF ABSTRACT	18. NUMBER OF PAGES	19a. NAME OF RESPONSIBLE PERSON
a. REPORT	b. ABSTRACT	c. THIS PAGE			Dr David R. Jacques, AFIT/ENV
U	U	U	UU	142	19b. TELEPHONE NUMBER (Include area code) (937) 255-6565, ext 3329 (David.Jacques@afit.edu)

Standard Form 298 (Rev. 8-98)
Prescribed by ANSI Std. Z39-18